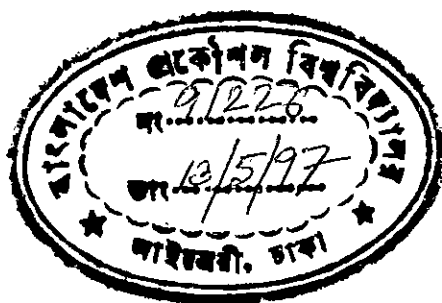


PERFORMANCE ANALYSIS OF DIRECT DETECTION OPTICAL FSK IN THE PRESENCE OF FIBRE CHROMATIC DISPERSION

A Thesis submitted to the Electrical and Electronic
Engineering Department of BUET, Dhaka,
in partial fulfillment of
the requirements for the degree of
Master of Science in Engineering
(Electrical and Electronic)



MD. ABDUL MOQADDEM

June 1996



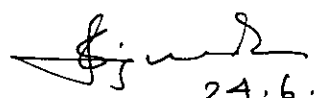



#91226#

DEDICATED TO
THE DEPARTED SOUL OF MY MOTHER

APPROVAL

The thesis titled "Performance analysis of direct detection optical FSK in the presence of fibre chromatic dispersion" submitted by Md. Abdul Moqaddem, Roll no. 881304F, Session 1986-87 to the Electrical and Electronic Engineering Department of B.U.E.T has been accepted as satisfactory for partial fulfillment of the requirements for the degree of Master of Science in Engineering (Electrical and Electronic).

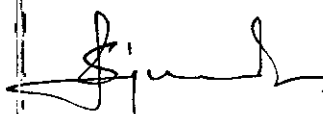
Board of Examiners

1. Dr. Satya Prasad Majumder
Associate Professor
Department of E.E.E
B.U.E.T, Dhaka- 1000.
Chairman
(Supervisor)

24.6.96
2. Dr. A. B. M. Siddique Hossain
Professor and Head
Department of E.E.E
B.U.E.T, Dhaka- 1000.
Member
(Ex-officio)

24/6/96
3. Dr. Md. Rezwan Khan
Associate Professor
Department of E.E.E
B.U.E.T, Dhaka- 1000.
Member

24.6.96
4. Md. Ashraf Alim
Divisional Engineer
Bangladesh T & T Board
37/E Eskaton Garden, Dhaka- 1000.
Member
(External)

24/6/96


DECLARATION

This work has been done by me and it has not been submitted elsewhere for the award of any degree or diploma.

Countersigned


24.6.96
(Dr. Satya Prasad Majumder)

Supervisor


24.6.96

(Md. Abdul Moqaddem)



CONTENTS

ACKNOWLEDGMENTS	viii
ABSTRACT	ix
LIST OF FIGURES	x
LIST OF PRINCIPAL SYMBOLS	xv
LIST OF ABBREVIATIONS	xvii
1. INTRODUCTION	1
1.1 Communication System	1
1.2 Brief review of Optical Fibre Communication System	3
1.3 Present Status and Future Prospects of Optical Fibre Communication in Bangladesh	10
1.3.1 Present Status	10
1.3.2 Future Prospect	16
1.4 Limitations of Optical Fibre Communications	20
1.5 Review of Previous Works	21

1.6	Objective of the Study	24
1.7	Brief Introduction to This Thesis	24
2.	PERFORMANCE ANALYSIS OF OPTICAL FSK WITH MACH-ZENDER INTERFEROMETER	26
2.1	Introduction	26
2.2	The Receiver Model	27
2.2.1	Mach-Zender Interferometer(MZI)	27
2.2.2	MZI Characteristics	29
2.3	Theoretical Analysis of Optical Direct Detection FSK	33
2.3.1	The Optical Signal	33
2.3.2	Receiver Output Signal	38
2.3.3	Bit Error Rate Expression	40
3.	RESULTS AND DISCUSSIONS	42

4.	CONCLUSION AND SUGESTIONS FOR FUTURE WORKS	81
4.1	Conclusions	81
4.2	Suggestions for Future Works	84
	REFERENCES	86
	APPENDICES	A-1
APPENDIX A	Expressions of $W_{\phi}^e(f)$ and $W_{\phi}^1(f)$	A-1
APPENDIX B	Program Listing	B-1

ACKNOWLEDGMENTS

The author would like to acknowledge his profound indebtedness and undoubted gratitude to his supervisor Dr. Satya Prasad Majumder, Associate Professor of the department of Electrical and Electronic Engineering, B.U.E.T for his sincere guidance, friendly supervision, constant encouragement and valuable suggestions during the important phases of the work.

The author wishes to express his thanks and regards to Dr. A.B.M Siddique Hossain, Professor and Head of the department of Electrical and Electronic Engineering, B.U.E.T for his support and encouragement to complete this work successfully.

The author also likes to thank Dr. Md. Rezwana Khan, Dr. Kazi Mohiuddin Ahmed, Dr. Shahidul Islam Khan, Dr. Mohammad Ali Chowdhury, Dr. M. M. Shahidul Hasan and many other faculty members of department of Electrical and Electronic engineering, B.U.E.T for their suggestions and helps.

Lastly, the author likes to thank his friends and colleagues especially Engr. Sadiqur Rahman Khan, Engr. Mohammad Tawrit, Engr. Yousuf Niaz, Engr. Sheik Riaz Ahmed for their constant encouragement to complete this work.

ABSTRACT

A novel theoretical analysis is provided for direct detection optical FSK transmission system with Mach-Zender interferometer (MZI) as an optical frequency discriminator (OFD). The analysis is carried out taking into account the combined effect of laser phase noise, chromatic dispersion of optical fibre, photodetector shot noise and receiver noise. The single mode fibre is modeled as a bandpass filter with flat amplitude response and linear group delay over the optical bandwidth of the modulated optical signal. The statistics of the signal phase fluctuations at the output of the fibre caused by non-linear filtering due to fibre chromatic dispersion are determined in terms of its moments and the probability density function (pdf) of the random phase fluctuation due to laser phase noise and fibre chromatic dispersion is evaluated. The total phase noise power at the output of the receiver photodetector is also expressed in terms of the powers of the cross-modulation and intermodulation frequency noise components.

Using the noise statistics and moments, the bit error rate (BER) performance of the receiver is then evaluated for different values of dispersion coefficient and laser linewidth at a bit rate of 10 Gbit/s. The penalty suffered by the system due to dispersion and phase noise is then determined at a bit error rate (BER) of 10^{-9} . For a specified power penalty of 1 dB, the maximum allowable fibre lengths are then determined for different values of the fibre dispersion coefficient and normalized laser linewidth.

LIST OF FIGURES

- Fig. 1.1 Frequency bands of radio frequency.
- Fig. 1.2 Different spectrum in the electromagnetic spectrum.
- Fig. 1.3 Generalized block diagram of an optical communication system.
- Fig. 1.4 Optical fibre network of Bangladesh Railway.
- Fig. 1.5 Optical fibre network (NEC) in Dhaka city of BTTB.
- Fig. 1.6 Optical fibre networks in Khulna, Rajshahi, Sylhet & Jessore.
- Fig. 1.7 Optical fibre network in Chittagong city (Alcatel) of BTTB.
- Fig. 1.8 Optical fibre network (Alcatel) in Dhaka city of BTTB.
- Fig. 1.9 Existing main micro-wave & UHF links of BTTB.
- Fig. 1.10 Proposed optical fibre & digital micro-wave links of BTTB.
- Fig. 2.1 Block diagram of an FSK direct detection receiver.
- Fig. 2.2 (a) An MZI with large ΔL or narrow wavelength spacing, (b) Transmittance characteristics of MZI and (c) Differential output of the balanced receiver.
- Fig. 3.1 The bit error rate (BER) performance of direct detection optical FSK transmission system at a bit rate of 10 Gb/s without fibre chromatic dispersion ($D_c=0.0$) and modulation index $m=0.8$ for several values of normalized laser linewidth $\Delta\nu T$.
- Fig. 3.2 The bit error rate (BER) performance of direct detection optical FSK transmission system at a bit rate of 10 Gb/s without fibre chromatic dispersion ($D_c=0.0$) and modulation index $m=1.0$ for several values of normalized laser linewidth $\Delta\nu T$.

- Fig. 3.3 The bit error rate (BER) performance of direct detection optical FSK transmission system at a bit rate of 10 Gb/s without fibre chromatic dispersion ($D_C=0.0$) and modulation index $m=1.2$ for several values of normalized laser linewidth $\Delta\nu T$.
- Fig. 3.4 The bit error rate (BER) performance of direct detection optical FSK transmission system at a bit rate of 10 Gb/s with fibre chromatic dispersion $D_C=1.0$ ps/ Km.nm, fibre length $L=150$ Km, at an wavelength of 1550 nm and modulation index $m=0.8$ for several values of normalized laser linewidth $\Delta\nu T$.
- Fig. 3.5 The bit error rate (BER) performance of direct detection optical FSK transmission system at a bit rate of 10 Gb/s with fibre chromatic dispersion $D_C=3.0$ ps/ Km.nm, fibre length $L=100$ Km, at an wavelength of 1550 nm and modulation index $m=0.8$ for several values of normalized laser linewidth $\Delta\nu T$.
- Fig. 3.6 The bit error rate (BER) performance of direct detection optical FSK transmission system at a bit rate of 10 Gb/s with fibre chromatic dispersion $D_C=15.0$ ps/ Km.nm, fibre length $L=50$ Km, at an wavelength of 1550 nm and modulation index $m=0.8$ for several values of normalized laser linewidth $\Delta\nu T$.
- Fig. 3.7 The bit error rate (BER) performance of direct detection optical FSK transmission system at a bit rate of 10 Gb/s with fibre chromatic dispersion $D_C=9.0$ ps/ Km.nm, fibre length $L=200$ Km, at an wavelength of 1550 nm and modulation index $m=0.8$ for several values of normalized laser linewidth $\Delta\nu T$.
- Fig. 3.8 The bit error rate (BER) performance of direct detection optical FSK transmission system at a bit rate of 10 Gb/s with fibre chromatic dispersion $D_C=1.0$ ps/ Km.nm, fibre length $L=150$ Km, at an wavelength of 1550 nm and modulation index $m=1.0$ for several values of normalized laser linewidth $\Delta\nu T$.
- Fig. 3.9 The bit error rate (BER) performance of direct detection optical FSK transmission system at a bit rate of 10 Gb/s with fibre chromatic dispersion $D_C=3.0$ ps/ Km.nm, fibre length $L=100$ Km, at an wavelength of 1550 nm and modulation index $m=1.0$ for several values of normalized laser linewidth $\Delta\nu T$.

- Fig. 3.10 The bit error rate (BER) performance of direct detection optical FSK transmission system at a bit rate of 10 Gb/s with fibre chromatic dispersion $D_C=15.0$ ps/ Km.nm, fibre length $L=50$ Km, at an wavelength of 1550 nm and modulation index $m=1.0$ for several values of normalized laser linewidth $\Delta\nu T$.
- Fig. 3.11 The bit error rate (BER) performance of direct detection optical FSK transmission system at a bit rate of 10 Gb/s with fibre chromatic dispersion $D_C=9.0$ ps/ Km.nm, fibre length $L=200$ Km, at an wavelength of 1550 nm and modulation index $m=1.0$ for several values of normalized laser linewidth $\Delta\nu T$.
- Fig. 3.12 The bit error rate (BER) performance of direct detection optical FSK transmission system at a bit rate of 10 Gb/s with fibre chromatic dispersion $D_C=1.0$ ps/ Km.nm, fibre length $L=150$ Km, at an wavelength of 1550 nm and modulation index $m=1.2$ for several values of normalized laser linewidth $\Delta\nu T$.
- Fig. 3.13 The bit error rate (BER) performance of direct detection optical FSK transmission system at a bit rate of 10 Gb/s with fibre chromatic dispersion $D_C=3.0$ ps/ Km.nm, fibre length $L=100$ Km, at an wavelength of 1550 nm and modulation index $m=1.2$ for several values of normalized laser linewidth $\Delta\nu T$.
- Fig. 3.14 The bit error rate (BER) performance of direct detection optical FSK transmission system at a bit rate of 10 Gb/s with fibre chromatic dispersion $D_C=15.0$ ps/ Km.nm, fibre length $L=50$ Km, at an wavelength of 1550 nm and modulation index $m=1.2$ for several values of normalized laser linewidth $\Delta\nu T$.
- Fig. 3.15 The bit error rate (BER) performance of direct detection optical FSK transmission system at a bit rate of 10 Gb/s with fibre chromatic dispersion $D_C=9.0$ ps/ Km.nm, fibre length $L=200$ Km, at an wavelength of 1550 nm and modulation index $m=1.2$ for several values of normalized laser linewidth $\Delta\nu T$.
- Fig. 3.16 Penalty in signal power due to combined effect of laser phase noise and fibre chromatic dispersion at $BER=10^{-9}$ versus dispersion coefficient D_C (ps/ Km.nm) with fibre length $L=150$ Km and modulation index $m=0.8$ for several values of normalized linewidth $\Delta\nu T$.

- Fig. 3.17 Penalty in signal power due to combined effect of laser phase noise and fibre chromatic dispersion at $BER=10^{-9}$ versus dispersion coefficient D_C (ps/ Km.nm) with fibre length $L=200$ Km and modulation index $m=0.8$ for several values of normalized linewidth $\Delta\nu T$.
- Fig. 3.18 Penalty in signal power due to combined effect of laser phase noise and fibre chromatic dispersion at $BER=10^{-9}$ versus dispersion coefficient D_C (ps/ Km.nm) with fibre length $L=150$ Km and modulation index $m=1.0$ for several values of normalized linewidth $\Delta\nu T$.
- Fig. 3.19 Penalty in signal power due to combined effect of laser phase noise and fibre chromatic dispersion at $BER=10^{-9}$ versus dispersion coefficient D_C (ps/ Km.nm) with fibre length $L=200$ Km and modulation index $m=1.0$ for several values of normalized linewidth $\Delta\nu T$.
- Fig. 3.20 Penalty in signal power due to combined effect of laser phase noise and fibre chromatic dispersion at $BER=10^{-9}$ versus dispersion coefficient D_C (ps/ Km.nm) with fibre length $L=50$ Km and modulation index $m=1.2$ for several values of normalized linewidth $\Delta\nu T$.
- Fig. 3.21 Penalty in signal power due to combined effect of laser phase noise and fibre chromatic dispersion at $BER=10^{-9}$ versus dispersion coefficient D_C (ps/ Km.nm) with fibre length $L=100$ Km and modulation index $m=1.2$ for several values of normalized linewidth $\Delta\nu T$.
- Fig. 3.22 Variation of power penalty (dB) due to combined effect of laser phase noise and fibre chromatic dispersion at $BER=10^{-9}$ with normalized linewidth $\Delta\nu T$ for modulation index $m=0.8$ and several values of dispersion factor γ .
- Fig. 3.23 Variation of power penalty (dB) due to combined effect of laser phase noise and fibre chromatic dispersion at $BER=10^{-9}$ with normalized linewidth $\Delta\nu T$ for modulation index $m=1.0$ and several values of dispersion factor γ .

- Fig. 3.24 Variation of power penalty (dB) due to combined effect of laser phase noise and fibre chromatic dispersion at $BER=10^{-9}$ with normalized linewidth $\Delta\nu T$ for modulation index $m=1.2$ and several values of dispersion factor γ .
- Fig. 3.25 Plots of power penalty (dB) at $BER=10^{-9}$ versus dispersion factor γ for modulation index $m=0.8$ with $\Delta\nu T$ as a parameter.
- Fig. 3.26 Plots of power penalty (dB) at $BER=10^{-9}$ versus dispersion factor γ for modulation index $m=1.0$ with $\Delta\nu T$ as a parameter.
- Fig. 3.27 Plots of power penalty (dB) at $BER=10^{-9}$ versus dispersion factor γ for modulation index $m=1.2$ with $\Delta\nu T$ as a parameter.
- Fig. 3.28 Plots of allowable fibre length corresponding to 1 dB penalty at $BER=10^{-9}$ as a function of normalized linewidth $\Delta\nu T$ for modulation index $m=0.8, 1.0$ and 1.2 and dispersion coefficient $D_C=1.0$ ps/Km.nm.
- Fig. 3.29 Plots of allowable fibre length corresponding to 1 dB penalty at $BER=10^{-9}$ as a function of normalized linewidth $\Delta\nu T$ for modulation index $m=0.8, 1.0$ and 1.2 and dispersion coefficient $D_C=3.0$ ps/Km.nm.
- Fig. 3.30 Plots of allowable fibre length corresponding to 1 dB penalty at $BER=10^{-9}$ as a function of normalized linewidth $\Delta\nu T$ for modulation index $m=0.8, 1.0$ and 1.2 and dispersion coefficient $D_C=15.0$ ps/Km.nm.

LIST OF PRINCIPAL SYMBOLS

T	Bit period
R_b	Bit rate
σ^2	Noise variance
$n(t)$	Complex additive Gaussian noise
Δf	Frequency deviation of FSK signal
ϕ_s	Angle modulation
ϕ_n	Phase noise of the transmitting laser
m	Modulation index
R_d	Photon responsivity
P_s	Input signal power
f_c	Optical carrier frequency
$H(f)$	Optical fibre transfer function
λ	Optical wavelength
ν	Frequency of optical carrier
$\Delta\nu$	Normalized linewidth of transmitting laser
τ	Delay occurred due to path difference in MZI
l_1, l_2	Lengths of arms I and II of MZI
T_I, T_{II}	Transmittance of arms I and II of MZI
ΔL	Path difference of MZI
η_{eff}	Effective refractive index of MZI

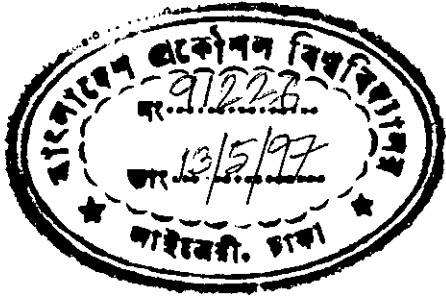
$E(t)$	Signal input to MZI
$D(\lambda)$	Fibre chromatic dispersion
γ	Dispersion factor
N_{SB}	Number of samples per bit
$I(t)$	Modulating signal
F	Fourrier transform
F^{-1}	Inverse fourrier transform
c	Velocity of light
K	Boltzman's constant
$\delta(t)$	Delta function of time
$W_0^c(f)$	PSD of cross-power component
$W_0^I(f)$	PSD of intermodulation power component
$P(\Delta\theta)$	PSD of $\Delta\theta$
M_{2r}	Even order moments
H_{2r}	Even order Hermite polynomial

LIST OF ABBREVIATIONS

ASK	Amplitude shift keying
APD	Avalanche photo diode
BER	Bit error rate
BPPM	Binary PPM
BPSK	Binary PSK
BTTB	Bangladesh Telegraph & Telephone Board
BW	Bandwidth
CPFSK	Continuous phase FSK
CPFSK-DD	CPFSK differential detection
dBm	Decibel relative to 1 mW
DFB	Distributed feedback
DPFSK	Discontinuous phase FSK
DPSK	Differential phase shift keying
erfc	Complementary error function
FM	Frequency modulation
FPF	Fabry Perot filter
FSK	Frequency shift keying
FS-SW	Frequency selection Switch
FDM	Frequency division multiplexing
FWM	Four wave mixing
GEC	General electric company

IF	Intermediate frequency
IM/DD	Intensity modulation direct detection
ISI	Inter-symbol interference
LAN	Local area network
LD	Laser diode
LED	Light emitting diode
LO	Local oscillator
LW	Linewidth
MSK	Minimum shift keying
MSK-FM	FM with MSK sub-carrier
MZI	Mach-Zender Interferometer
NEC	Nippon electric company
NRZ	Non-return to zero
OOK	On-off keying
OFD	Optical frequency discriminator
OFDM	Optical frequency division multiplexing
OQPSK	Orthogonal QPSK
PDF	Probability density function
PIN	Positive intrinsic negative
PPM	Pulse position modulation
PRBS	Pseudo-random bit sequence
PSD	Power spectral density

PSK	Phase shift keying
SBS	Stimulated Brillouin scattering
SCM	Sub-carrier modulation
SNR	Signal to noise ratio
WAN	Wide area network
WDM	Wavelength division multiplexing



CHAPTER - 1

INTRODUCTION

1.1 Communication System :

With the advent of telecommunication technology human civilization had a great leap in its development. Till today this technology has got enormous achievements. Telecommunication requires transmission of information from one place to another. Basic concept behind telecommunication technology is that information is first converted to electrical signal which after transferring to another place is again reconverted back to information. Transmission of this information signal to a distant place is done by using electromagnetic wave. For this transmission, information signal is superimposed (modulated) on an electromagnetic wave called carrier. This modulated carrier is then transmitted to the destination, where information is recovered (demodulated) from the carrier. The carrier electromagnetic waves are designated by its location in the frequency spectrum. Fig. 1.1 shows the frequency bands of radio frequency (RF) part of the electromagnetic spectrum.

Band name	VLF	LF	MF	HF	VHF	UHF	SHF	EHF		
Band number	4	5	6	7	8	9	10	11	12	
Frequency	3 Khz	30 khz	300 khz	3 Mhz	30 Mhz	300 Mhz	3 Ghz	30 Ghz	300 Ghz	3 THz

Fig. 1.1 Frequency bands of radio frequency

The electromagnetic wave can be transmitted either through guided channel such as wire or wave guide or through unguided atmosphere or free space. When information is modulated on the carrier it occupies certain band of frequency around the carrier called transmission bandwidth. Amount of information transmitted per unit time is called information rate. Transmission bandwidth is directly proportional to the information rate and on the other hand available transmission bandwidth increases with the increase of carrier frequency. With the development of telecommunication technology demand for higher and higher information rate was felt and hence the higher bands were called for.

When it was very difficult to meet the growing demand by RF spectra, development of technology made it possible to utilize another spectra called optical spectra and thus a wide window for information transmission channel was open to mankind. Fig. 1.2 shows the position of this spectra in the electromagnetic spectra. Optical communication system utilizes the infra red portion of the optical spectra.

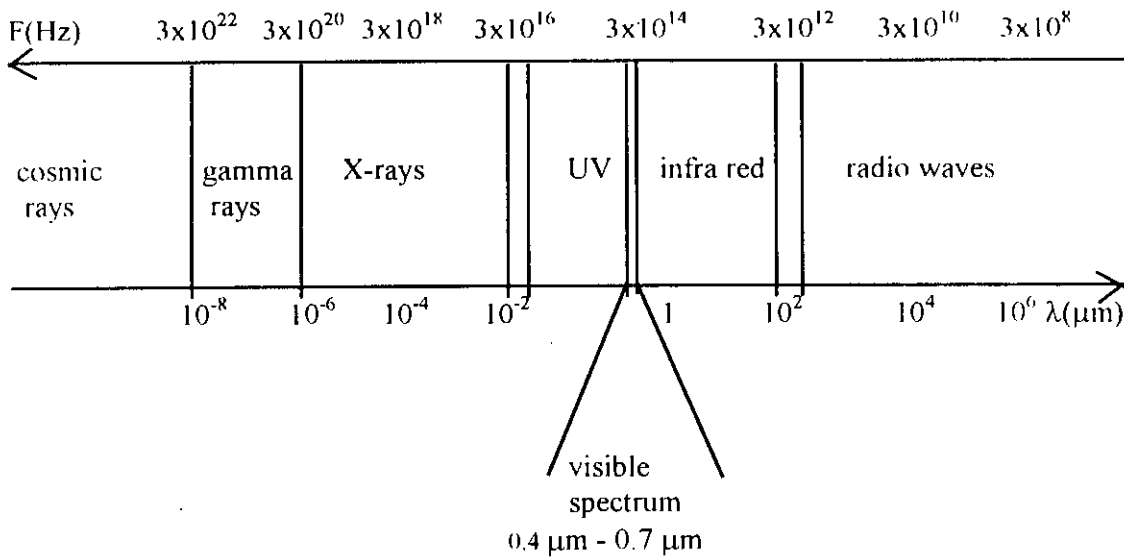


Fig. 1.2 Different spectrum in the electromagnetic spectrum

1.2 Brief Review of Optical Fibre Communication System :

The invention of LASER in 1960 made the optical fibre communication possible. During the last thirty years enormous developments have been done in this field. The period 1965-75 was devoted to the development of graded index fibre system which utilized wavelengths of 850-900 nm and achieved information rates in the range of 8-140 Mbit/s. Then in 1978, research started for single mode fibre technology and it led to the establishment of 1300 nm range single mode fibre system. Present trend is towards 1500 nm range fibre for long haul system.

Optical fibre communication system has the following advantages by virtue of its characteristics:

1. Low losses: It enables reducing number of repeaters.
2. High bandwidth: Low cost per channel is achieved.
3. Small bulk: Requires less space.
4. Low weight: Lightened the cable.
5. Flexibility: Easy to install.
6. Resistant to radiation: Less costly protection is required.
7. Immunity to radio interference: Increased reliability.
8. Difficult to intercept: Security is ensured.
9. No conductor: Adequate electrical insulation is assured.

Due to these and other features led today to have around 50 million kilometers of optical fibre installed world wide[1].

The generalized block diagram of an optical communication system is shown in fig. 1.3. The main components are:

1. The optical source
2. A means to modulate the optical carrier from the source with the information signal to be transmitted.

3. The transmission medium.

4. The photo detector which converts the received optical power to electrical wave form.

5. A means to demodulate the electrical wave form and recover the information signal.

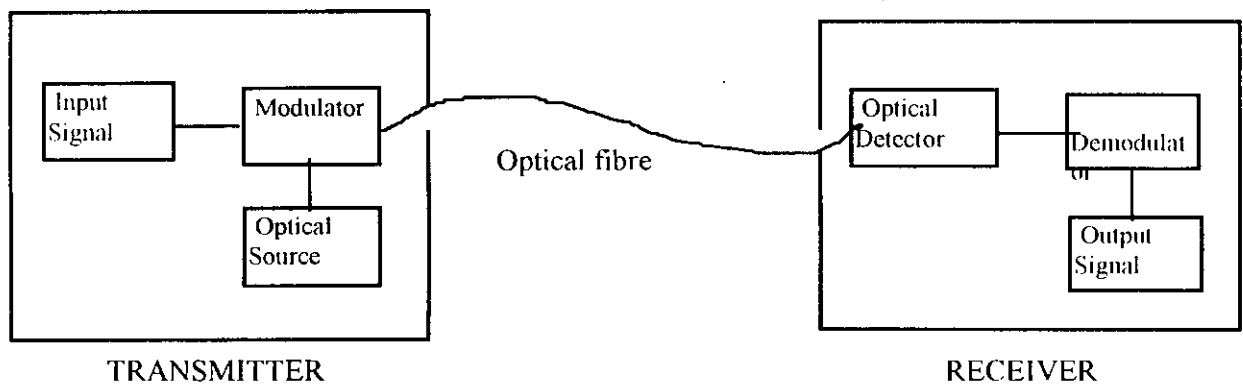


Fig. 1.3 Generalized block diagram of an optical communication system

The two conventional sources used in fibre optics are LEDs and Laser diodes (LDs). The advantages of LED are (i) low sensitivity to retroreflection (ii) no interference problem (iii) low sensitivity to temperature (iv) high reliability (v) simple electronic excitation and (vi) low cost. But main disadvantages are (i) low coupling efficiency between an LED and a fibre (ii) low modulation bandwidth, typically limited to 100-200 Mhz (iii) wide spectrum, around 50 nm[2].

The advantages of LD are (i) high conversion gain i.e. with small bias current relatively high power output (ii) low numerical aperture, as a result coupling efficiency high (iii) high modulation bandwidth (Ghz) (iv) narrow spectrum. Main disadvantages of LD are (i) high sensitivity to temperature (ii) produce supplementary to return reflected power (iii) less reliable (iv) more costly[2].

In Summary, for short links (< 10 km) LED is suitable, but for medium and long links LD is suitable[2].

Two types of detectors are frequently used in optical fibre communication system: (i) PIN photo diode and (ii) avalanche photo diode (APD). For short links GE PIN is used. For medium links GE III/V PIN or GE APD are used and for long links III/V APD is used[2].

After optical signal has been launched into fibre, it becomes progressively attenuated and distorted with increasing distance because of scattering, absorption, dispersion in the fibre. At the receiver the attenuated and distorted optical power is detected by a photo diode. Principle figure of merit for a fibre is the attenuation and distortion as less as possible and that for a receiver is the minimum optical power necessary at the desired data rate to attain either a given error probability for a digital system or a specified signal to noise ratio for an analog system.

In light wave communication system, broadly categorizing, two important detection strategies are normally employed: (i) direct detection and (ii) coherent detection. In direct detection, the intensity of the received optical field is directly converted to a current by a photo detector. Whereas in coherent detection, the received optical field is combined with the light output from a local oscillator (LO) laser and the mixed optical field is converted to an intermediate frequency (IF) signal by heterodyning or directly to base band by homodyning. The first optical communication system employed intensity modulation direct detection (IM/DD) technique and in spite of a lot of research, this scheme is still very popular for commercial application due to its low cost and simplicity. However, direct detection technique has limitation of data rate for application in power limited free space optical channels due to relatively low optical power output of semiconductor laser diode (LD). To increase the data rate throughput of all semiconductor free space optical channels, extensive research for bandwidth, power efficient coding and modulation schemes were carried out in the last decade. Direct detection optical communication systems are very promising for future deep space applications, inter satellite links and terrestrial line of sight communications[3]-[7].

Coherent optical transmission systems using heterodyne or homodyne are attractive due to their improved receiver sensitivity compared to conventional IM/DD systems and its enhanced frequency selectivity on optical frequency

division multiplexing (OFDM) system. In coherent optical communication system, information can be impressed on the optical carrier in one of the three ways: (i) phase shift keying (PSK) (ii) frequency shift keying (FSK) or (iii) amplitude shift keying (ASK). Depending on the specific application various modulation and demodulation formats similar to those of traditional radio frequency communication are also employed in coherent light wave transmission. These include: binary PSK (BPSK), quadrature PSK (QPSK), orthogonal QPSK (OQPSK), continuous phase FSK (CPFSK), discontinuous phase FSK (DPFSK), binary pulse position modulation (BPPM) etc. Each of the modulation schemes viz. ASK, FSK, DPFSK etc. and combinations thereof, with homodyne, heterodyne or diversity receivers has its own merits and demerits and non has emerged as absolutely preferable. However, FSK systems are more promising than ASK or PSK due to several reasons. First, modulation can be easily performed using direct modulation of laser diode (LD) through its injection current[8]-[10]. FSK is flexible enough to allow generation of either compact spectra, which is advantageous in multi channel OFDM or two lobe spectra which allows for receiver envelop detection by properly selecting the modulation index. Further, a laser FM transmitter and a receiver front-end can easily be converted to encompass subcarrier modulation scheme, such as MSK-FM for instance and subcarrier multiplexing[8].

The enormous bandwidth of the optical fibre can be utilized when hundreds of channels can be multiplexed over a single fibre. Optical frequency division multiplexing (OFDM) networks have an ultra large transmission capacity potential[11]. To increase the number of multiplexed channel the signals should be spaced densely. A sharp cut-off filter and a modulation scheme with a compact spectrum are necessary to construct densely spaced multiplexing systems utilizing a direct detection scheme. A periodic filter that consists of an anti-symmetric Mach-Zender Interferometer (MZI) is promising because it can multiplex/demultiplex optical carrier with channel spacing in the order of giga hertz. An FSK scheme has a compact spectrum. A tunable Fabry-Perot filter (FPF) that functions as a channel selective filter is useful for frequency division multiplexed FSK signals and acts as an optical frequency discriminator (OFD). However, a MZI that can act both as modulator/ demodulator is more promising as it is 3 dB more power efficient compared to FPF. The periodic filter which consists of anti-symmetric MZI, also functions as a channel selective filter and OFD[12]. When it is used as an OFD, 'mark' and 'space' are differentially detected with two outputs from OFD. Recently an experiment employing 10 Gbit/s modulation using a III-IV semiconductor MZI has been reported[13].

1.3 Present Status and Future Prospects of Optical Fibre Communication in Bangladesh

1.3.1 Present Status

Bangladesh Railway is the pioneer in introducing optical fibre communication system in Bangladesh. NORAD aided project implemented by GEC Telecommunication Ltd. commenced in the year 1987 and its Dhaka-Chittagong link was commissioned on January 10, 1989. Total length of the link is about 1450 km, which covers almost the whole railway link (fig. 1.4). Maximum repeater distance is 68 km and minimum is 8 km. Laser sources used are mainly Laser diodes (LDs), but for shorter distances LEDs are used. Fibre used is mono-mode and transmission wavelength is 1310 nm. Speed of transmission is 8 Mb/s. Depending on requirement no. of channels transmitted is 30, 60 or 120.

Bangladesh T & T Board (BTTB) introduced its first optical fibre communication system in the year 1989-90. It came along with the first digital exchanges installed in Dhaka city. These links connected the telephone exchanges (mainly digital) of the city (fig. 1.5). Transmission speed is 140 Mb/s. The system was implemented by NEC, Japan.

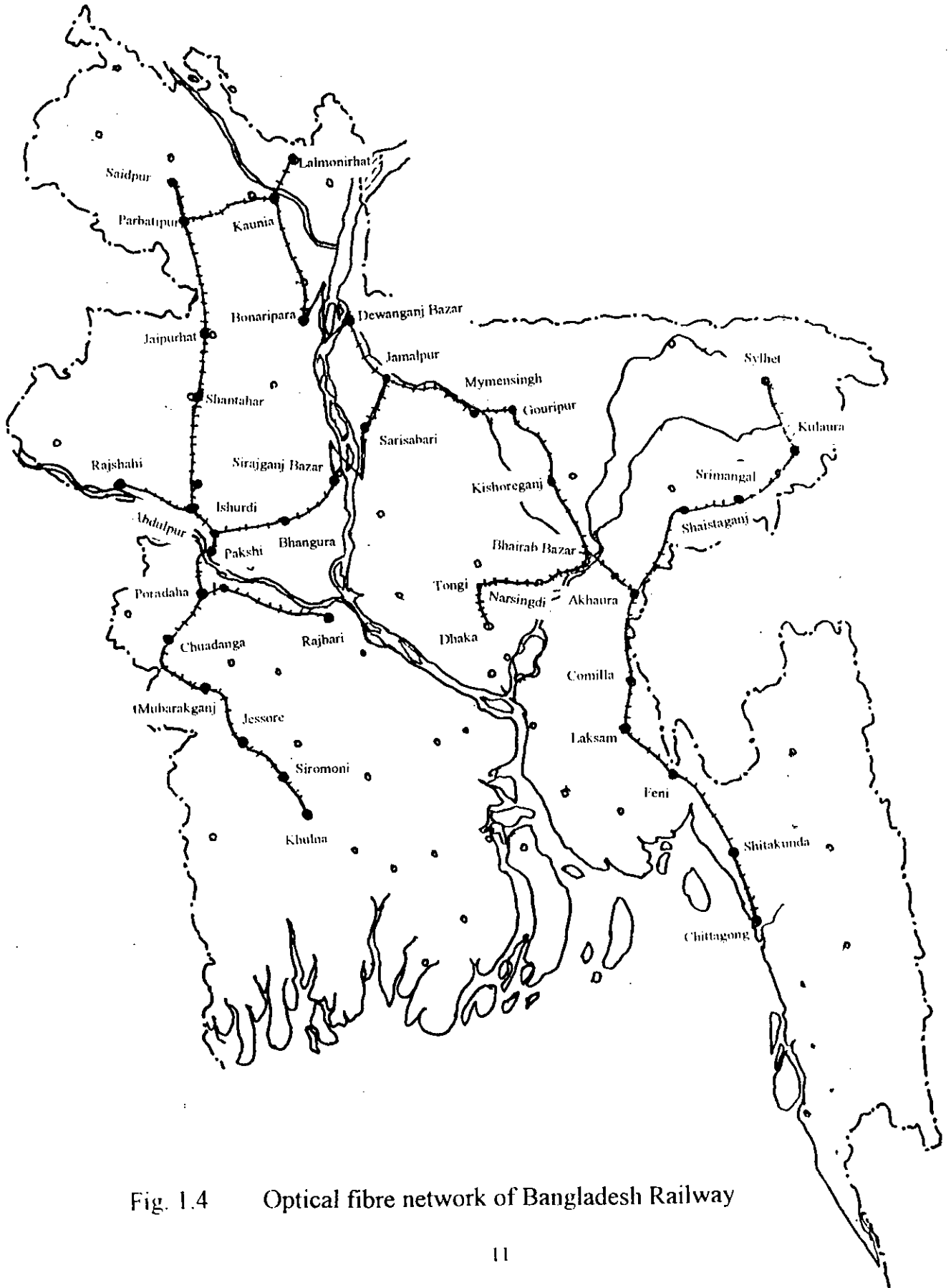


Fig. 1.4 Optical fibre network of Bangladesh Railway

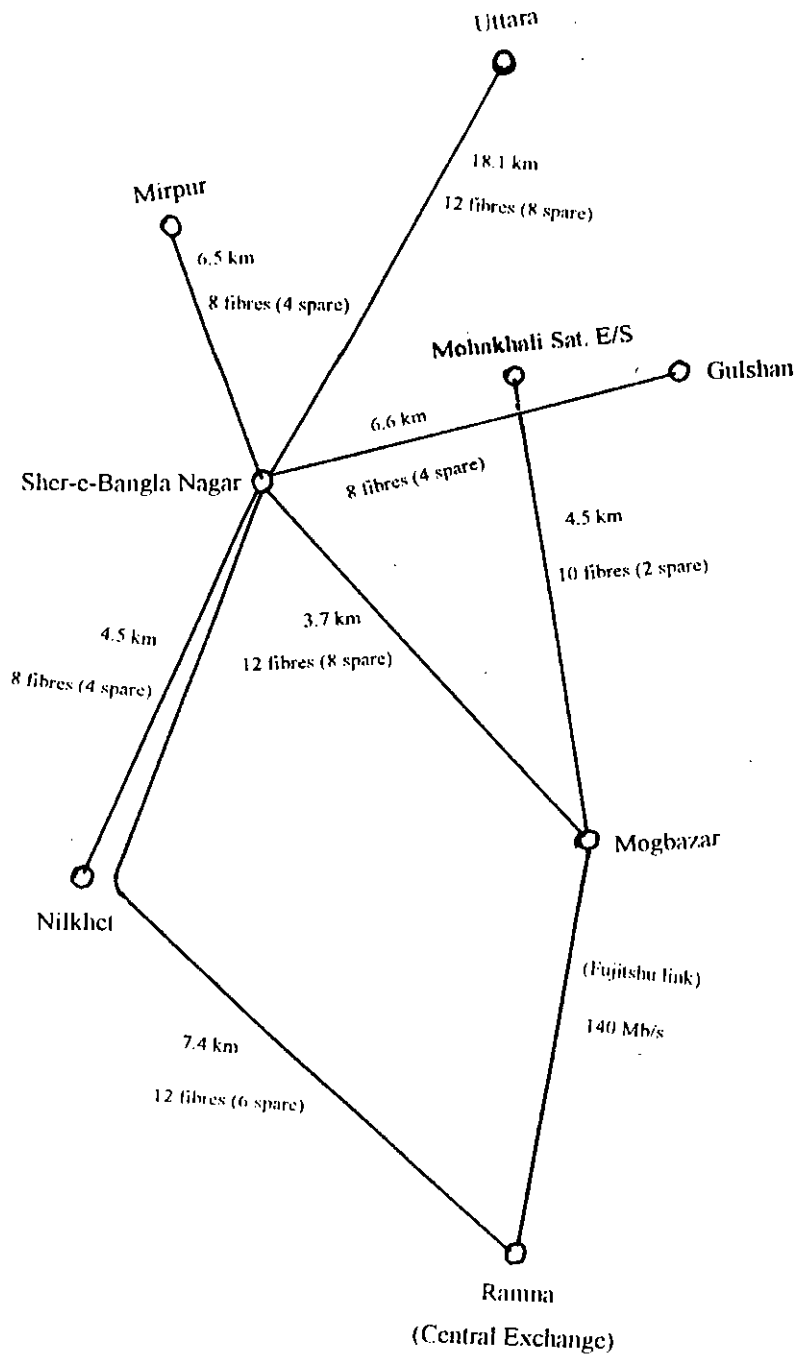


Fig. 1.5 Optical fibre network (NEC) in Dhaka city of BTTB

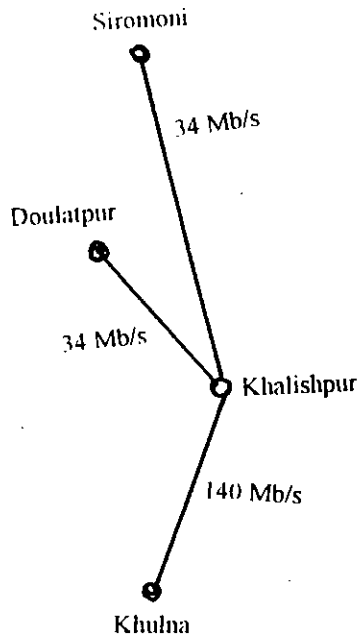
BTTB then had Fujitsu system with it's Dhaka-Khulna digital microwave project. It has two links, Moghbazar-Ramna link is 140 Mb/s (fig. 1.5) and Jessore-Rajarhat link is 34 Mb/s (fig. 1.6).

BTTB then had it's Chittagong 30,000 telephone project which introduced optical fibre links connecting it's exchanges at Chittagong (fig. 1.7). Transmission speed is 140 Mb/s. The system was implemented by Alcatel, France.

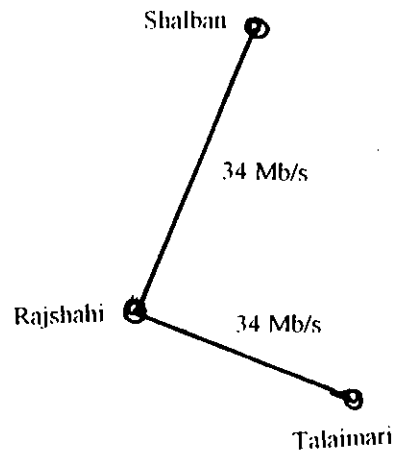
With the installation of satellite earth station and international switching centre at Mohakhali at the end of 1994, BTTB had one optical fibre link (4.5 km) between Mohakhali and Moghbazar (fig. 1.5). Transmission speed is 140 Mb/s and was implemented by NEC, Japan.

Then BTTB had it's biggest 1,50,000 telephone project which is nearly completed. It included optical fibre links in Dhaka (fig. 1.8), Khulna, Rajshahi and Sylhet (fig. 1.6). Transmission speeds are 34 Mb/s, 140 Mb/s and 560 Mb/s. This project is being implemented by Alcatel, France.

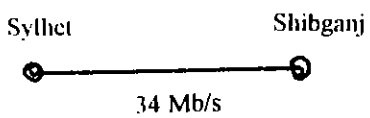
All the systems of BTTB used LDs as Laser sources and APDs as detectors. Each of the system uses IM/DD and transmission wavelength is 1310 nm. Fibres used are mono-mode fibres.



(a) Optical fibre network in Khulna city (Alcatel)



(b) Optical fibre network in Rajshahi city (Alcatel)



(c) Optical fibre link in Sylhet (Alcatel)



(d) Optical fibre link in Jessore (Fujitsu)

Fig. 1.6 Optical fibre networks in Khulna, Rajshahi, Sylhet & Jessore

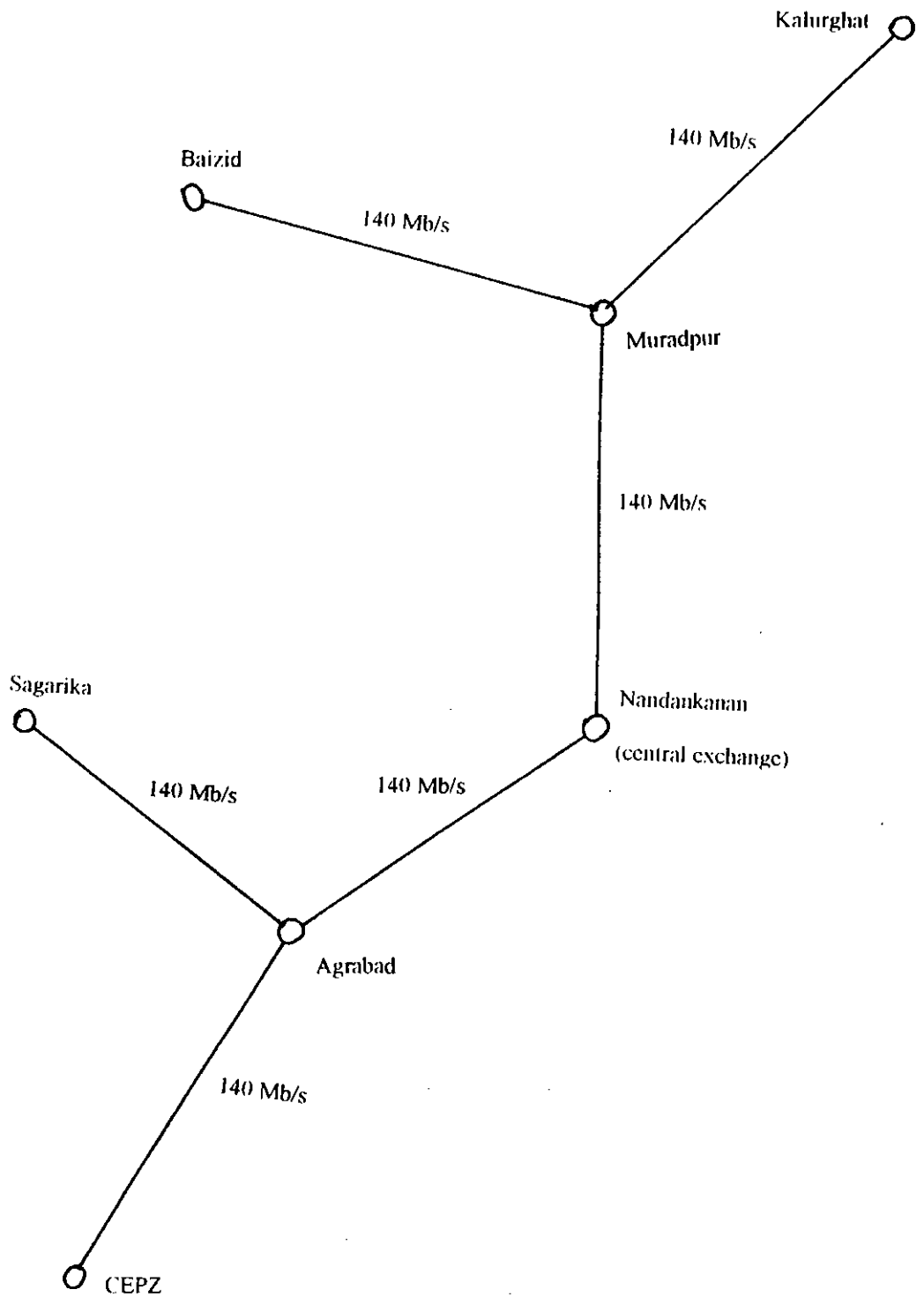


Fig. 1.7 Optical fibre network in Chittagong city (Alcatel) of BTTB

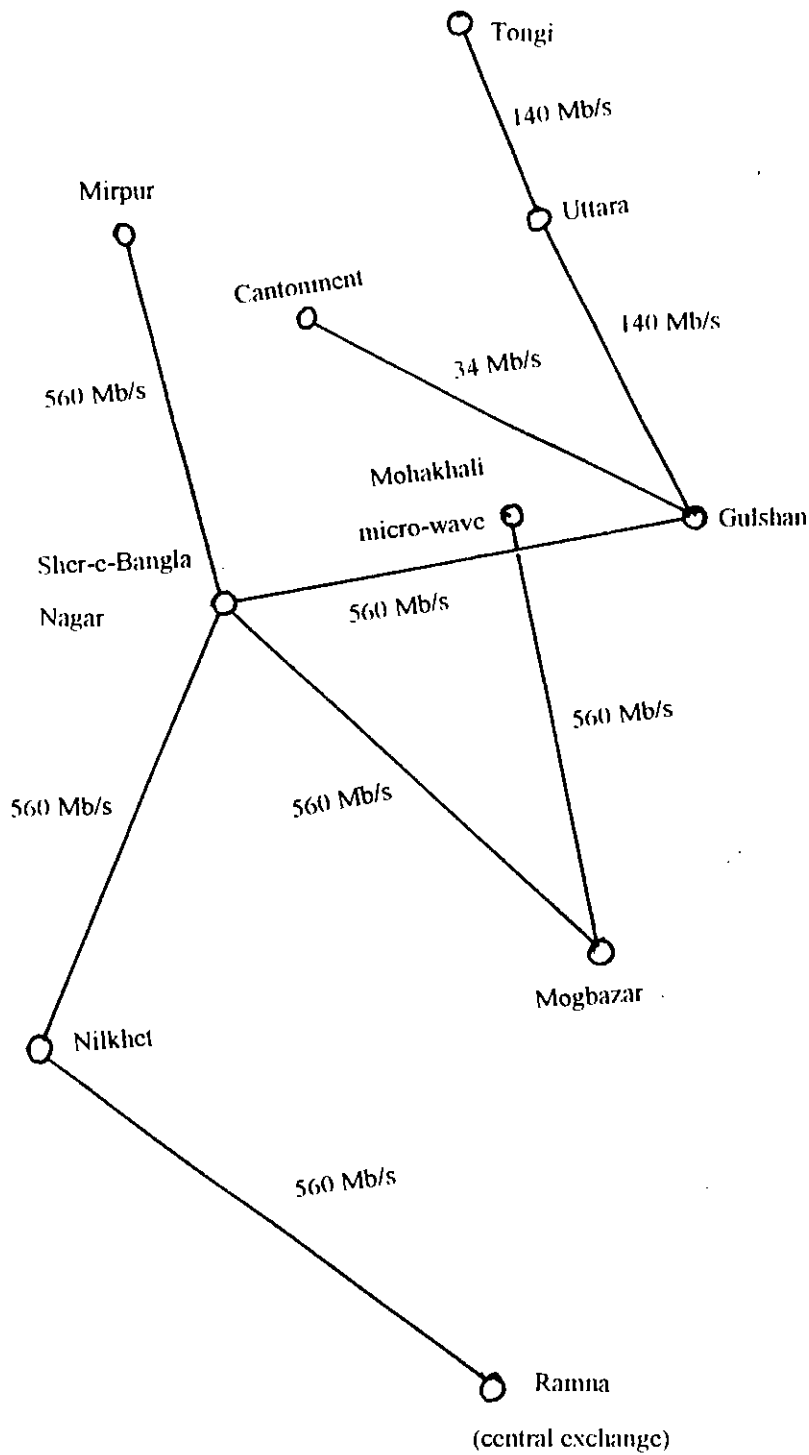


Fig. 1.8 Optical fibre network (Alcatel) in Dhaka city of BTTB

Bangladesh Railway has only one pair of fibre with no standby or spare fibres installed, whereas BTTB's system has 8 to 12 fibres in every link and one pair is always hot-standby and in most cases there are spare fibres also.

1.3.2 Future Prospect

In the near future, Bangladesh Railway is going to upgrade its transmission speed from 8 Mb/s to 140 Mb/s. Channels increased by this up-gradation will be offered to telephone companies either public (BTTB) or private.

BTTB has its back-bone micro-wave link (fig. 1.9) connecting its main cities and most of these links are now digital micro-wave links. BTTB is now preparing for a network (fig. 1.10) complementary to existing links and thus turning almost its whole network into digital. It is expected that main parts of this network will be optical fibre. It will extend its link up to Cox's Bazar, so that it can be connected to international fibre link, though it has not yet finalised any such connection.

In Bangladesh telecommunication sector is now open for private investment and on the other hand all sort of telecommunication services including cable TV and computer networks LAN/WAN are becoming popular. Private telephone operators are planning to have their own optical fibre telecommunication networks. Computer

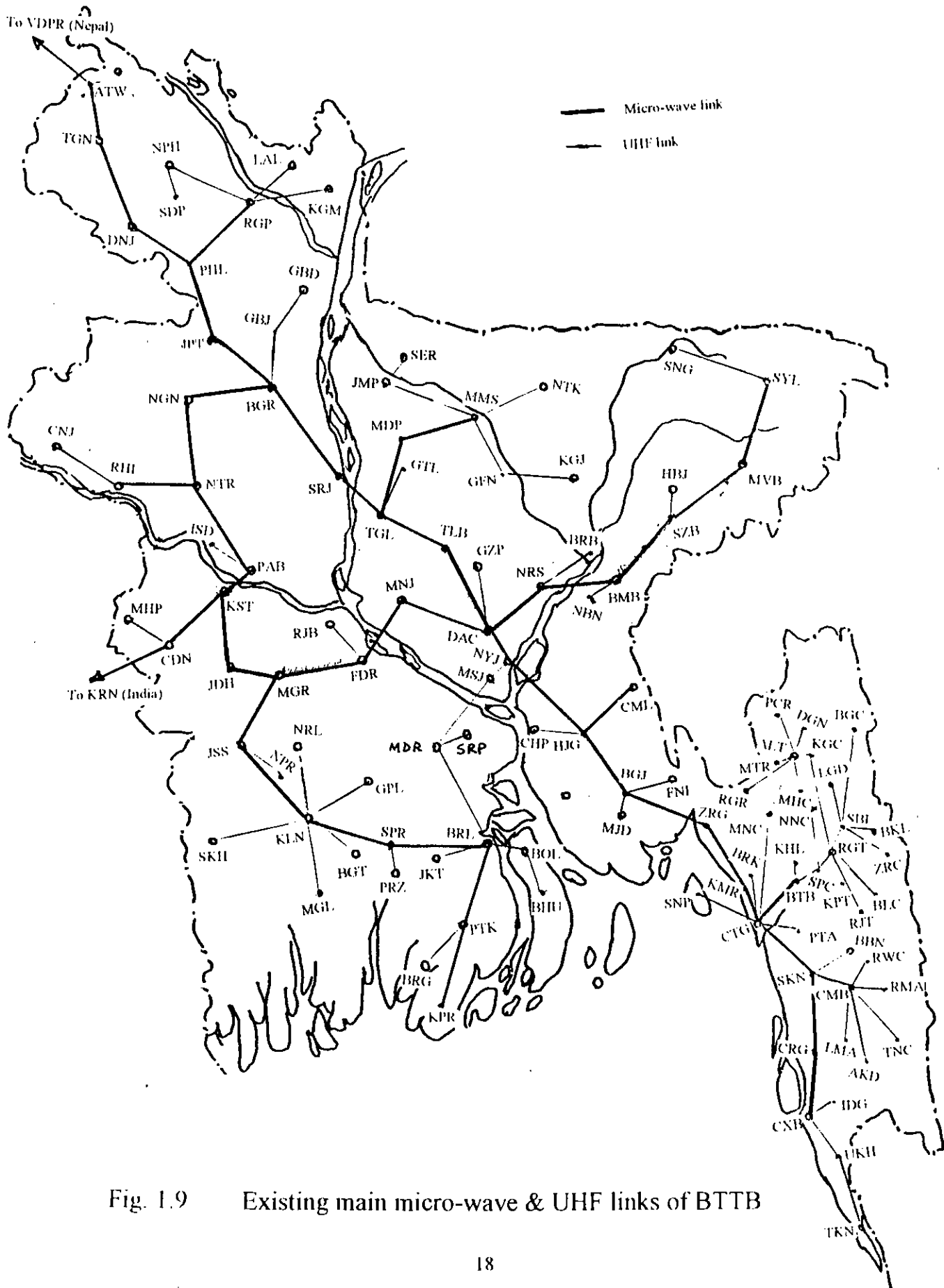


Fig. 1.9 Existing main micro-wave & UHF links of BTTB

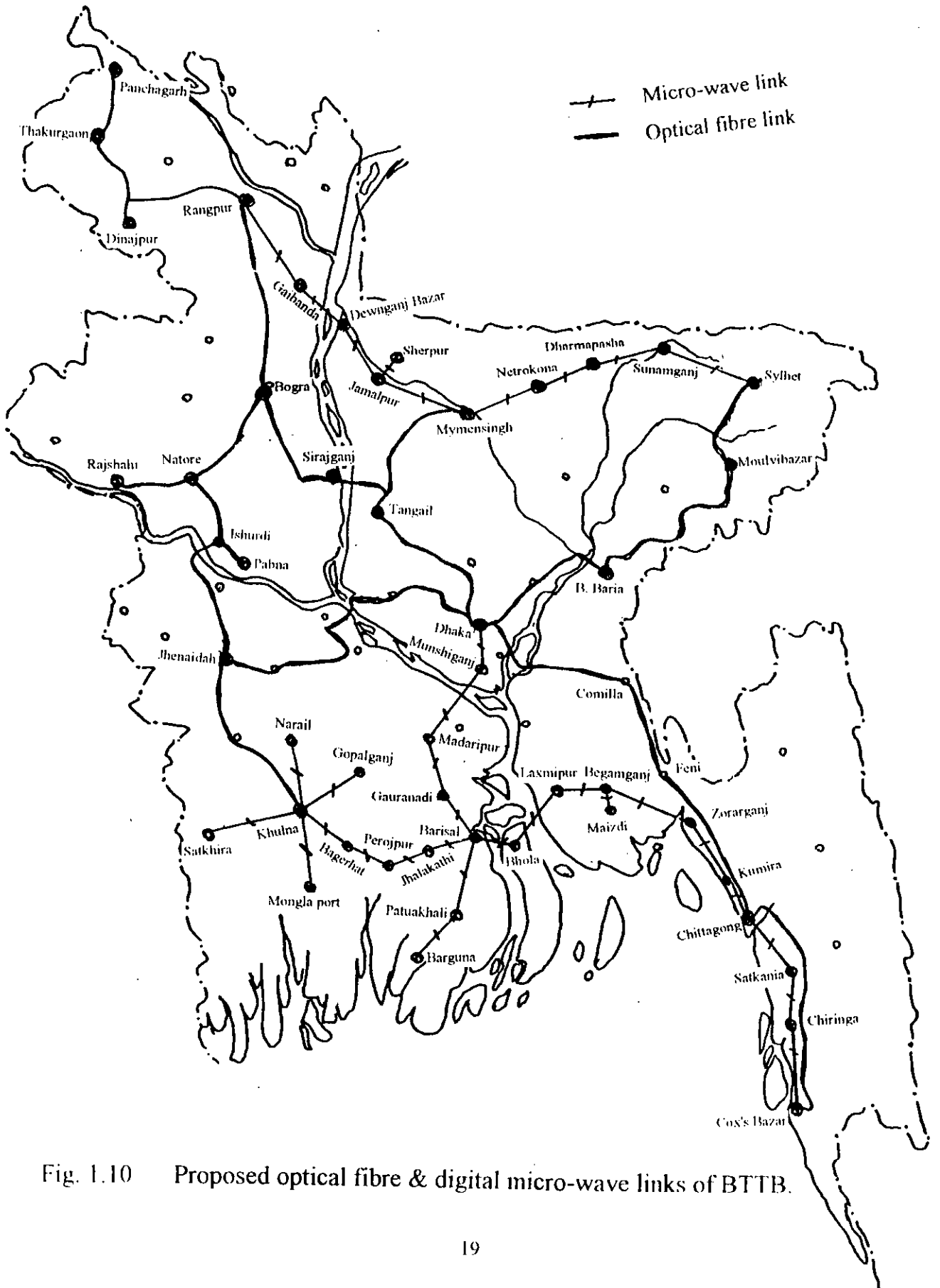


Fig. 1.10 Proposed optical fibre & digital micro-wave links of BTTB.

networks were earlier copper networks, now optical fibre networks are also becoming popular. So, it is expected that optical fibre will soon play an important role in solving future requirements and bring the world to the hands of the citizens of Bangladesh.

1.4 Limitations of Optical Fibre Communication :

There exists a rich collection of non-linear optical effects in fused silica fibres, each of which manifests itself in a unique way[14]-[16]. Stimulated Raman Scattering, an interaction between light and vibrations of silica molecules, causes attenuation of short-wavelength channels in wavelength-multiplexed systems. Stimulated Brillouin Scattering, an interaction between light and sound waves in the fibre, causes frequency conversion and reversal of the propagation direction of light[16]. Cross-phase modulation is an interaction, via the non-linear refractive index, between the intensity of one light wave and the optical phase of other light waves. Four-photon mixing or Four wave mixing is analogous to third order intermodulation distortion whereby two or more optical waves at different wave lengths mix to produce new waves at other wave lengths[14]. Optical non-linear effects, such as Stimulated Brillouin Scattering (SBS)[16] and Four Wave Mixing (FWM)[17] processes are likely to impose severe restrictions on transmitter power

in frequency division multiplexing (FDM) systems employing narrow linewidth single frequency lasers[17]-[19].

Some other limitations of optical fibre communications are fibre chromatic dispersion, laser phase noise, relative intensity noise etc. The various colors contained in an optical impulse travel at different speeds causing widening of the impulses at the end of the fibre[20],[21]. Thus, widening of the impulse depends on the spectral width of the source. This effect is known as chromatic dispersion. If the bit rate increases i.e. if time slot T decreases the impulses will overlap and can no longer be distinguished from each other, thus limiting the transmittable bit rate. The expression of propagation time dispersion shows that this is proportional to fibre length. Consequently, the bit rate limit with a given fibre against its length will be known as the bandwidth and is expressed in Hz-Km. Chromatic dispersion results in limiting of the fibre transmission capability, due to variation in propagation time as a function of the wavelength. So, limitation due to this phenomenon is obviated by using a narrower spectrum laser like DFB laser.

1.5 Review of Previous Works :

There is increasing interest in optical fibre transmission systems which operate at 10 Gbit/s to meet future demand for higher transmission capacity in exchange

networks. A key problem for high speed ($>5\text{Gbit/s}$) light wave systems at 1550 nm wave length is high chromatic dispersion of conventional single-mode fibres which are optimized for transmission at 1310 nm[20],[21]. A lot of works have been reported on optical FSK systems or on fibre chromatic dispersions or on optical phase noise etc.

The detection performance of a coherent light wave transmission link can be sharply degraded by laser phase noise. This problem has been the focus of many recent studies, a representative sampling of which is given by[22]-[28]. The modulation schemes considered in these papers treat are phase shift keying (PSK), amplitude shift keying (ASK) and frequency shift keying (FSK). A study performed with on-off keying (OOK), which is equivalent to binary ASK and binary FSK, wherein the frequency shift keying is large and a dual filter detection was used[29]. A conceptional design was done on optical frequency division multiplexing distribution systems with optical tunable filters, investigating periodic filters for frequency division multiplexers and frequency selection switches (FS-SW) and the optical source as well as single-mode fibre polarization mode dispersion[30]. A 100 channel optical FDM transmission/ distribution experiment at 622 Mbit/s is demonstrated for a fibre length of 50 km, verifying the feasibility of a polarization insensitive wave guide frequency selection switch for 10 Ghz intervals and an FSK/ direct detection scheme employing a Mach-Zender filter[31]. Experimental results for coherent digital subcarrier multiplexed (SCM)

light wave system with a total of 20 frequency shift keyed (FSK) channels at 100 Mbit/s each were demonstrated[32]. Performance of coherent optical CPFSK-DD (differential detection) with intersymbol interference, noise correlation and phase noise was studied[33]. Study of soliton propagation at 10 Gbit/s in standard fibre systems at 1550 nm showed that using 36 km amplifier spacing and 30 ps solitons up to 200 km propagation is possible. In order to extend this distance and increase the range of usable pulse widths, the use of dispersion compensating fibre, as part of each amplifier, was established[1].

An experimental study for comparison of performance of 10 Gbit/s ASK, FSK and DPSK light wave systems which operate near 1550 nm with directly modulated DFB laser transmitters and conventional 1310 nm dispersion optimized fibre was reported[20]. A study showing that narrow spectral width is desired to minimize the intersymbol interference due to fibre chromatic dispersion was reported[34]. Chromatic dispersion limitations for FSK and DPSK system using narrow line width lasers and direct detection receivers are found to depend strongly on the receiver configuration. In the previous studies the system penalty was determined from eye-patterns[21]. A simplified dispersion limit formula for IM/DD systems and its comparison with experimental results were done[35]. Effects of fibre chromatic dispersion on optical FSK and DPSK transmission system using eye closure pattern was done[36]. But so far no theoretical analysis was reported on direct detection optical FSK considering the fibre chromatic dispersion.

1.6 Objective of The Study :

A novel theoretical analysis of direct detection optical FSK system in the presence of fibre chromatic dispersion is to be developed taking into consideration the effect of laser phase noise and receiver noise. The moments and the probability density function of the random phase fluctuation due to the combined effect of group velocity dispersion and phase noise are to be determined. The single mode fibre will be modeled as a band pass filter with flat amplitude response and linear group-delay over the optical bandwidth of the modulated optical signal[21]. Using the noise statistics the signal to noise ratio and the bit error rate performance of the receiver are to be computed for different dispersion factor and laser line width at a bit rate of 10 Gbit/s. The penalty suffered by the system due to dispersion and phase noise will then be determined at a bit error rate 10^{-9} .

1.7 Brief Introduction to This Thesis :

Chapter -1 presents a brief introduction to communication system with special emphasis on optical communication and a review of the research works currently going on in the related field.

Chapter -2 presents performance analysis of optical FSK with Mach-Zender Interferometer. It includes the MZI based receiver model, theoretical analysis of optical direct detection FSK receiver, receiver output signal and BER expression.

Chapter -3 presents the results and discussions and comments on further works in this topic.

Chapter -4 presents conclusions and suggestions for future works.

CHAPTER - 2

PERFORMANCE ANALYSIS OF OPTICAL FSK WITH MACH-ZENDER INTERFEROMETER

2.1 Introduction :

Direct Detection optical FSK systems are very promising for future multi-channel optical networks due to the direct frequency modulation capability of semiconductor lasers and low cost in comparison to coherent receivers. There is an increasing interest in optical fibre transmission systems which operate at 10 Gbit/s to meet future demand for higher transmission capacity in the exchange networks. A key problem for 10 Gb/s light wave transmission is the high chromatic dispersion for conventional single-mode fibres which are optimized for transmission at 1310 nm. When distributed feedback lasers are frequency modulated for direct detection systems, they are normally driven with currents that swing from near threshold to well above threshold producing significant wavelength chirp as well as intensity modulation. The resulting broad optical spectral width causes severe system degradation when fibre dispersion is present. Nearly all of the presently deployed fibres are optimized for 1310 nm operation and have a high dispersion of about 15 ps/nm.km in the low-loss window near 1550 nm. Although several experimental demonstrations and computer simulation are reported[20],[21], no theoretical

analysis taking into account the effect of fibre chromatic dispersion on optical FSK systems is available.

In this chapter, we provide the theoretical analysis of direct detection optical FSK receiver with Mach-Zender interferometer (MZI) as an optical frequency discriminator (OFD) considering the effects of laser phase noise and receiver noise. This chapter begins with an introduction of the receiver model which is followed by a brief description of the OFD, the Mach-Zender interferometer. Then single-mode fibre is modeled as a band-pass filter with flat amplitude response and linear group delay over the optical band width of the modulated optical signal[21]. The statistics of the phase fluctuations due to chromatic dispersion in the presence of laser phase noise are determined analytically and the expression for the bit error probability of the FSK receiver is developed.

2.2 The Receiver Model :

2.2.1 Mach-Zender Interferometer (MZI):

The block diagram of the FSK direct detection receiver with MZI considered for analysis is shown in fig. 2.1. The MZI acts as an optical filter and differentially detects the 'mark' and 'space' of received FSK signal which are then directly fed to a pair of photodetectors. The difference of the two photo currents are applied to the amplifier which is followed by an equalizer. The equalizer is required to

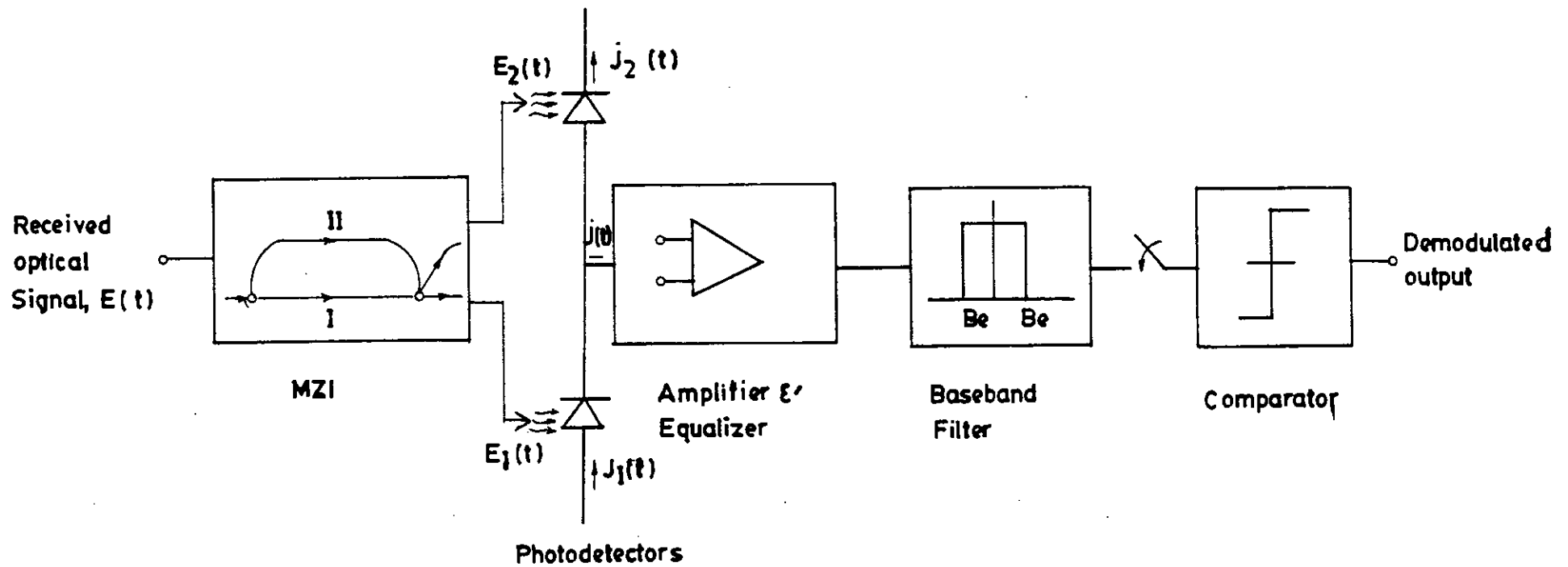


Fig. 2.1 Block diagram of an FSK direct detection receiver.

equalize the pulse shape distortion caused by the photo detector capacitance and due to the input resistance and capacitance of amplifier. After passing through the base band filter, the signal is detected at the decision circuit by comparing it with a threshold of zero value.

MZI has two input ports, two output ports, two 3 dB couplers and two wave guide arms with length difference ΔL . A thin film heater is placed in one of the arms to act as a phase shifter, because light path length of heated wave guide arm changes due to the change of refractive index. The phase shifter is used for precise frequency tuning. Frequency spacing of the peak to bottom transmittance of the OFD is set equal to the peak frequency deviation $2\Delta f$ of the FSK signal. Consequently the 'mark' and the 'space' appear at the two output ports of the OFD. These outputs are differentially detected by the photo detectors with balanced configuration.

2.2.2 MZI Characteristics :

If $E(t)$ represents the signal input to the MZI, then the signals received at the output ports can be expressed as[21],[37]

$$|E_2(t)| = |E(t)| \sin \left[\frac{k(l_2 - l_1)}{2} \right] \quad (2.1)$$

and

$$|E_1(t)| = |E(t)| \cos \left[\frac{k(l_2 - l_1)}{2} \right] \quad (2.2)$$

where l_1 and l_2 are the length of two arms of MZI and k is the wave number which can be expressed as

$$k = \frac{w}{v} = \frac{2\pi}{\lambda} = \frac{2\pi f n_{\text{eff}}}{c} \quad (2.3)$$

n_{eff} , f and c are the effective refractive index of the wave guide, frequency of optical input signal and velocity of light in vacuum, respectively.

The transmittance of arm II of MZI

$$T_{II}(f) = \frac{|E_2(t)|^2}{|E(t)|^2} = \sin^2 \left[\frac{k(l_2 - l_1)}{2} \right] = \sin^2 \theta \quad (2.4)$$

and that of arm I of MZI is

$$T_I(f) = \frac{|E_1(t)|^2}{|E(t)|^2} = \cos^2 \left[\frac{k(l_2 - l_1)}{2} \right] = \cos^2 \theta \quad (2.5)$$

where, θ is the phase factor related to the arm path difference $\Delta L = l_2 - l_1$ and can be expressed as

$$\theta = \frac{k\Delta L}{2} = \frac{\pi f n_{\text{eff}} \Delta L}{c} \quad (2.6)$$

Normally ΔL is chosen as

$$\Delta L = \frac{c}{4n_{\text{eff}} \Delta f} \quad (2.7)$$

Therefore,

$$\theta = \frac{\pi f}{4\Delta f} \quad (2.8)$$

Then we get

$$T_{II}(f) = \sin^2\left(\frac{\pi f}{4\Delta f}\right) \quad (2.9)$$

and

$$T_I(f) = \cos^2\left(\frac{\pi f}{4\Delta f}\right) \quad (2.10)$$

The outputs of the MZI are therefore anti-symmetric and are shown in fig. 2.2

For an MZI used as an OFD, Δf is so chosen that [21],[37], $\Delta f = \frac{f_c}{2n+1}$, f_c is the

carrier frequency of the FSK signal and n is an integer. The 'mark' and 'space' of FSK signals are represented by f_1 and f_2 respectively where $f_1 = f_c + \Delta f$ and $f_2 = f_c - \Delta f$.

Therefore, when 'mark' (f_1) is transmitted

$$T_I = 1 \text{ and } T_{II} = 0$$

Similarly, for transmission of 'space'

$$T_I = 0 \text{ and } T_{II} = 1$$

Thus, two different signals f_1 and f_2 can be extracted from two output ports of MZI.

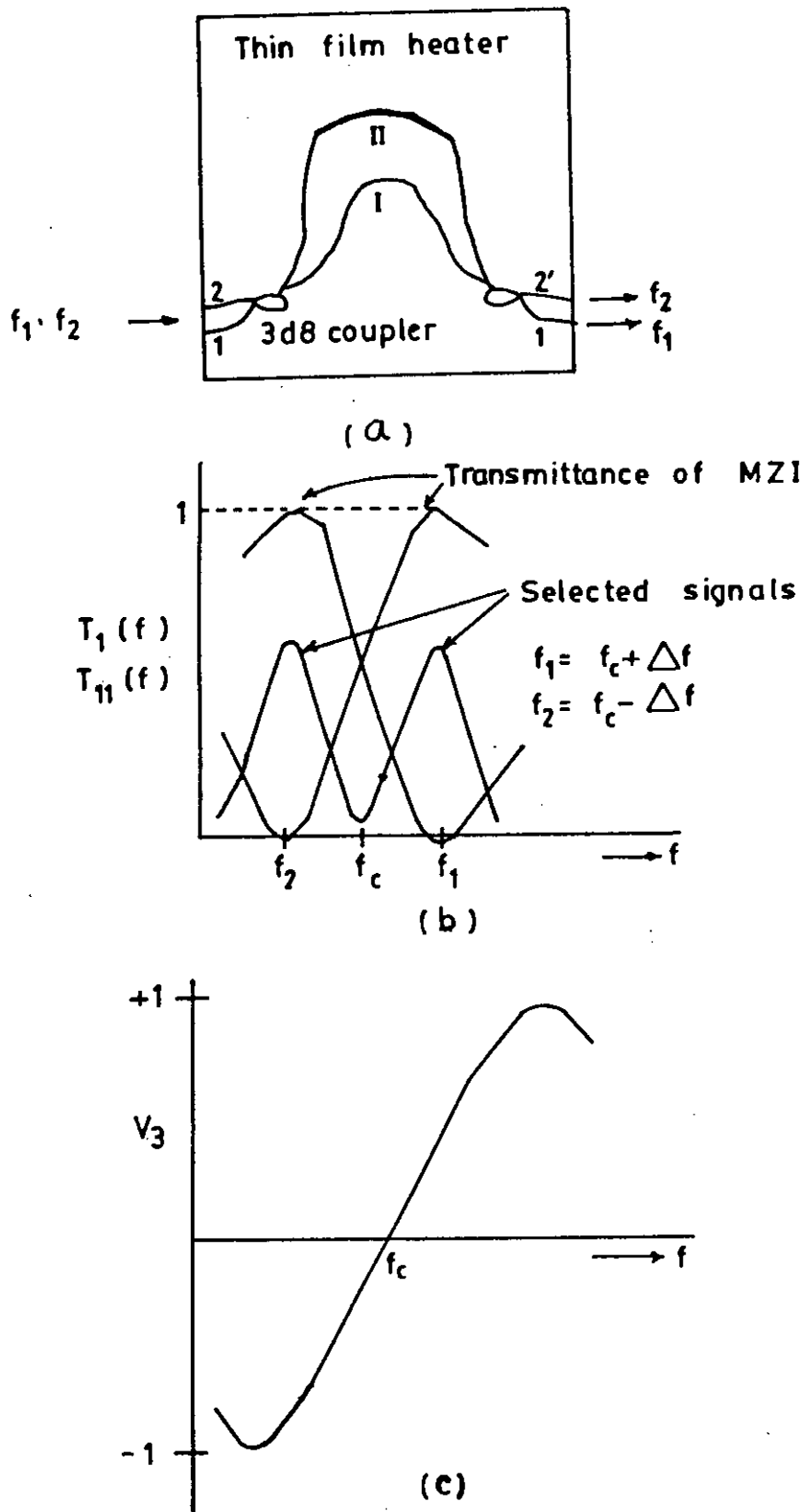


Fig. 2.2 (a) An MZI with large ΔL or narrow wavelength spacing. (b) Transmittance characteristics of MZI and (c) Differential output of the balanced receiver.

The MZI is used in our analysis only as an OFD as our analysis is based on single channel operation. The complete potential of an MZI can be extracted when a multiplexer/ demultiplexer or a frequency selection switch for a multi channel WDM/ FDM system is fabricated utilizing the periodicity of the transmittance versus frequency characteristic of an MZI[21],[37].

2.3 Theoretical Analysis of Optical Direct Detection FSK :

2.3.1 The Optical Signal :

The optical FSK signal input to the fibre is given by

$$\chi_i(t) = \sqrt{2P_s} \exp[j\{2\pi f_c t + \phi(t)\}] \quad (2.11)$$

where $\phi(t) = \phi_s(t) + \phi_n(t)$ and f_c is the optical carrier frequency, P_s is the optical signal power, $\phi_s(t)$ is the angle modulation and $\phi_n(t)$ is the phase noise of the transmitting laser.

The single-mode fibre transfer function due to chromatic dispersion[38] is

$$H(f) = e^{-j\alpha f^2} \quad (2.12)$$

where $\alpha = \pi D(\lambda)L \frac{\lambda^2}{c}$; $D(\lambda)$ is the fibre chromatic dispersion, λ is the optical wavelength, c is the speed of light and L is the length of fibre.

The optical signal at the output of fibre can be obtained as

$$\begin{aligned}
 x_0(t) &= \int_0^{\infty} h(\tau) x_i(t-\tau) d\tau \\
 &= \left[\int_0^{\infty} h(\tau) e^{-j2\pi f_c \tau} e^{j\phi(t-\tau)} d\tau \right] e^{j2\pi f_c t} \times \sqrt{2P_s}
 \end{aligned} \tag{2.13}$$

Output phase is the given by,

$$\begin{aligned}
 &\text{Im} \left\{ \log \int_0^{\infty} h(\tau) e^{-j2\pi f_c \tau} e^{j\phi(t-\tau)} d\tau \right\} \\
 &= \text{Im} \left\{ \log \int_0^{\infty} h(\tau) e^{j\phi(t-\tau)} d\tau \right\} + \text{Im} \log e^{-j2\pi f_c \tau} \\
 &= \theta(t) + \beta_0
 \end{aligned} \tag{2.14}$$

where[38] considering small values of $\phi(t) < 1$ radian

$$\begin{aligned}
 \theta(t) &= \text{Re} \left\{ \int_0^{\infty} h(\tau) \phi(t-\tau) d\tau \right\} + \sum_{n=2}^{\infty} \frac{1}{n!} I_n(i^n f_n) \\
 &= \theta_s(t) + \theta_n(t)
 \end{aligned} \tag{2.15}$$

and the coefficients f_n upto $n=7$ are given by [38]

$$f_2 = F_2$$

$$f_3 = F_3$$

$$f_4 = F_4 - 3F_2^2$$

$$f_5 = F_5 - 10F_3F_2$$

$$f_6 = F_6 - 15F_4F_2 - 10F_3^2 + 30F_2^3$$

$$f_7 = F_7 - 21F_5F_2 - 35F_4F_2 + 210 F_3F_2^2$$

$$\text{with } F_n = \int_0^{\infty} h(\tau) [\phi(t-\tau) - \phi(t)]^n d\tau$$

Here, $\theta_s(t)$ represents the linear filtering terms and $\theta_n(t)$ represents the non-linear filtering terms consisting of the cross-term and the inter-modulation term.

The output of fibre can be written as (from equation 2.13)

$$\begin{aligned} x_o(t) &= \sqrt{2P_s} \cdot e^{j\theta(t) + j2\pi f_c t} \\ &= \sqrt{2P_s} \cdot e^{j2\pi f_c t + j\theta_s(t) + j\theta_n(t)} \end{aligned} \quad (2.16)$$

If $W_\phi(f)$ denotes the power spectral density of $\phi(t)$, then psd of the linear signal component of output phase is

$$W_\theta^L = W_\phi(f) \cdot |H(f)|^2 = W_{\theta_s}(f) \quad (2.17)$$

The psd of non-linear signal component is

$$W_{\theta_n}(f) = W_\theta^C(f) + W_\theta^I(f) \quad (2.18)$$

where $W_\theta^C(f)$ and $W_\theta^I(f)$ represent the psd of the cross-power components and inter-modulation components and are given by [see Appendix A]

$$W_\theta^C(f) = 2W_\phi(f) \int_{-\infty}^{\infty} W_\phi(\rho) [\text{Cos}\{2\alpha(f^2 + f\rho + \rho^2)\} - 1] d\rho \quad (2.19)$$

$$W_\theta^I(f) = \frac{1}{6} \int_{-\infty}^{\infty} d\rho \int_{-\infty}^{\infty} d\sigma W_\phi(\rho) W_\phi(\sigma) W_\phi(f - \rho - \sigma) |S(f)|^2 \quad (2.20)$$

where

$$|S(f)|^2 = |S_1(f)|^2 + |S_2(f)|^2$$

$$S_1(f) = 2\text{Cos}(\alpha a) - \text{Cos}(\alpha b) - \text{Cos}(\alpha c) - \text{Cos}(\alpha d) + \text{Cos}(\alpha e)$$

$$S_2(f) = 2\text{Sin}(\alpha a) + \text{Sin}(\alpha b) + \text{Sin}(\alpha c) + \text{Sin}(\alpha d) - \text{Sin}(\alpha e)$$

with

$$a = 2\rho^2 + 2\sigma^2 + f^2 - 2f\rho + 2\rho\sigma - 2f\sigma$$

$$b = f^2 + 2\rho^2 + 2\sigma^2 - 2f\rho + 4\rho\sigma - 2f\sigma$$

$$c = f^2 + 2\rho^2 - 2f\rho$$

$$d = f^2 + 2\sigma^2 - 2f\sigma$$

$$e = f^2$$

The final form of $|S(f)|^2$ is formed to be

$$\begin{aligned} |S(f)|^2 = & 8 - 4\text{Cos}\alpha(a+b) - 4\text{Cos}\alpha(a+c) - 4\text{Cos}\alpha(a+d) + 4\text{Cos}\alpha(a-e) + 2\text{Cos}\alpha(b-d) \\ & - 2\text{Cos}\alpha(b+e) + 2\text{Cos}\alpha(b-c) + 2\text{Cos}\alpha(c-d) - 2\text{Cos}\alpha(c+e) - 2\text{Cos}\alpha(d+e) \end{aligned}$$

Since $|H(f)|^2 = 1.0$ i.e. the chromatic dispersion transfer function has flat amplitude,

$$\text{therefore, } W_{\theta_s}(f) = W_{\theta}(f) \tag{2.21}$$

We can rewrite $\theta_s(t)$ as

$$\begin{aligned}
 \theta_s(t) &= \text{Re} \left[\int_0^{\infty} h(\tau) \phi(t-\tau) d\tau \right] \\
 &= \text{Re} \left[\int_0^{\infty} h(\tau) \{ \phi_s(t-\tau) + \phi_n(t-\tau) \} d\tau \right] \\
 &= \text{Re} \left[\int_0^{\infty} h(\tau) \phi_s(t-\tau) d\tau \right] + \text{Re} \left[\int_0^{\infty} h(\tau) \phi_n(t-\tau) d\tau \right] \\
 &= \theta'_s(t) + \theta'_{PN}(t)
 \end{aligned} \tag{2.22}$$

The fibre output can now be rewritten as

$$\begin{aligned}
 x_0(t) &= \sqrt{2P_s} \cdot e^{j2\pi f_c t + j\theta_s(t) + j\theta_n(t)} \\
 &= \sqrt{2P_s} \cdot e^{j2\pi f_c t + j\theta'_s(t) + j\theta'_{PN}(t) + j\theta_n(t)} \\
 &= \sqrt{2P_s} \cdot e^{j2\pi f_c t + j\theta'_s(t) + j\theta_t(t)} \quad [\theta_t(t) = \theta'_{PN}(t) + \theta_n(t)]
 \end{aligned} \tag{2.23}$$

The chromatic-dispersion thus produces an additional phase-noise $\theta_n(t)$ at the output of the fibre without affecting the signal amplitude.

Variance of $\theta_t(t)$ is

$$\sigma^2 = \sigma_{\theta_n}^2 + \sigma_{\theta'_{PN}}^2 \tag{2.24}$$

where $\sigma_{\theta_n}^2 = \int_{-\infty}^{\infty} [W_{\theta_n}(f)] df$

$$\sigma_{\theta'_{PN}}^2 = |H(f)|^2 \sigma_{\phi_n}^2 = |H(f)|^2 \cdot 2\pi \Delta\gamma\tau \tag{2.25}$$

2.3.2 Receiver Output Signal :

For a 'mark' transmission; the current at the photo detector output is

$$i_m(t) = R_d P_s \text{Cos}[2\pi f_c \tau + \Delta\theta'_s(t) + \Delta\theta_t(t)] \quad (2.26)$$

where,

$$\Delta\theta'_s(t) = \theta'_s(t) - \theta'_s(t - \tau)$$

$$\begin{aligned} \Delta\theta_t(t) &= \theta_t(t) - \theta_t(t - \tau) \\ &= \Delta\theta'_{PN}(t) + \Delta\theta_n(t) \end{aligned}$$

and

the psd of $\Delta\theta'_{PN}(t)$ and $\Delta\theta_n(t)$ are given by

$$W_{\Delta\theta'_{PN}}(f) = W_{\phi_n}(f) |H(f)|^2 \quad (2.27)$$

$$W_{\Delta\theta_n}(f) = W_{\Delta\theta}^c(f) + W_{\Delta\theta}^l(f) = W_{\theta}^c(f) + W_{\theta}^l(f) \quad (2.28)$$

The psd of that phase noise $\Delta\theta_t(t)$ is

$$W_{\Delta\theta_t}(f) = W_{\Delta\theta'_{PN}}(f) \otimes W_{\Delta\theta_n}(f) \quad (2.29)$$

Since,

$$\phi_s(t) = 2\pi \Delta f \int_0^t I(t) dt$$

and $I(t) = \sum a_k p(t - kT)$; $a_k = \pm 1$ for NRZ data and $p(t)$ is the elementary pulse

shape.

Therefore,

$\theta'_s(t)$ can be expressed as

$$\begin{aligned}
 \theta'_s(t) &= h(t) \otimes \phi_s(t) \\
 &= 2\pi\Delta f \int_0^t I(t) \otimes h(t) dt \\
 &= 2\pi\Delta f \int_0^t \sum_k a_k p(t - kT) \otimes h(t) dt \\
 &= 2\pi\Delta f \int_0^t \sum_k a_k g(t - kT) dt
 \end{aligned} \tag{2.30}$$

where, $g(t) = p(t) \otimes h(t)$

Thus chromatic dispersion produces distortion of the optical pulse shape.

Therefore, $\Delta\theta'_s(t) = \theta'_s(t) - \theta'_s(t - \tau)$

$$= 2\pi\Delta f \int_{t-\tau}^t \sum_k a_k g(t - kT) dt \tag{2.31}$$

Thus, output of the balanced photodetector is

$$\begin{aligned}
 i(t) &= R_d P_s \text{Cos} \left[2\pi f_c \tau + 2\pi\Delta f \int_{t-\tau}^t \sum_k a_k g(t - kT) dt + \Delta\theta_s(t) \right] \\
 &= R_d P_s \text{Cos} \left[2\pi f_c \tau + 2\pi\Delta f \int_{t-\tau}^t a_0 g(t) dt + 2\pi\Delta f \int_{t-\tau}^t \sum_{k \neq 0} a_k g(t - kT) dt + \Delta\theta_s(t) \right]
 \end{aligned} \tag{2.32}$$

For a 'mark' transmission ($a_0 = +1$), the current at any sampling instant can be

$$\begin{aligned}
 \text{expressed as } i_m(t) &= R_d P_s \text{Cos} \left[2\pi f_c \tau + \frac{\pi}{2} - \frac{\pi}{2} + 2\pi\Delta f \tau \cdot q(t) + 2\pi\Delta f \tau \sum_{k \neq 0} a_k q(t - kT) + \Delta\theta_s(t) \right] \\
 &= R_d P_s \text{Cos} \left[2\pi f_c \tau + \frac{\pi}{2} - \frac{\pi}{2} + \frac{\pi}{2} \cdot q(t) + \frac{\pi}{2} \sum_{k \neq 0} a_k q(t - kT) + \Delta\theta_s(t) \right]
 \end{aligned} \tag{2.33}$$

where, $\tau = T/2m$ and $m = 2\Delta fT$ and $q(t)$ is defined as

$$q(t) = \frac{1}{\tau} \int_{t-\tau}^t g(t) dt \quad (2.34)$$

Denoting the phase noise due to chromatic dispersion by $\Delta\theta_{cd}(t)$ as

$$\begin{aligned} \Delta\theta_{cd}(t) &= -\pi/2 + \pi/2 q(t) + \pi/2 \sum_{k \neq 0} \alpha_k q(t - kT) \\ &= \bar{\theta}_{cd} + \pi/2 \sum_{k \neq 0} \alpha_k q(t - kT) \end{aligned} \quad (2.35)$$

where $\bar{\theta}_{cd} = -\pi/2 + \pi/2 q(t)$

The output current $i_m(t)$ can be expressed as

$$i_m(t) = R_d P_s \text{Cos} \left[2\pi f_c \tau + \pi/2 + \Delta\theta_{cd}(t) + \Delta\theta_i(t) \right] \quad (2.36)$$

2.3.3 Bit Error Rate Expression :

Under ideal CPFSK demodulation condition

$$\omega_c \tau = (2n+1)\pi/2 \text{ and } n \text{ is an integer}$$

and $2\pi f \tau = \pi/2$ for NRZ data, then

$$i_m(t) = R_d P_s [x(t)] \quad (2.37)$$

where $x(t) = \text{Cos}[\Delta\theta(t)]$

$$\begin{aligned}\Delta\theta(t) &= \Delta\theta_{cd}(t) + \Delta\theta_t(t) \\ &= \bar{\theta}_{cd} + \Delta\theta'(t)\end{aligned}$$

$$\Delta\theta'(t) = \pi/2 \sum a_k q(t - kT) + \Delta\theta_t(t)$$

Assuming $\Delta\theta_t$ as Gaussian with zero mean variance σ^2 , the psd of $\Delta\theta'_t$ is given by[39]

$$P_{\Delta\theta'}(\Delta\theta') = P_{\Delta\theta_t}(\Delta\theta_t) \left[1 + \sum \frac{M_{2r}}{2r!} \left(\frac{1}{\sigma^2}\right)^r H_{2r}\left(\frac{\Delta\theta_t}{\sigma}\right) \right] \quad (2.38)$$

where $M_{2i} = Y_{2r}(k)$ and $Y_{2r} = \sum_{j=0}^r \binom{2r}{2j} Y_{2j} (i-1) h_i^{2r-2j}$ and k is the actual number of interfering terms in the summation eqn. 2.35.

The psd of the balanced photo detector output is

$$S_{pd}(f) = eR_d P_s + 0.5R_d P_s^2 [S_x - \bar{X}^2 \delta(f)] \quad (2.39)$$

where $x(t) = \text{Cos}[\Delta\theta(t)]$

and $S_x(f) = W_{\Delta\theta_{cd}}(f) \otimes W_{\Delta\theta_t}(f)$

$$= W_{\Delta\theta_{cd}}(f) \otimes W_{\Delta\theta_n}(f) \otimes W_{\Delta\theta_n}(f) \quad (2.40)$$

Total noise power at the LPF output is

$$\sigma^2 = \sigma_m^2 = \sigma_s^2 = \int_{-\infty}^{\infty} [S_{pd}(f) + S_{th}(f)] |H_{LPF}(f)|^2 df \quad (2.41)$$

$$BER = \frac{1}{2} \int_{-\infty}^{\infty} \text{erfc} \left[\frac{2R_d P_s \text{Cos}\Delta\theta}{\sqrt{2\sigma^2}} \right] P(\Delta\theta) d(\Delta\theta) \quad (2.42)$$

$P(\Delta\theta)$ is the psd of $\Delta\theta$ which can be obtained from $P(\Delta\theta')$ with mean value θ_{cd} .

CHAPTER - 3

RESULTS AND DISCUSSIONS

Following the theoretical analysis presented in chapter 2, the performance results for direct detection optical FSK system are evaluated at a bit rate of 10 Gb/s with different sets of receiver and system parameters. The parameters of the single-mode fibre used for numerical computations are: chromatic dispersion coefficient $D_C = 0, 1, 3, 9, 15$ for wavelength $\lambda=1550$ nm. Dispersion factor γ is calculated as

$$\gamma = R_b^2 \cdot D(\lambda) \cdot L \cdot \frac{\lambda^2}{\pi c} = \alpha \frac{R_b^2}{\pi^2} \text{ where } R_b = \text{bit rate and } L = \text{fibre length.}$$

The bit error rate (BER) performance of direct detection FSK system is depicted in fig.3.1 in presence of laser phase noise and receiver noise without considering the effect of fiber chromatic dispersion. The BER is plotted as a function of the received optical power P_s (dBm) and the receiver sensitivity is defined as the optical power required to achieve a BER of 10^{-9} . In this figure, results are given for several values of the normalized laser linewidth ($\Delta\nu T$) when the modulation index $m (=2\Delta f T)=0.8$ and chromatic dispersion coefficient $D_C=0.0$. The figure reveals that the BER decreases with increase in the input power and when the value of $\Delta\nu T=0.0$ the receiver sensitivity is found to be -19.6 dBm. At increased value of laser linewidth, the required amount of signal power is higher to achieve the same

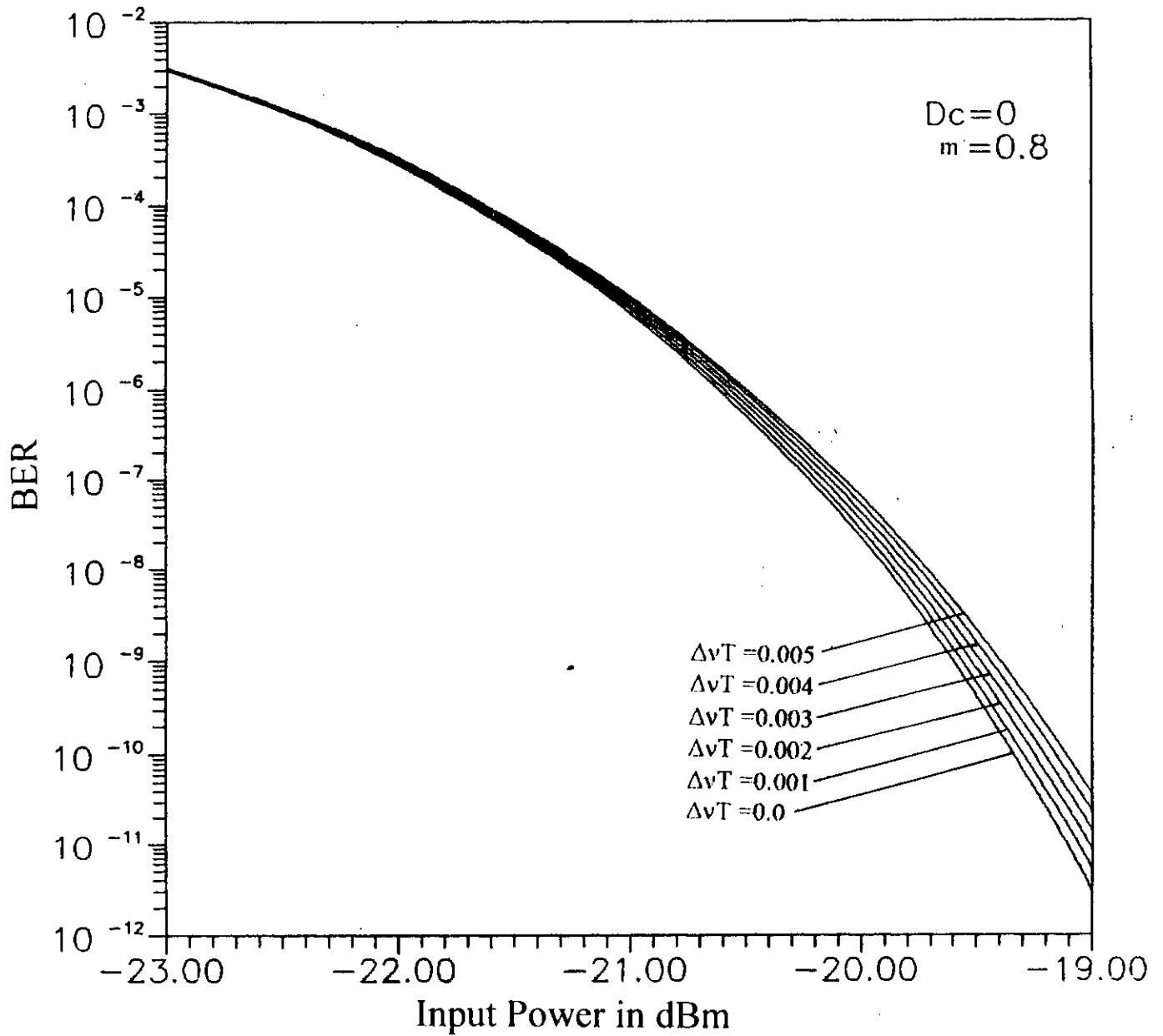


Fig. 3.1 The bit error rate (BER) performance of direct detection optical FSK transmission system at a bit rate of 10 Gb/s without fibre chromatic dispersion ($D_c=0.0$) and modulation index $m=0.8$ for several values of normalized laser linewidth $\Delta\nu T$.

BER. The additional signal power compared to the case of $\Delta\nu T=0.0$ may be termed as the power penalty at $\text{BER}=10^{-9}$ due to the effect of laser phase noise caused by non-zero linewidth. Phase noise causes the spectrum of the FSK signal to be broadened and for a given receiver bandwidth, the signal power is less at the output of the receiver bandpass filter. As a result more signal power is required to achieve the same BER. The effect of phase noise is more at higher values of linewidth.

When the modulation index is increased to $m=1.0$, the BER performance results are plotted in fig. 3.2 for $D_C=0.0$ with $\Delta\nu T$ as a parameter. Compared to fig. 3.1 it becomes evident that the power penalty suffered by the system due to non-zero linewidth is slightly decreased when m is increased from 0.8 to 1.0. This is due to the fact that as m increases the difference between the 'mark' and 'space' frequencies in the FSK signal spectrum increases. As a consequence intersymbol interference caused by laser phase noise is less at increased values of modulation index m . The power penalty due to laser phase noise is further decreased as m is increased to 1.2 as is evident from fig. 3.3.

In the presence of fibre chromatic dispersion, the BER performance of FSK direct detection transmission system is shown in fig. 3.4 for fibre length $L=150$ Km, chromatic dispersion coefficient $D_C=1.0$, dispersion factor $\gamma=0.038$ and modulation index $m=0.8$ with and without laser phase noise. Comparing this figure with fig. 3.1

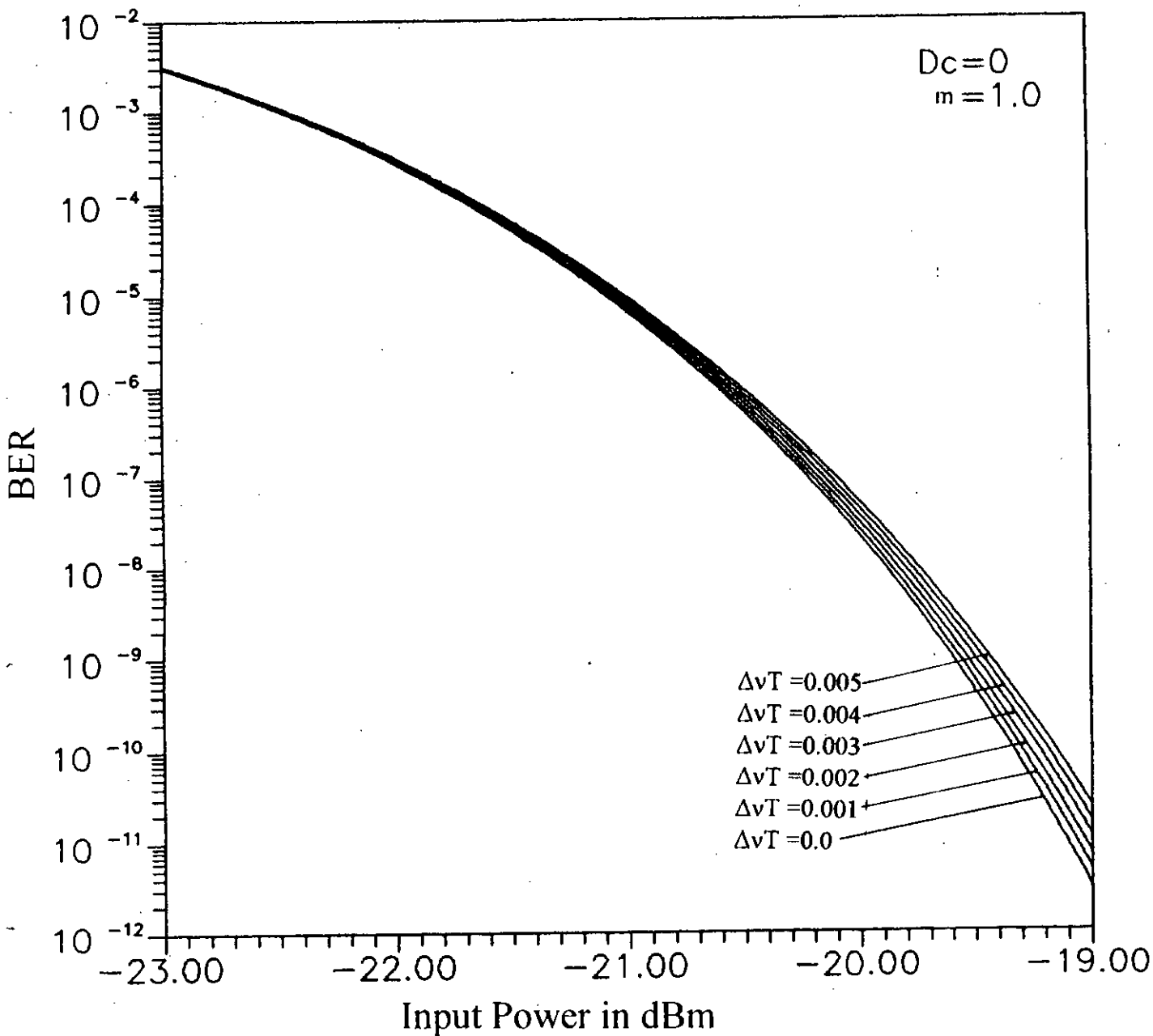


Fig. 3.2 The bit error rate (BER) performance of direct detection optical FSK transmission system at a bit rate of 10 Gb/s without fibre chromatic dispersion ($D_c=0.0$) and modulation index $m=1.0$ for several values of normalized laser linewidth $\Delta\nu T$.

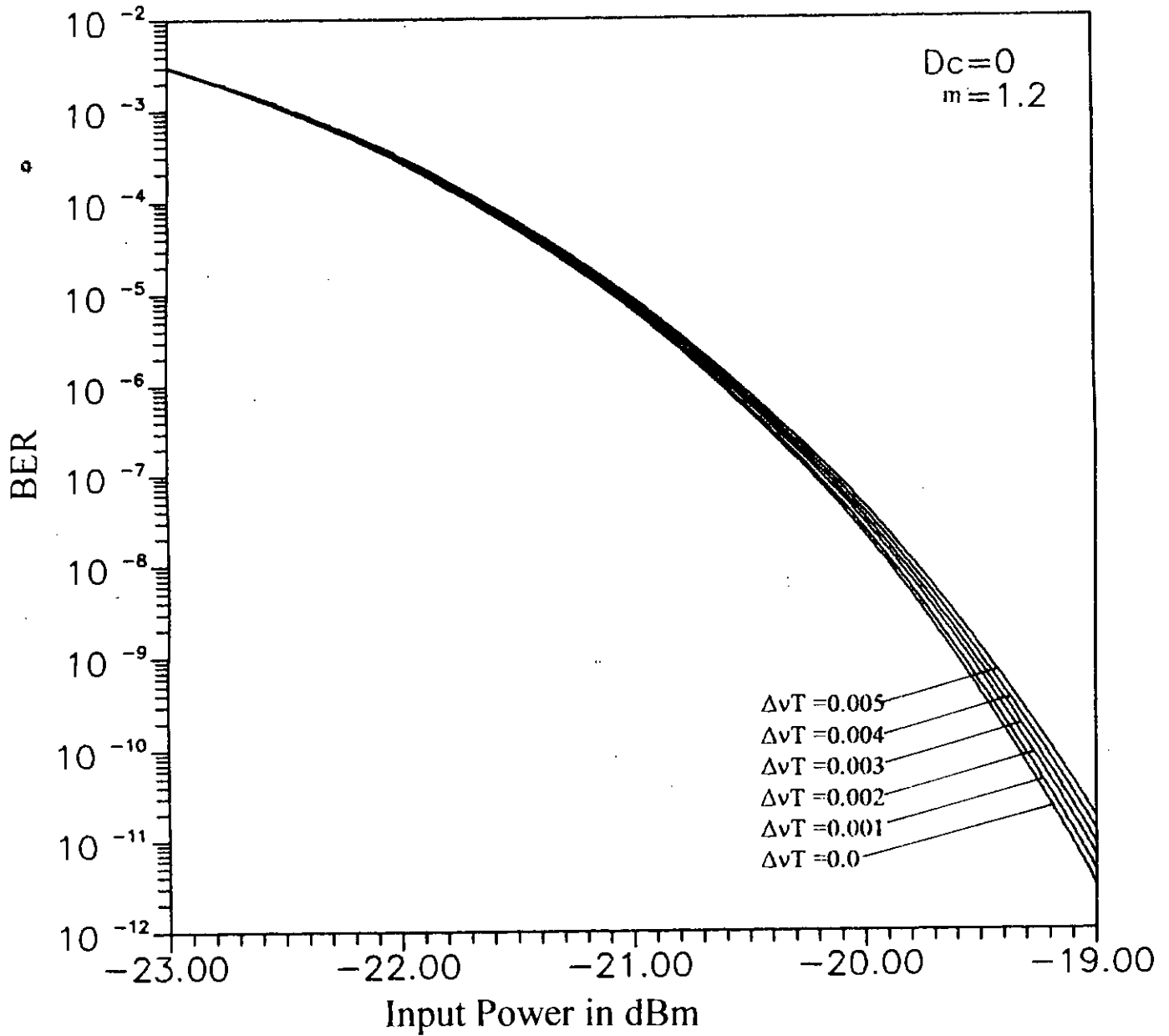


Fig. 3.3 The bit error rate (BER) performance of direct detection optical FSK transmission system at a bit rate of 10 Gb/s without fibre chromatic dispersion ($D_c=0.0$) and modulation index $m=1.2$ for several values of normalized laser linewidth $\Delta\nu T$.

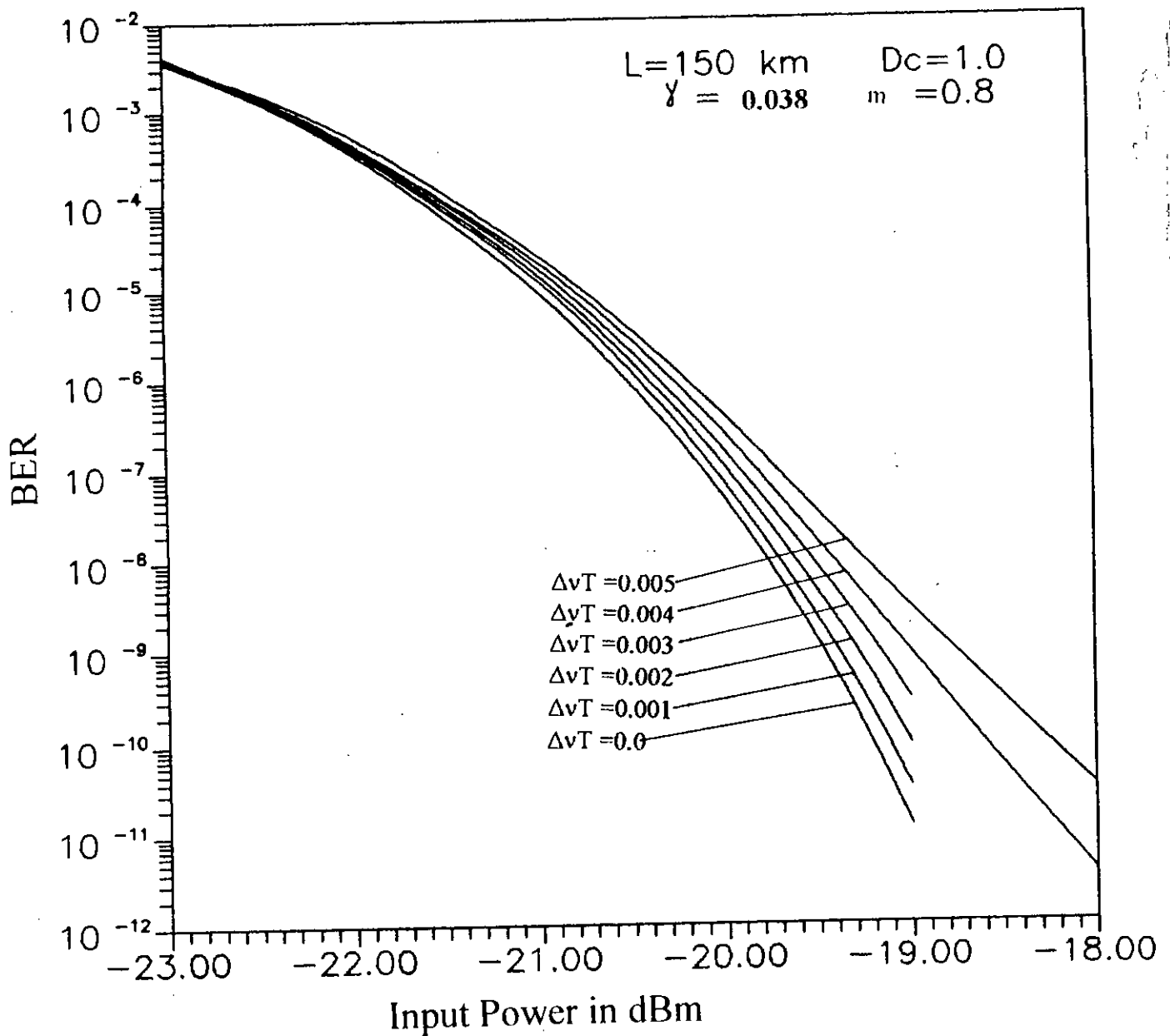


Fig. 3.4 The bit error rate (BER) performance of direct detection optical FSK transmission system at a bit rate of 10 Gb/s with fibre chromatic dispersion $D_c=1.0$ ps/ Km.nm, fibre length $L=150$ Km, at an wavelength of 1550 nm and modulation index $m=0.8$ for several values of normalized laser linewidth $\Delta\nu T$.

we notice that the performance of the system is degraded due to the effect of fibre chromatic dispersion. At a given input power the BER is higher in the presence of dispersion compared to the case when there is no dispersion. The receiver sensitivity thus degrades and there is additional power penalty due to the effect of dispersion. For example, the receiver sensitivity to achieve $BER=10^{-9}$ is -19.6 dBm when there is no dispersion ($D_C=0.0$) whereas in the presence of dispersion with $D_C=1.0$, the receiver sensitivity is found to be -19.47 dBm when $m=0.8$ and $\Delta\nu T=0.0$. The sensitivity degradation is more pronounced in the presence of both dispersion and laser phase noise. For $\Delta\nu T=0.005$, the receiver sensitivity is -19.38 dBm when $D_C=0.0$ (from fig.3.1) and it is found to be -18.78 dBm when $D_C=1.0$ (from fig. 3.4).

It is also noticed that the penalty due to combined effect of laser phase noise and chromatic dispersion is higher at higher values of normalized linewidth $\Delta\nu T$.

When the dispersion coefficient D_C is increased to 3.0 with fibre length $L=100$ Km, the results are shown in fig. 3.5 for dispersion factor $\gamma=0.076$ and $m=0.8$. Compared to fig. 3.4 where $\gamma=0.038$, it is evident that increased dispersion factor causes the system performance to be more degraded by around 0.15 dB at $BER=10^{-9}$ when $\Delta\nu T=0.005$.

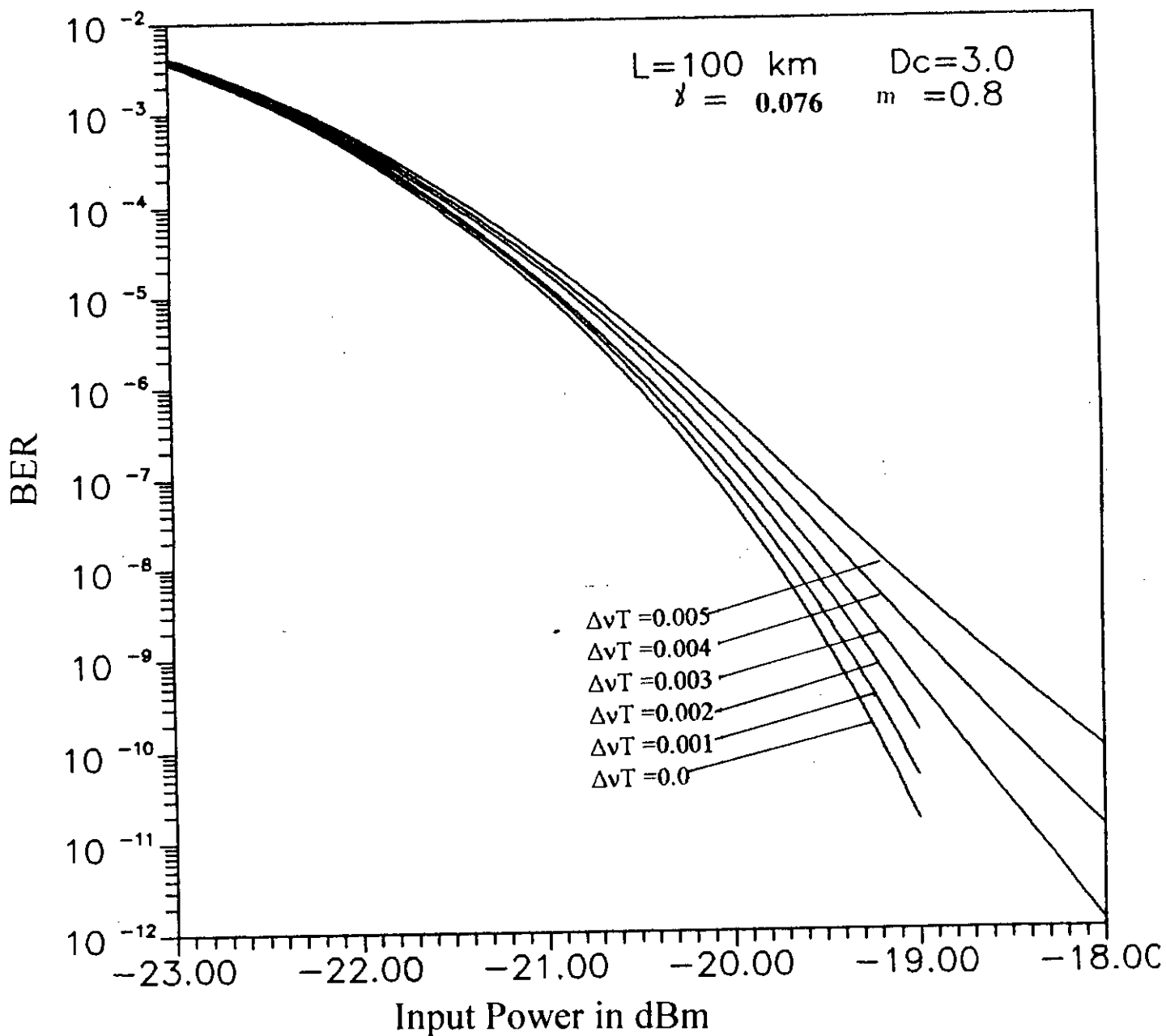


Fig. 3.5 The bit error rate (BER) performance of direct detection optical FSK transmission system at a bit rate of 10 Gb/s with fibre chromatic dispersion $D_c=3.0$ ps/ Km.nm, fibre length $L=100$ Km, at an wavelength of 1550 nm and modulation index $m=0.8$ for several values of normalized laser linewidth $\Delta\nu T$.

For the same value of modulation index and at higher value of dispersion factor $\gamma=0.19$, with $D_C=15$ and $L=50$ Km, the BER is plotted in fig. 3.6. Similar conclusion are also revealed from this figure when compared to fig. 3.4 and fig. 3.5. Similar plots are also shown in fig. 3.7 when $\gamma=0.46$.

When the modulation index m is increased from 0.8 to 1.0, the receiver performance results are given in fig. 3.8 through fig. 3.11 for different sets of values of fibre span L and chromatic dispersion coefficient D_C and $\gamma=0.038, 0.076, 0.19$ and 0.46. The effects of increased modulation index on the system performance is noticed when these curves are compared to fig. 3.4 through fig. 3.7. It becomes clear that the BER increases with increase in the value of the modulation index m for a given value of input power. As a consequence the system suffers more penalty in signal power at increased modulation index. This may be due to the fact that the FSK spectrum becomes broadened at higher modulation index and the effect of dispersion is more prominent at increased bandwidth of the signal spectrum. When the intermodulation index is further increased to $m=1.2$ the performance results are shown in fig. 3.12 through fig. 3.15 for $\gamma=0.038, 0.076, 0.19, 0.46$ corresponding to different values of D_C and fibre span L (Km). Comparing these curves with fig. 3.8 through fig. 3.11 we see that there is much higher degradation in the receiver performance due to increased value of m and increased γ .

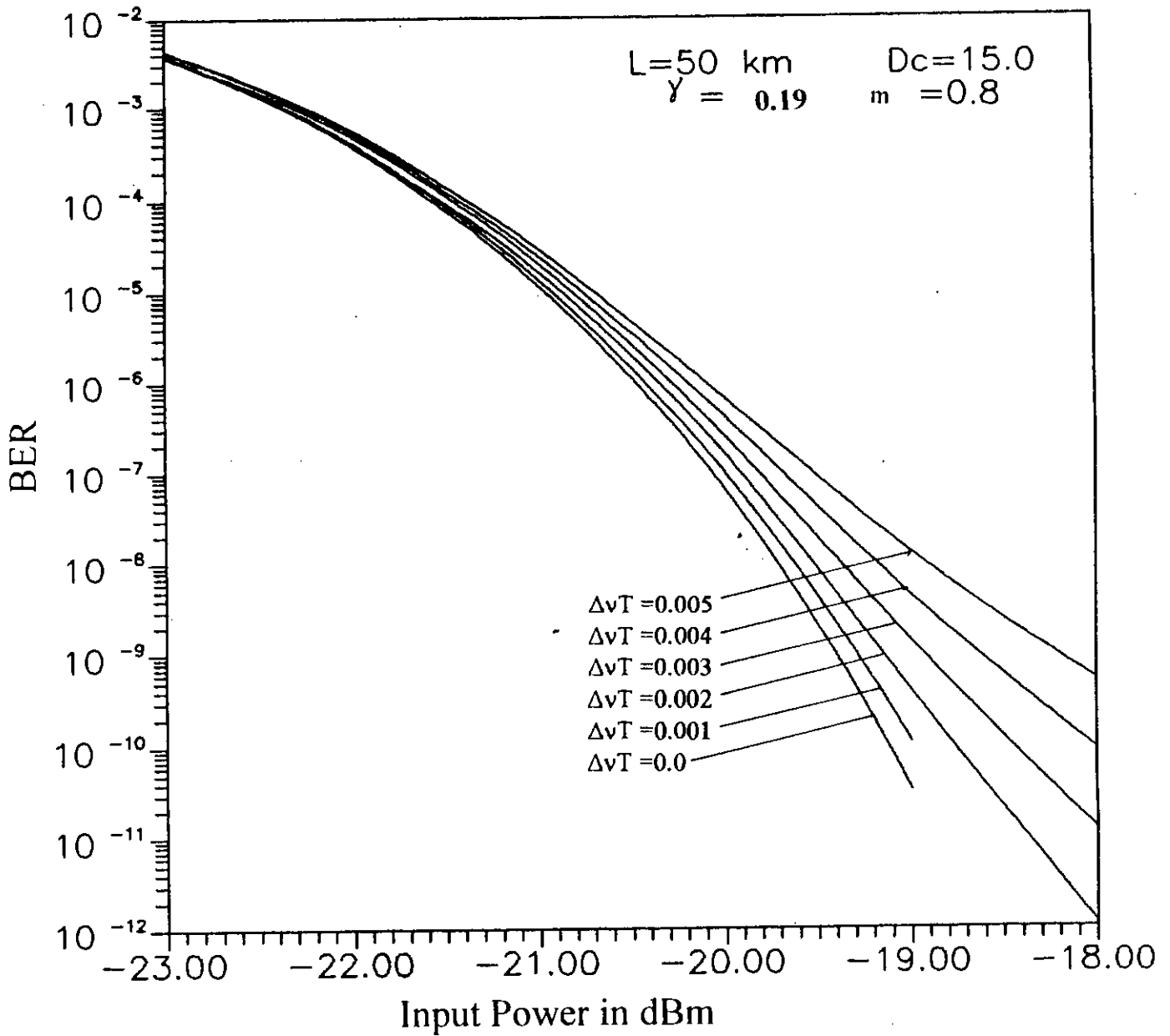


Fig. 3.6 The bit error rate (BER) performance of direct detection optical FSK transmission system at a bit rate of 10 Gb/s with fibre chromatic dispersion $D_c=15.0 \text{ ps/ Km.nm}$, fibre length $L=50 \text{ Km}$, at an wavelength of 1550 nm and modulation index $m=0.8$ for several values of normalized laser linewidth $\Delta\nu T$.

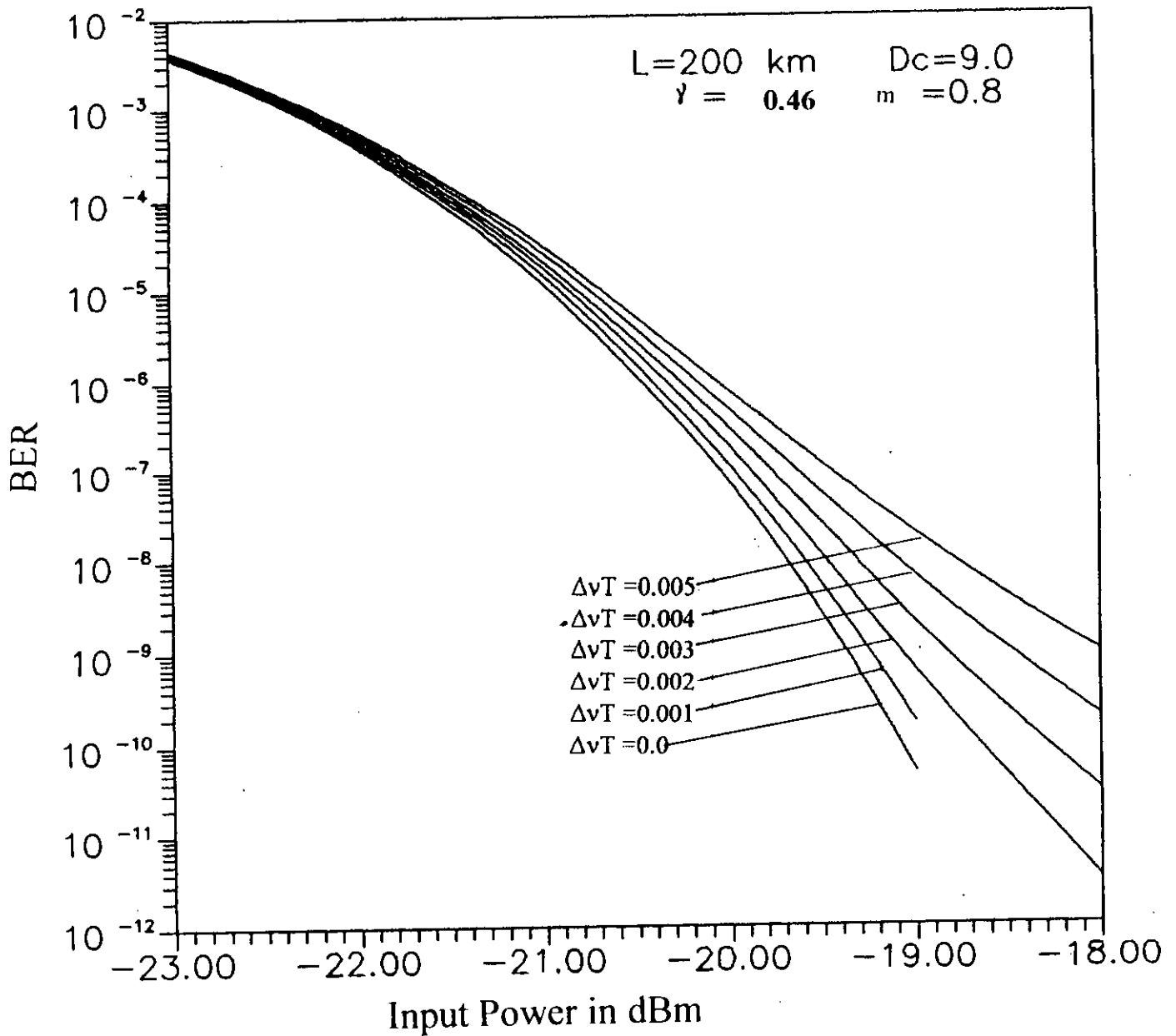


Fig. 3.7 The bit error rate (BER) performance of direct detection optical FSK transmission system at a bit rate of 10 Gb/s with fibre chromatic dispersion $D_c=9.0$ ps/ Km.nm, fibre length $L=200$ Km, at an wavelength of 1550 nm and modulation index $m=0.8$ for several values of normalized laser linewidth $\Delta\nu T$.

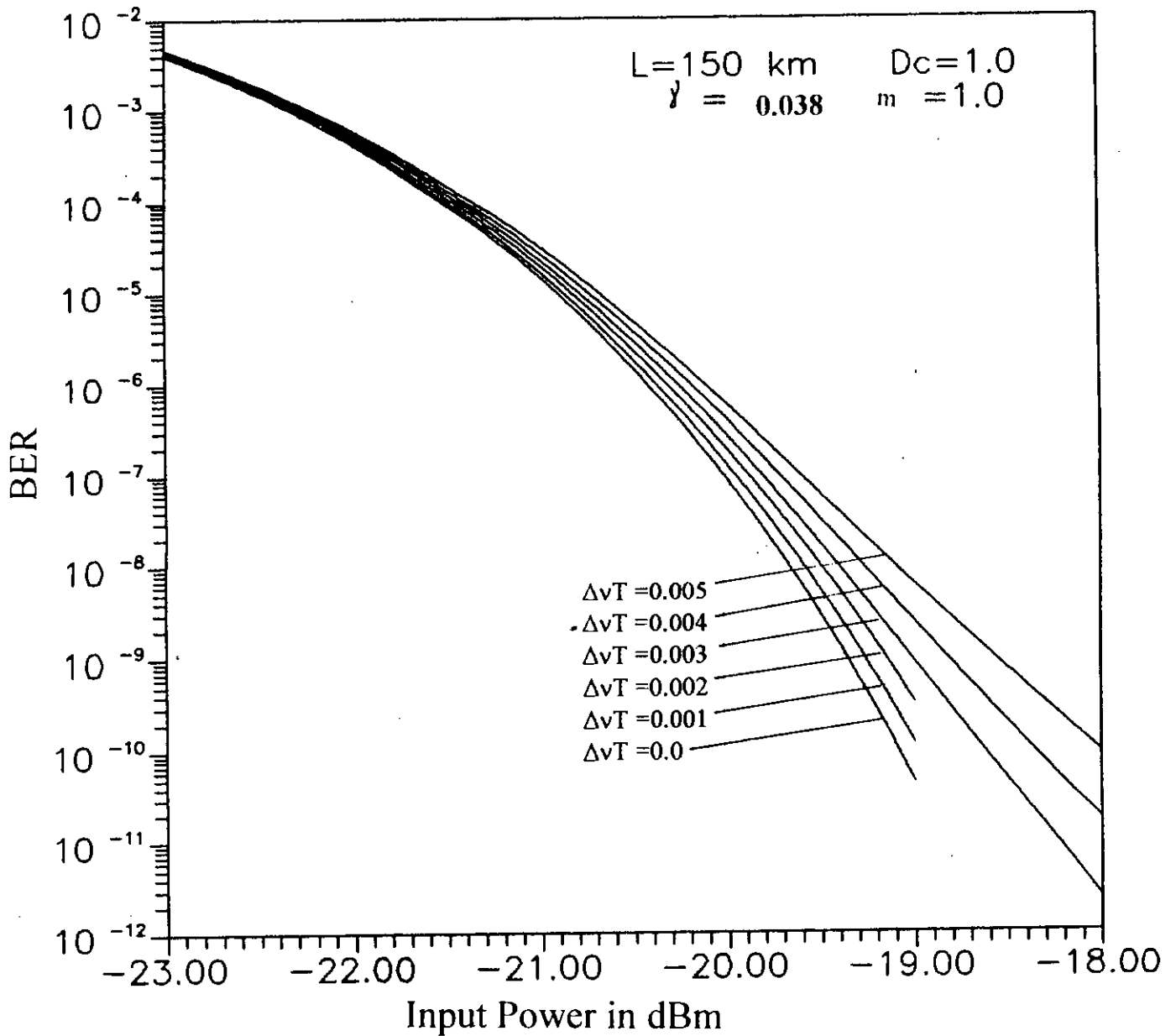


Fig. 3.8 The bit error rate (BER) performance of direct detection optical FSK transmission system at a bit rate of 10 Gb/s with fibre chromatic dispersion $D_c=1.0 \text{ ps/ Km.nm}$, fibre length $L=150 \text{ Km}$, at an wavelength of 1550 nm and modulation index $m=1.0$ for several values of normalized laser linewidth $\Delta\nu T$.

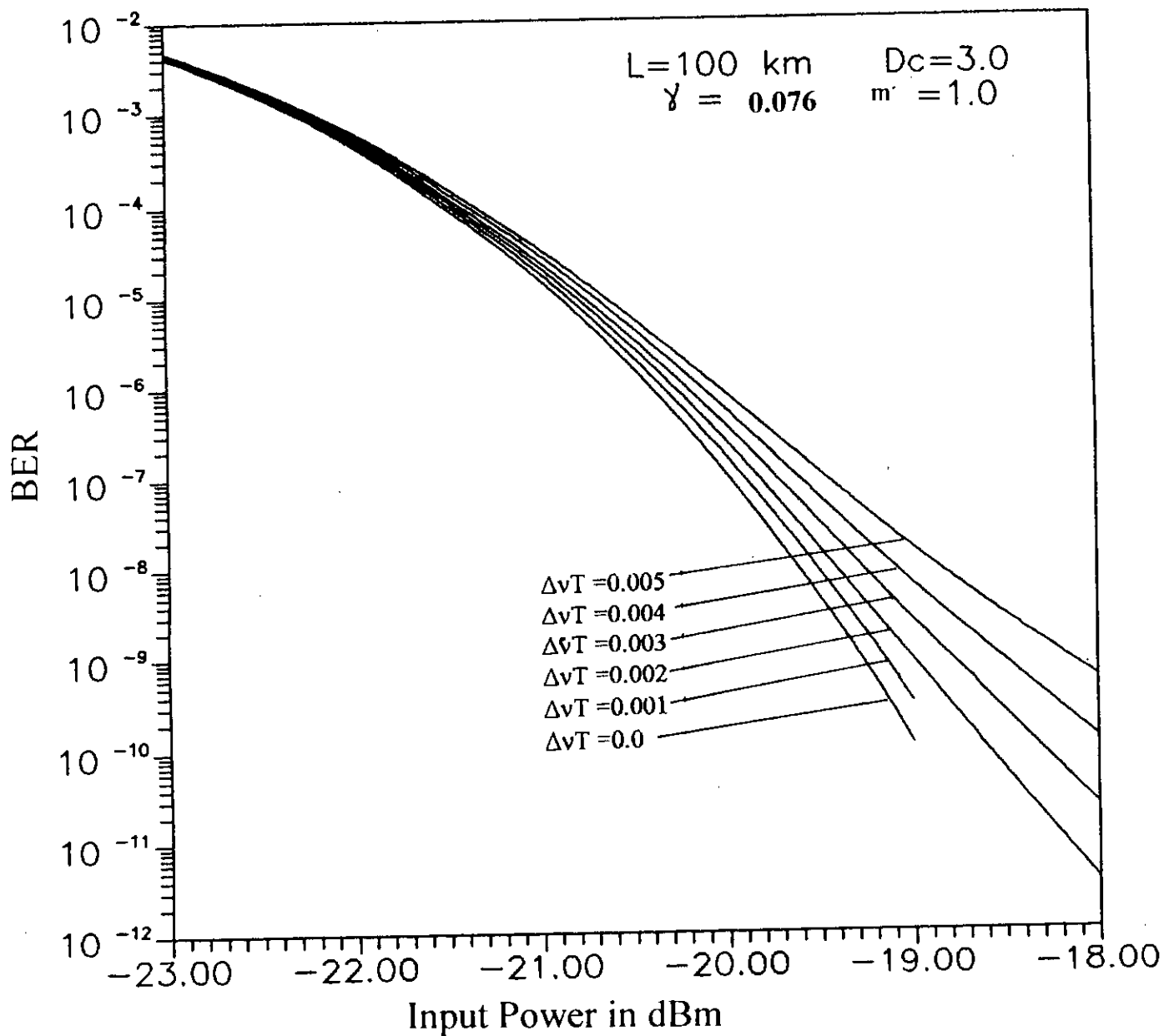


Fig. 3.9 The bit error rate (BER) performance of direct detection optical FSK transmission system at a bit rate of 10 Gb/s with fibre chromatic dispersion $D_c=3.0$ ps/ Km.nm, fibre length $L=100$ Km, at an wavelength of 1550 nm and modulation index $m=1.0$ for several values of normalized laser linewidth $\Delta\nu T$.

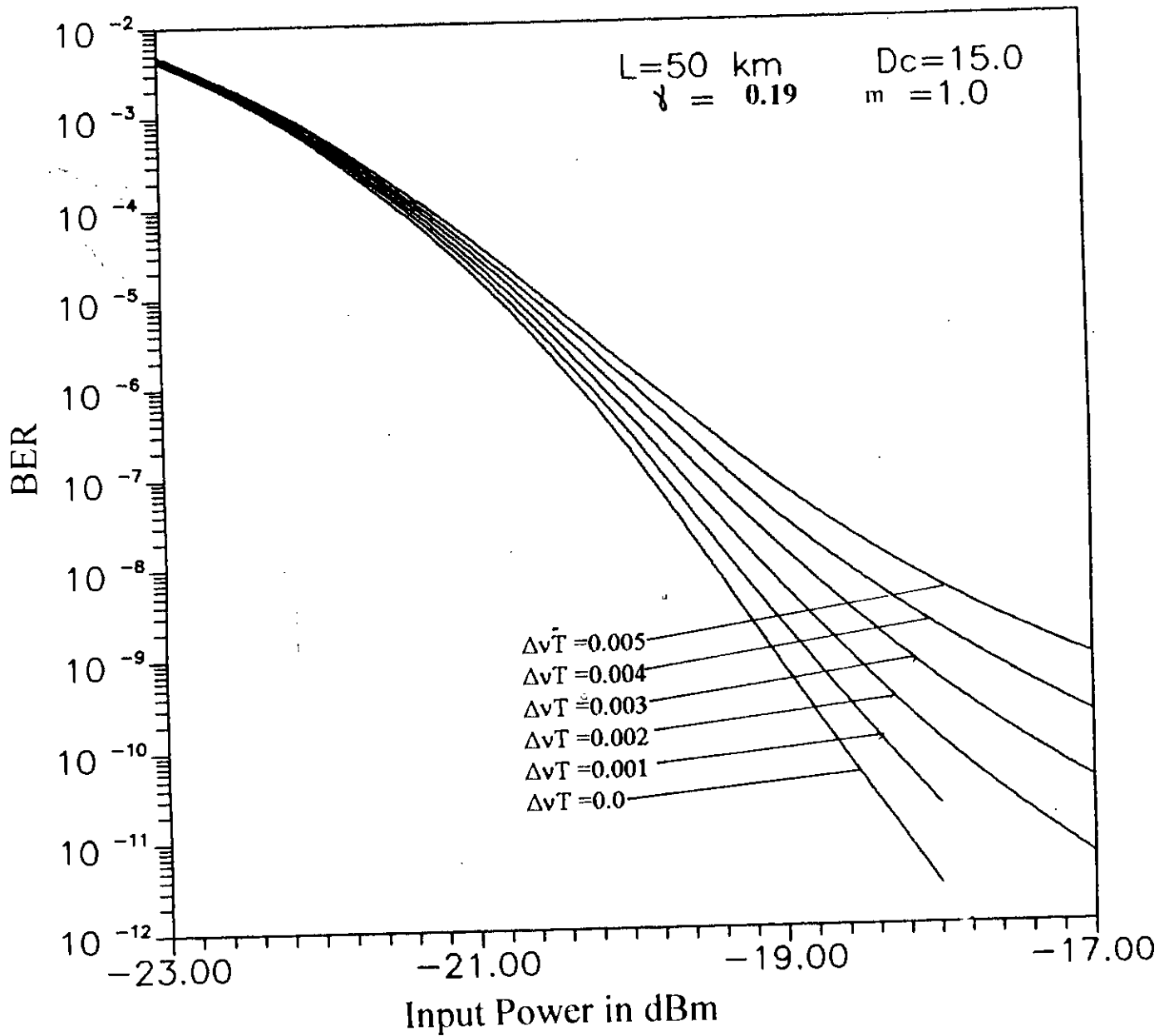


Fig. 3.10 The bit error rate (BER) performance of direct detection optical FSK transmission system at a bit rate of 10 Gb/s with fibre chromatic dispersion $D_c=15.0 \text{ ps/Km.nm}$, fibre length $L=50 \text{ Km}$, at an wavelength of 1550 nm and modulation index $m=1.0$ for several values of normalized laser linewidth $\Delta\nu T$.

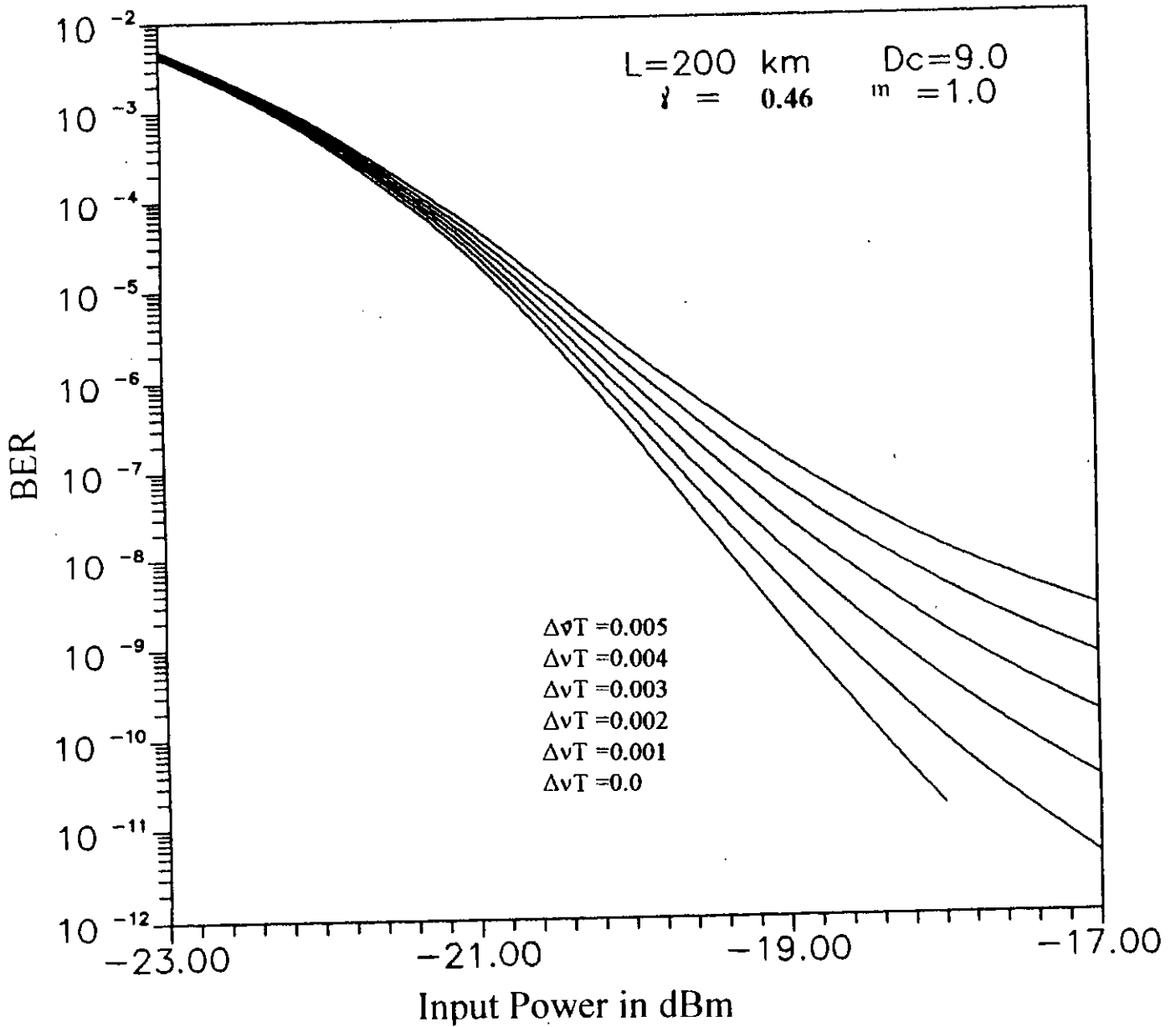


Fig. 3.11 The bit error rate (BER) performance of direct detection optical FSK transmission system at a bit rate of 10 Gb/s with fibre chromatic dispersion $D_c=9.0$ ps/ Km.nm, fibre length $L=200$ Km, at an wavelength of 1550 nm and modulation index $m=1.0$ for several values of normalized laser linewidth $\Delta\nu T$.

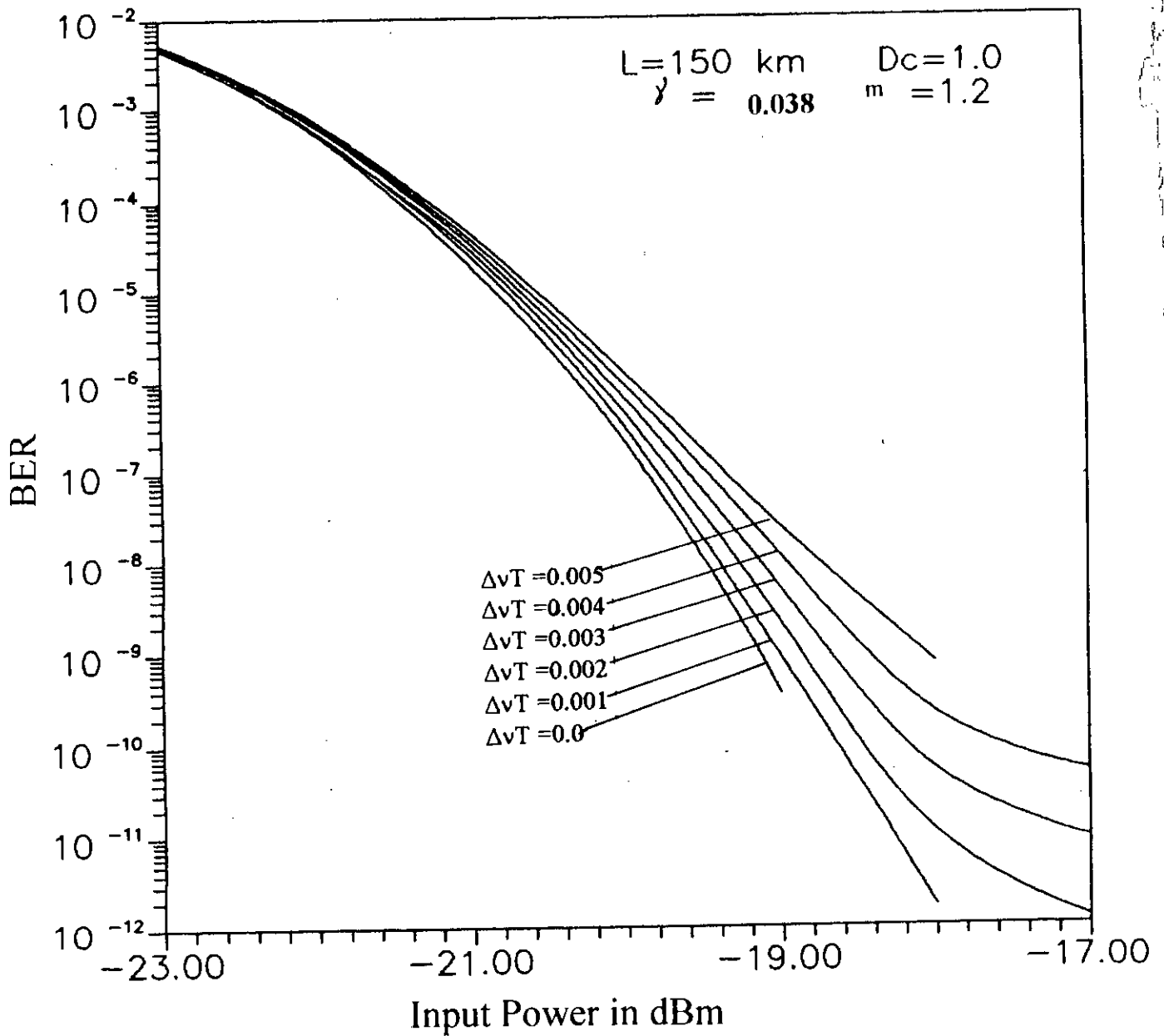


Fig. 3.12 The bit error rate (BER) performance of direct detection optical FSK transmission system at a bit rate of 10 Gb/s with fibre chromatic dispersion $D_c=1.0 \text{ ps/ Km.nm}$, fibre length $L=150 \text{ Km}$, at an wavelength of 1550 nm and modulation index $m=1.2$ for several values of normalized laser linewidth $\Delta\nu T$.

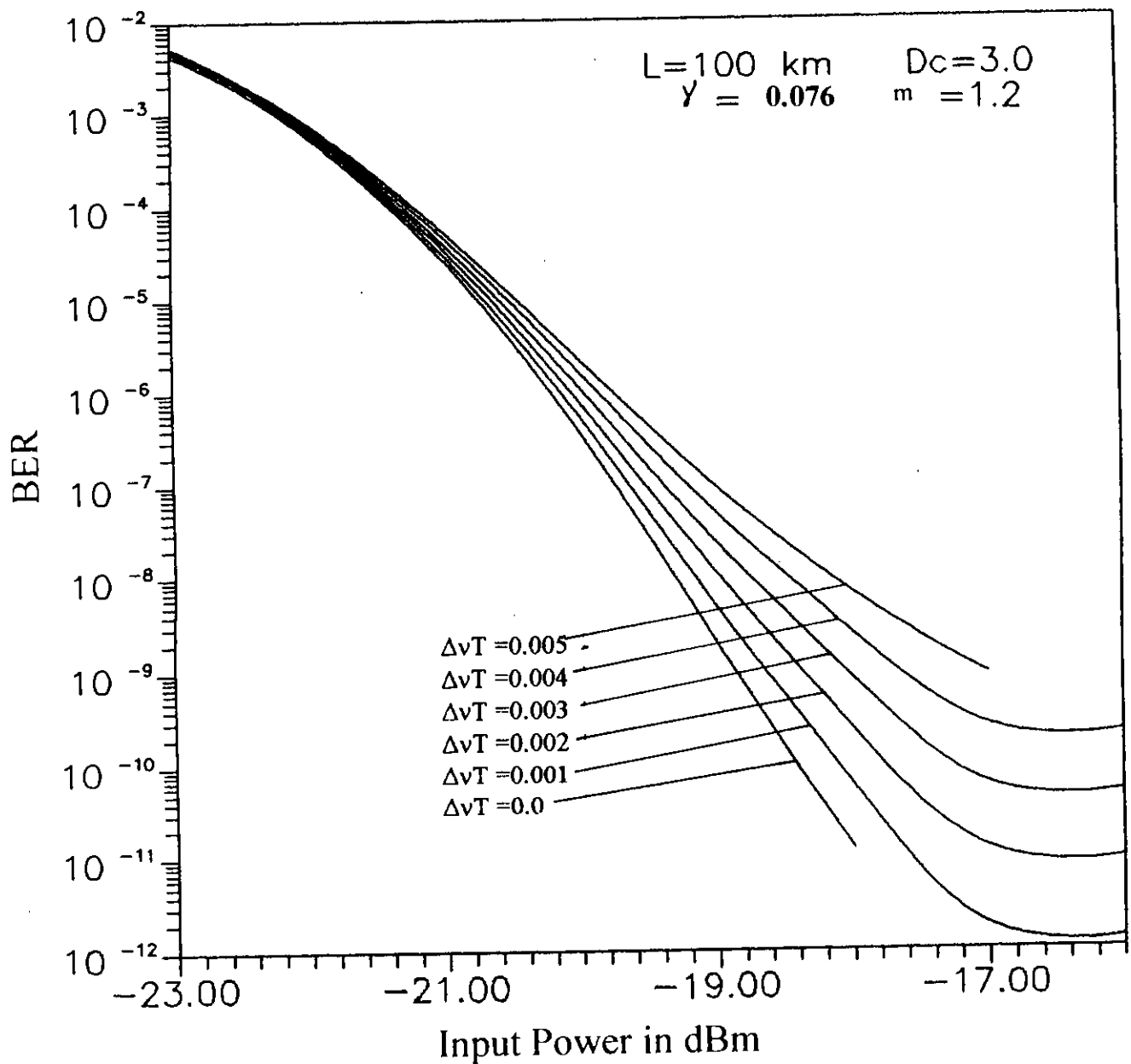


Fig. 3.13 The bit error rate (BER) performance of direct detection optical FSK transmission system at a bit rate of 10 Gb/s with fibre chromatic dispersion $D_c=3.0 \text{ ps/Km.nm}$, fibre length $L=100 \text{ Km}$, at an wavelength of 1550 nm and modulation index $m=1.2$ for several values of normalized laser linewidth $\Delta\nu T$.

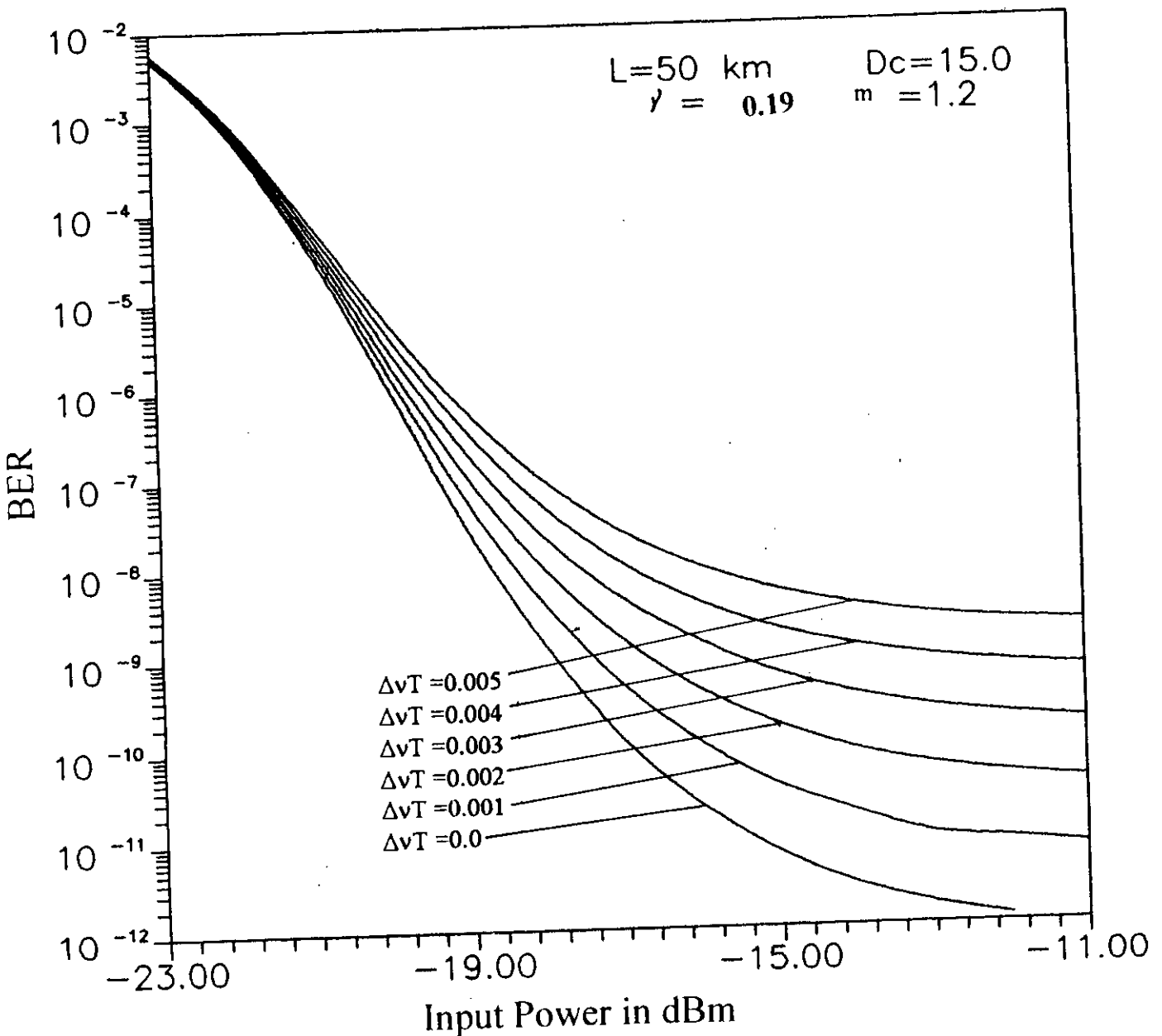


Fig. 3.14 The bit error rate (BER) performance of direct detection optical FSK transmission system at a bit rate of 10 Gb/s with fibre chromatic dispersion $D_c=15.0 \text{ ps/ Km.nm}$, fibre length $L=50 \text{ Km}$, at an wavelength of 1550 nm and modulation index $m=1.2$ for several values of normalized laser linewidth $\Delta\nu T$.

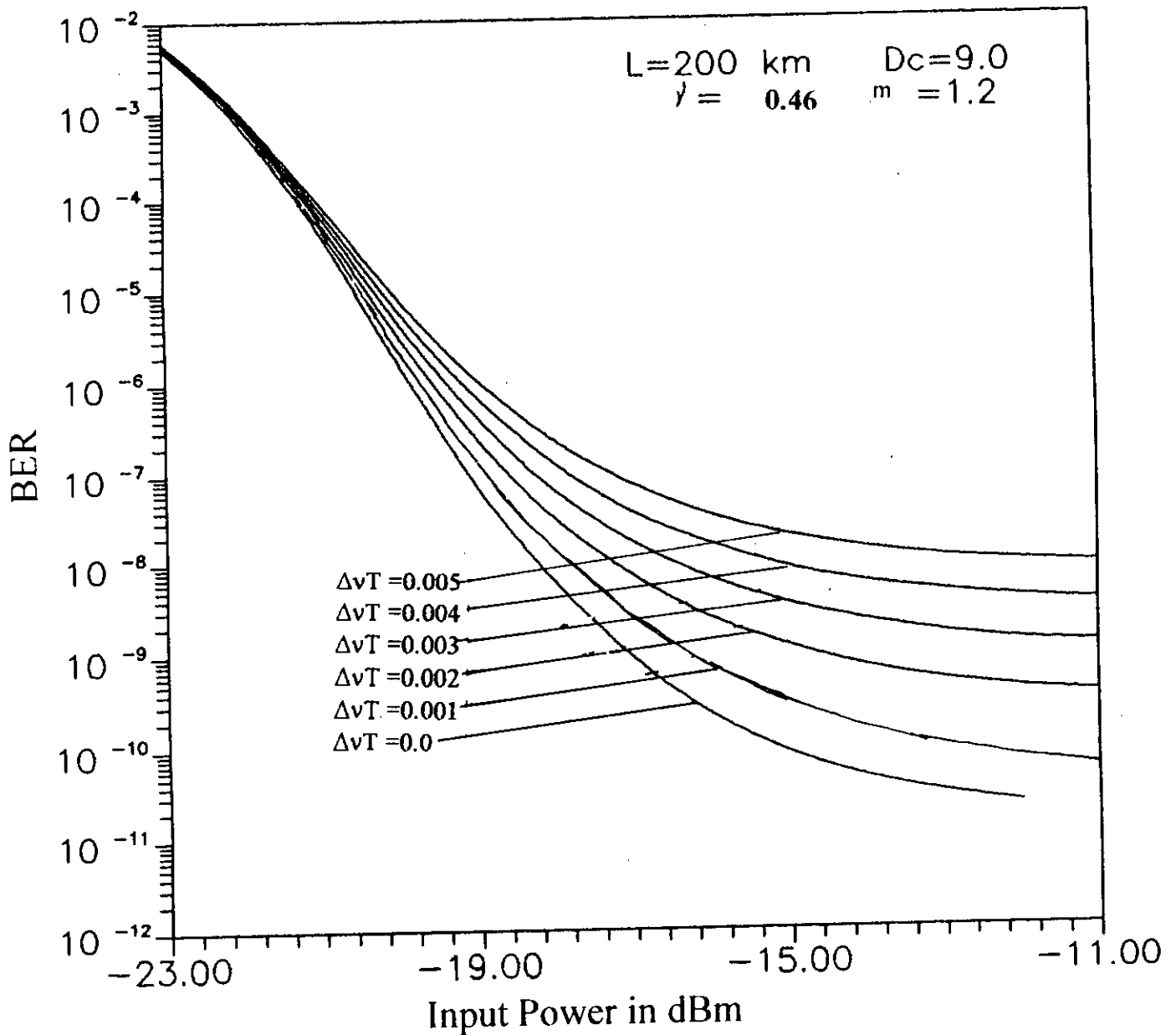


Fig. 3.15 The bit error rate (BER) performance of direct detection optical FSK transmission system at a bit rate of 10 Gb/s with fibre chromatic dispersion $D_c=9.0 \text{ ps/ Km.nm}$, fibre length $L=200 \text{ Km}$, at an wavelength of 1550 nm and modulation index $m=1.2$ for several values of normalized laser linewidth $\Delta\nu T$.

It is further noticed that at increased value of $\Delta\nu T$, there occurs bit error rate (BER) floor at increased signal power, i.e. the BER does not decrease with increase in signal power. As seen from fig. 3.13, the BER floor occurs around 10^{-12} corresponding to $\Delta\nu T=0.001$ and around 4×10^{-11} for $\Delta\nu T=0.003$. Also, the BER floor goes upward for the same value of $\Delta\nu T$ when γ is increased from 0.076 to 0.46 as is evident by comparing fig. 3.13, fig. 3.14 and fig. 3.15.

From fig. 3.14 it is further observed that BER floor occurs around 10^{-11} and 10^{-9} corresponding to $\Delta\nu T=0.001$ and 0.005 respectively when $m=1.2$ and $\gamma=0.19$. When γ is increased to 0.46 as shown in fig. 3.15 we see that the corresponding BER floor occurs around 5×10^{-10} and 10^{-8} respectively. Thus the system suffers BER floor at larger values of the chromatic dispersion coefficient D_C and/or larger fibre length.

The penalty in signal power suffered by the system due to the combined effect of laser phase noise and fibre chromatic dispersion are determined from bit error rate (BER) curves at $BER=10^{-9}$. The plots of power penalty versus chromatic dispersion coefficient D_C (ps/ Km.nm) are shown in fig. 3.16 and fig. 3.17 for modulation index $m=0.8$ and fibre span $L=150$ Km and 200 Km respectively. The figure depicts the variation of power penalty with D_C and it is revealed that for small values of the

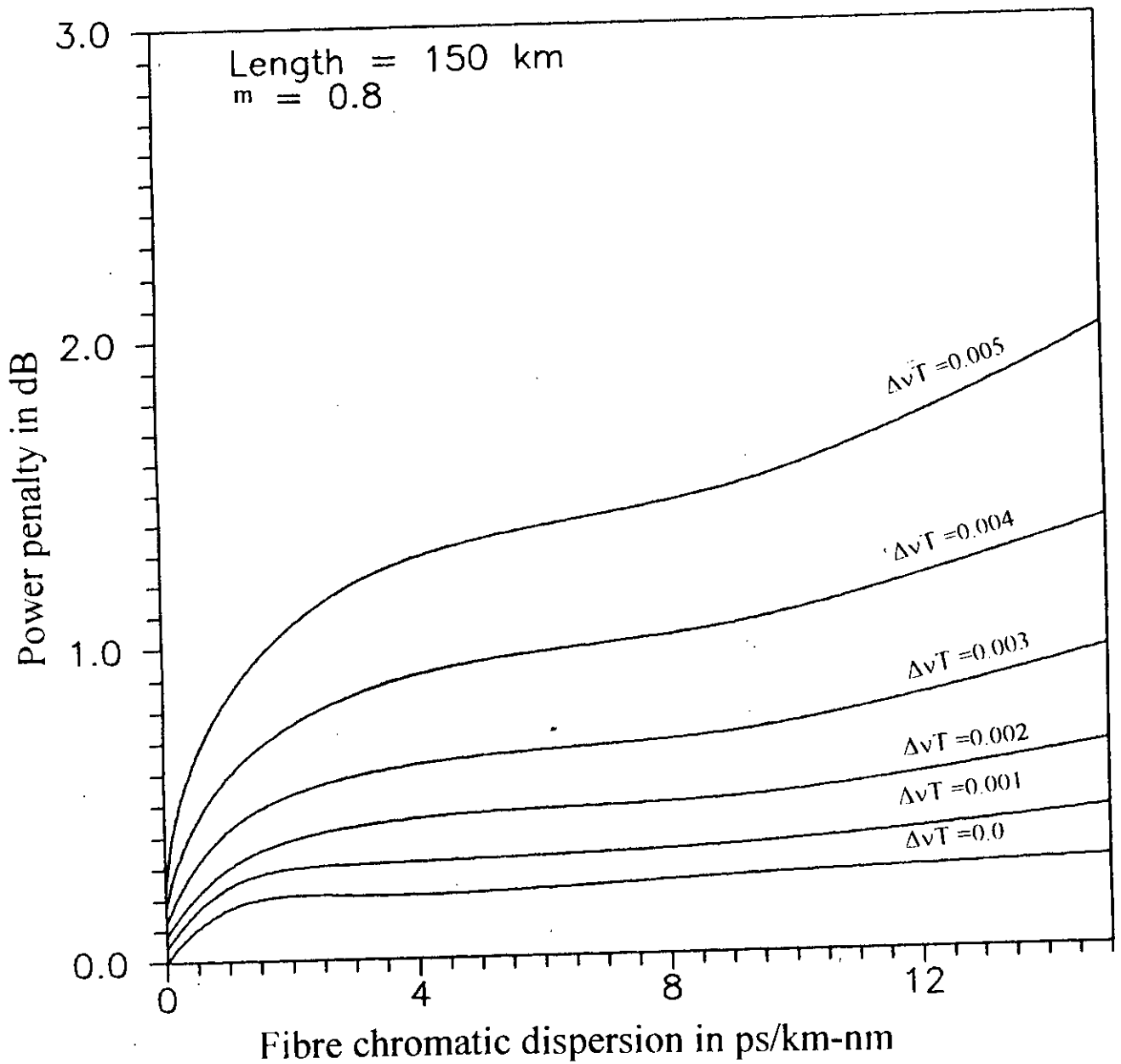


Fig. 3.16 Penalty in signal power due to combined effect of laser phase noise and fibre chromatic dispersion at BER=10⁻⁹ versus dispersion coefficient D_c (ps/ Km.nm) with fibre length L=150 Km and modulation index m=0.8 for several values of normalized linewidth $\Delta\nu T$.

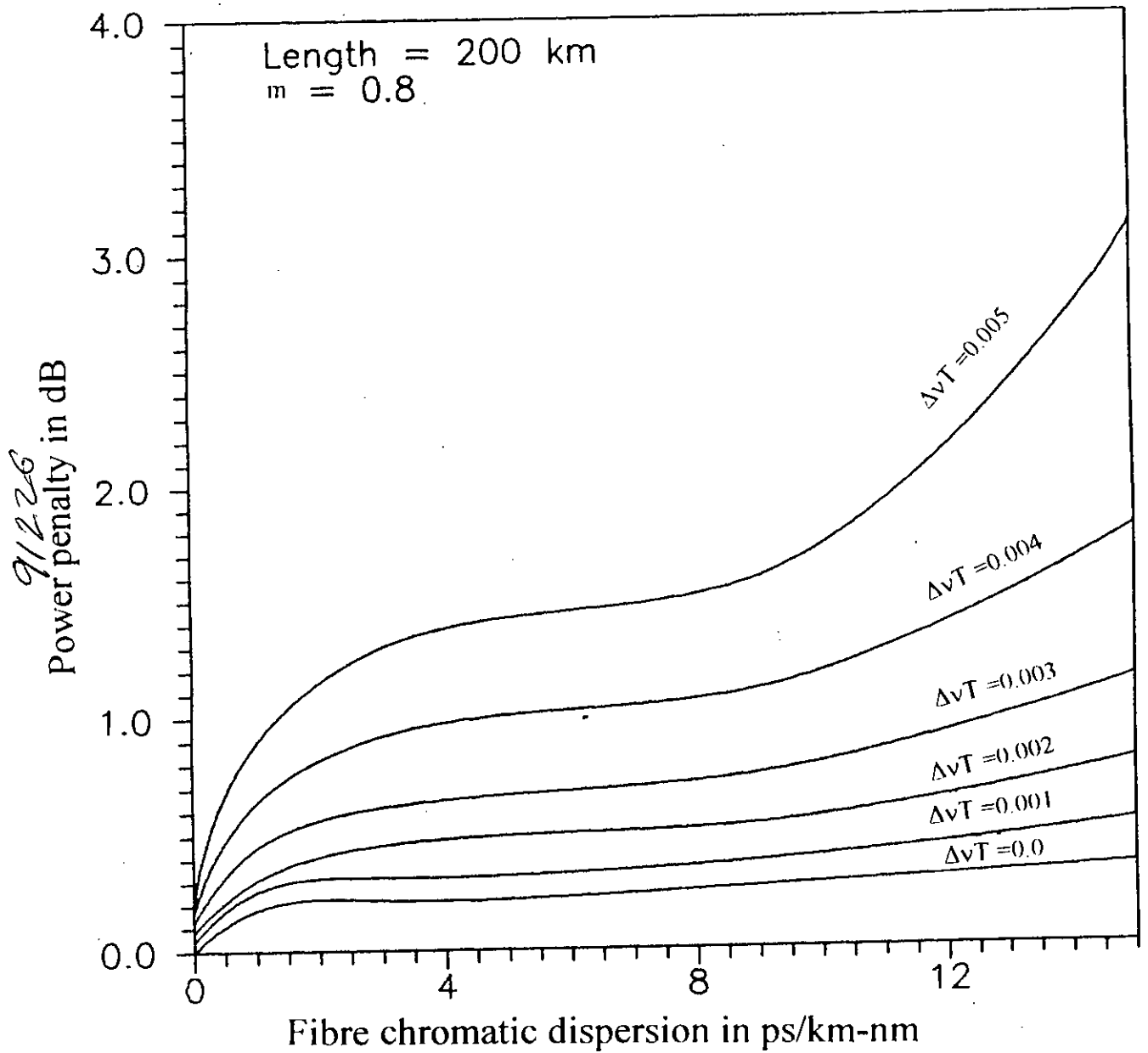


Fig. 3.17 Penalty in signal power due to combined effect of laser phase noise and fibre chromatic dispersion at $BER=10^{-9}$ versus dispersion coefficient D_c (ps/ Km.nm) with fibre length $L=200$ Km and modulation index $m=0.8$ for several values of normalized linewidth $\Delta\nu T$.

dispersion coefficient D_C the penalty increases almost linearly. At higher values of dispersion coefficient penalty tends to increase more rapidly.

Further, it is also observed that for zero and smaller values of linewidth, the penalty is below 1 dB. When the normalized linewidth $\Delta\nu T \geq 0.004$ and $D_C > 8$ ps/ Km.nm, the penalty is more than 1 dB and further increases with increase in $\Delta\nu T$ and/ or dispersion coefficient D_C . Comparing fig. 3.16 and fig. 3.17 we also found that for the same modulation index and dispersion coefficient, the penalty is more for larger fibre span. As seen from the figures, the penalty is approximately 1.7 dB (for $D_C=12$ ps/ Km.nm and $\Delta\nu T=0.005$) corresponding fibre span $L= 150$ Km whereas it increases to 2.1 dB when L is increased to 200 Km.

Similar plots of penalty versus dispersion coefficient D_C are also shown in fig. 3.18 & fig. 3.19 for higher $m=1.0$ and fig. 3.20 & fig. 3.21 for $m=1.2$. Comparing fig. 3.16 and fig. 3.18 we note that for same fibre span L (Km) and same values of D_C and $\Delta\nu T$, the penalty is higher for higher values of modulation index. This may be due to the fact that the effect of chromatic dispersion is higher at higher spectral bandwidth of FSK signal at increased modulation index. For $L=150$ Km, $\Delta\nu T=0.005$, $D_C=12$ the penalty is 2.1 dB when $m=0.8$ (fig. 3.16) whereas the penalty is approximately 4.0 dB when m is increased to 1.0 (fig. 3.18). There is

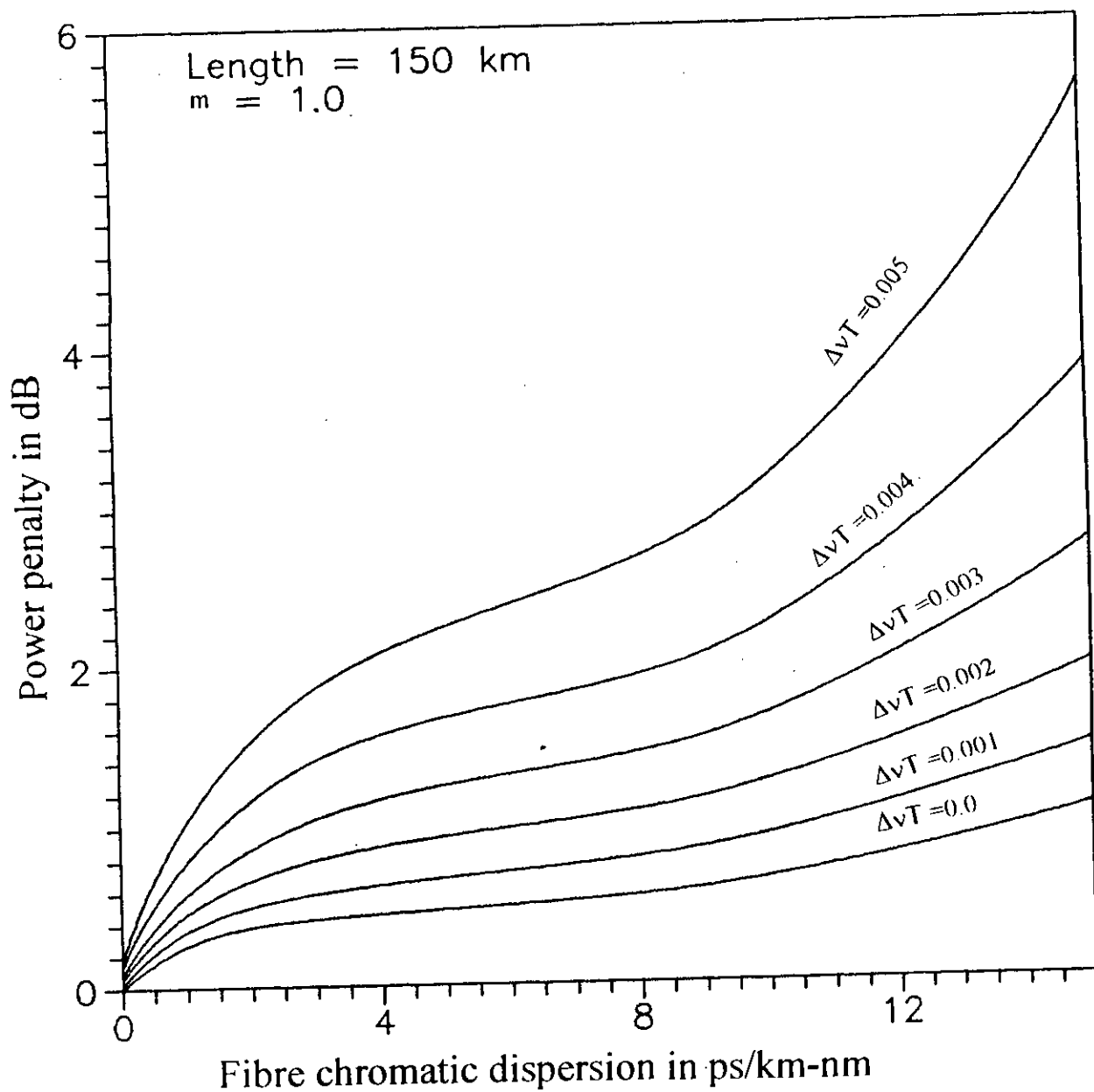


Fig. 3.18 Penalty in signal power due to combined effect of laser phase noise and fibre chromatic dispersion at $BER=10^{-9}$ versus dispersion coefficient D_C (ps/ Km.nm) with fibre length $L=150$ Km and modulation index $m=1.0$ for several values of normalized linewidth $\Delta\nu T$.

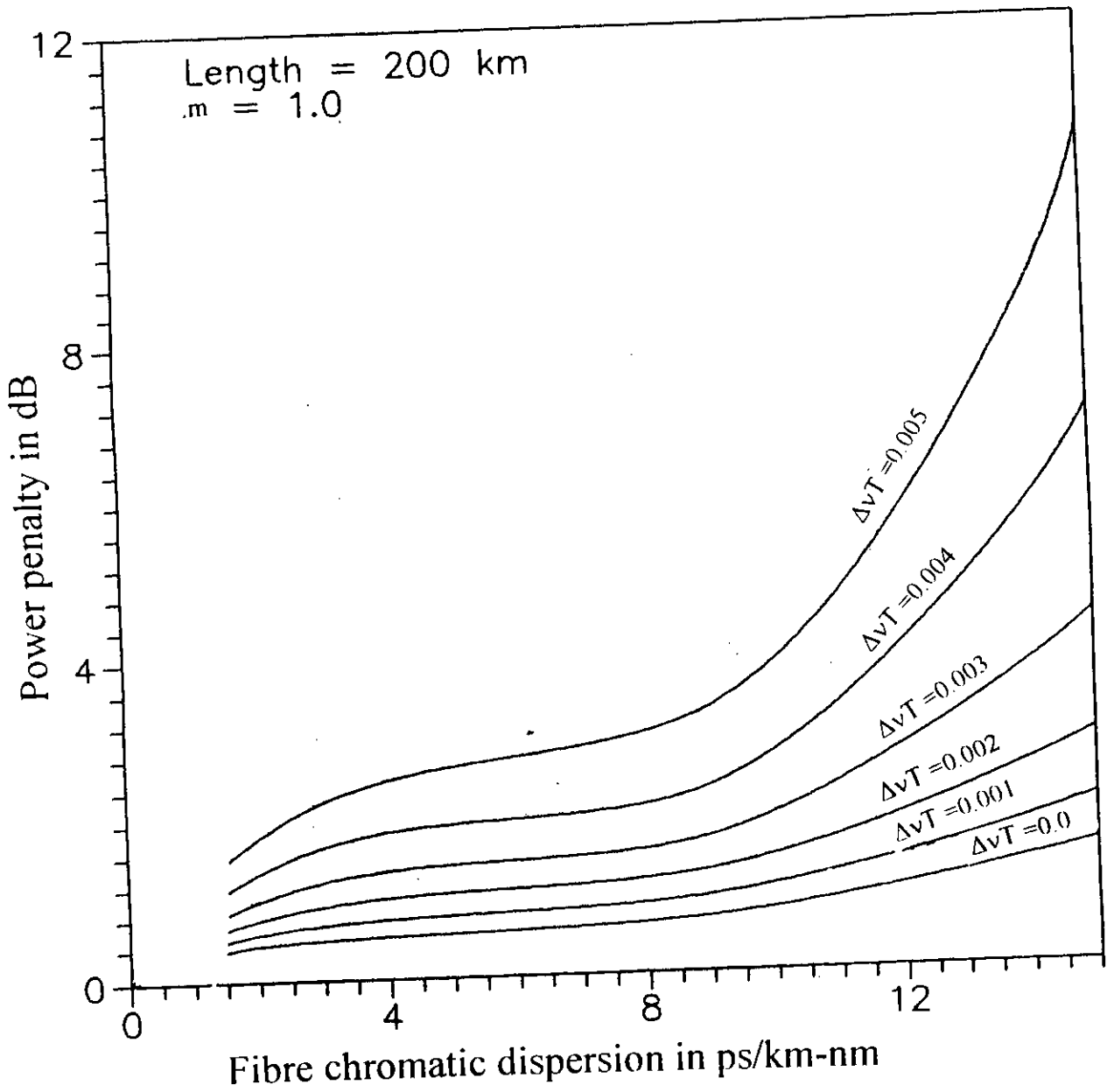


Fig. 3.19 Penalty in signal power due to combined effect of laser phase noise and fibre chromatic dispersion at BER= 10^{-9} versus dispersion coefficient D_c (ps/ Km.nm) with fibre length $L=200$ Km and modulation index $m=1.0$ for several values of normalized linewidth $\Delta\nu T$.

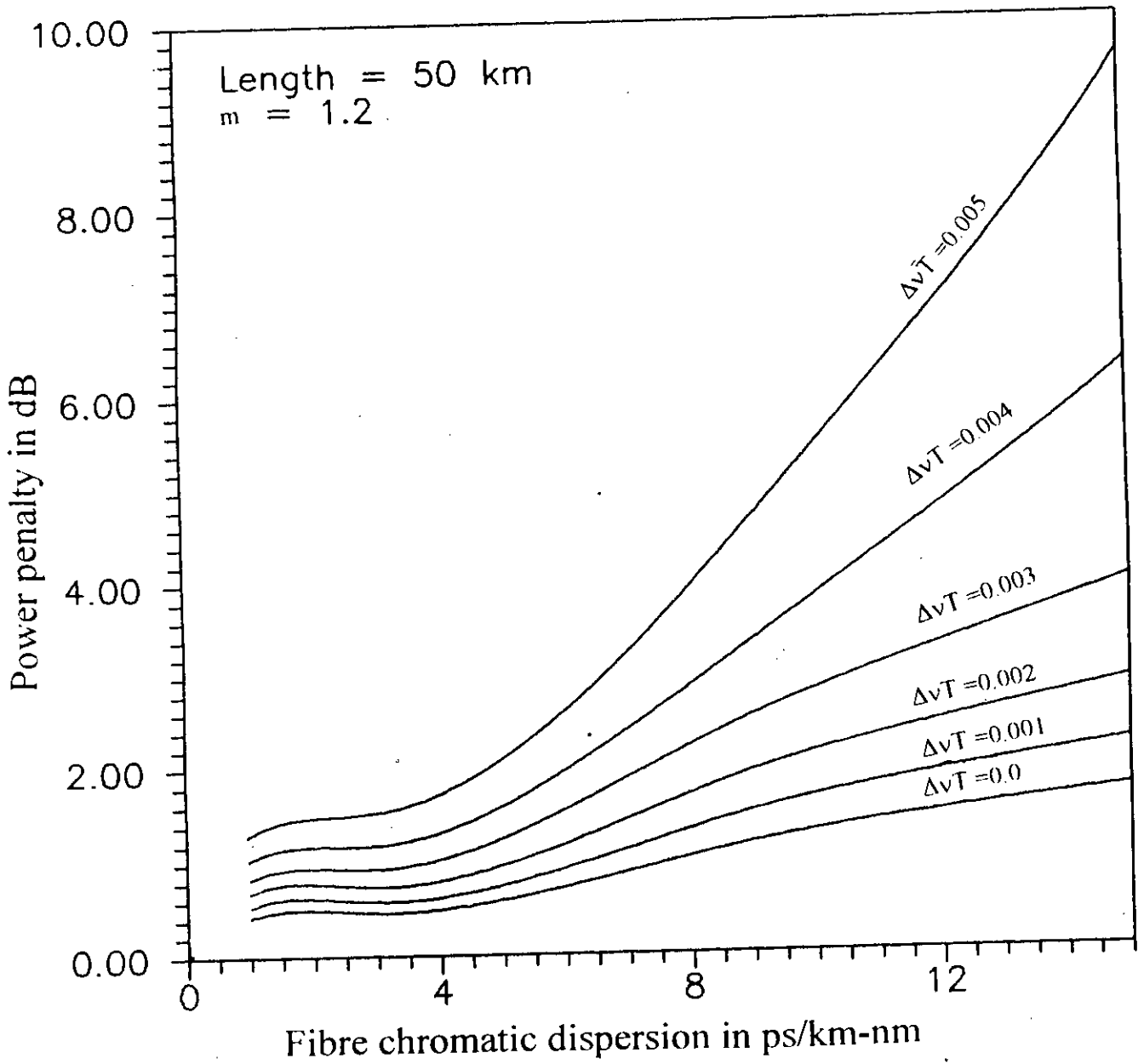


Fig. 3.20 Penalty in signal power due to combined effect of laser phase noise and fibre chromatic dispersion at $BER=10^{-9}$ versus dispersion coefficient D_C (ps/ Km.nm) with fibre length $L=50$ Km and modulation index $m=1.2$ for several values of normalized linewidth $\Delta\nu T$.

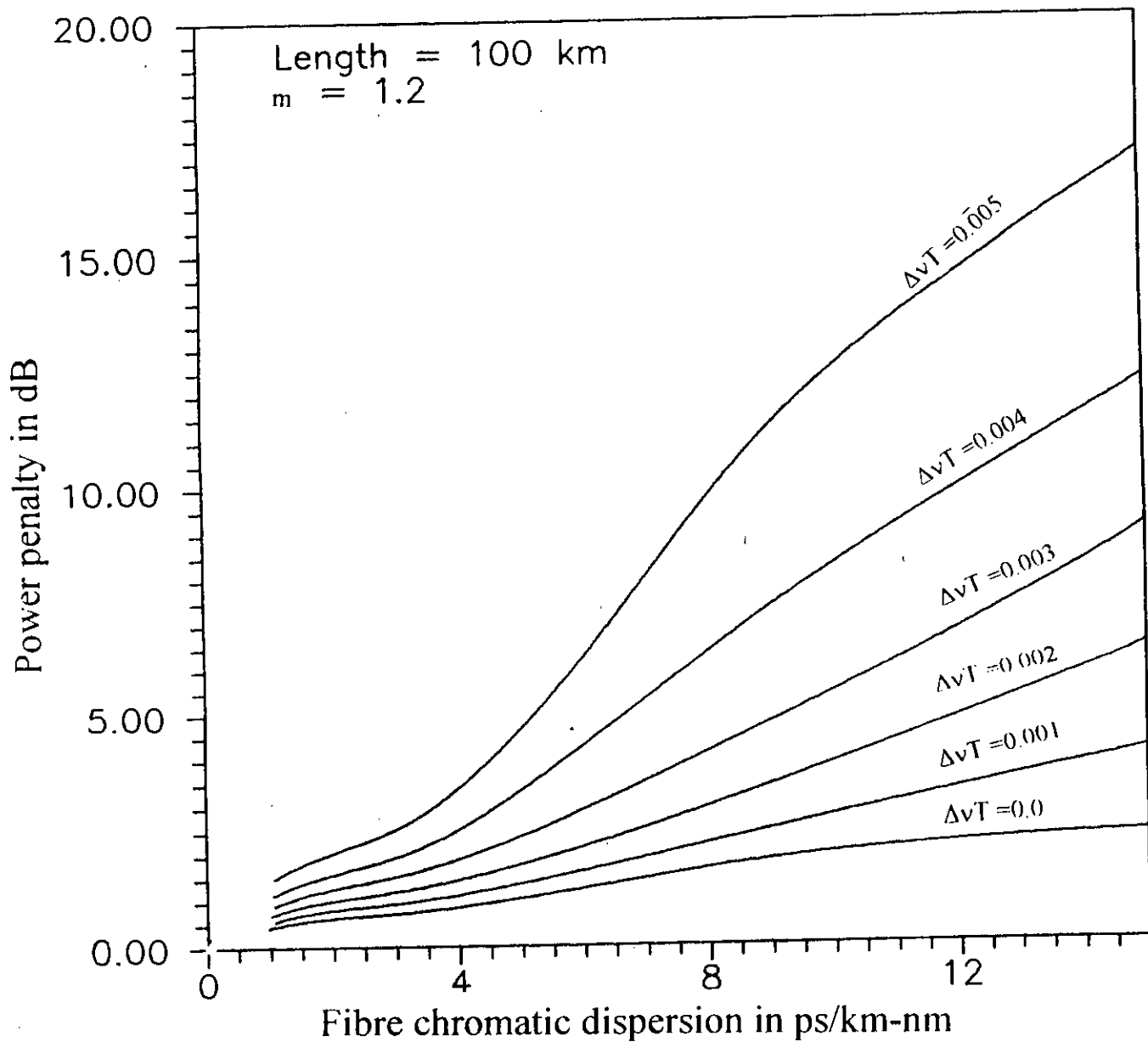


Fig. 3.21 Penalty in signal power due to combined effect of laser phase noise and fibre chromatic dispersion at $BER=10^{-9}$ versus dispersion coefficient D_c (ps/ Km.nm) with fibre length $L=100$ Km and modulation index $m=1.2$ for several values of normalized linewidth $\Delta\nu T$.

further increase in the penalty when the modulation index is further increased (as shown in fig. 3.19 and fig. 3.20).

To get more insight into the effect of dispersion on the system performance, the penalty in signal power at $\text{BER}=10^{-9}$ is plotted as a function of the normalized linewidth $\Delta\nu T$ in fig. 3.22, fig. 3.23 and fig. 3.24 for $m= 0.8, 1.0$ and 1.2 respectively with dispersion factor γ as a parameter. In the absence of dispersion ($\gamma=0.0$) i.e. when only laser phase noise is present, the penalty is significantly less (< 0.25 dB for $\Delta\nu T=0.005$) compared to the case of non-zero value of γ . When $\Delta\nu T=0.0$, the penalty suffered by the system is only due to chromatic dispersion and for $\Delta\nu T>0.0$ and $D_c>0.0$ the penalty is due to combined effect of dispersion and phase noise. For a given linewidth, the penalty increases with increase in the value of dispersion factor γ . For 1 dB penalty, the maximum allowable laser linewidth is significantly less at higher values of dispersion factor γ . For example, from fig. 3.22 corresponding to $m=0.8$ we see that for penalty less than or equal to 1 dB, the allowable laser linewidth is sufficiently large ($>0.005/T$) when $\gamma=0.0$. When $\gamma=0.076$, the allowable laser linewidth is slightly higher than $0.005/T$. When γ is further increased to 0.46, the allowable laser linewidth is reduced to less than $0.004/T$. Thus chromatic dispersion imposes restriction on the allowable laser linewidth for a specified system penalty at a given BER.

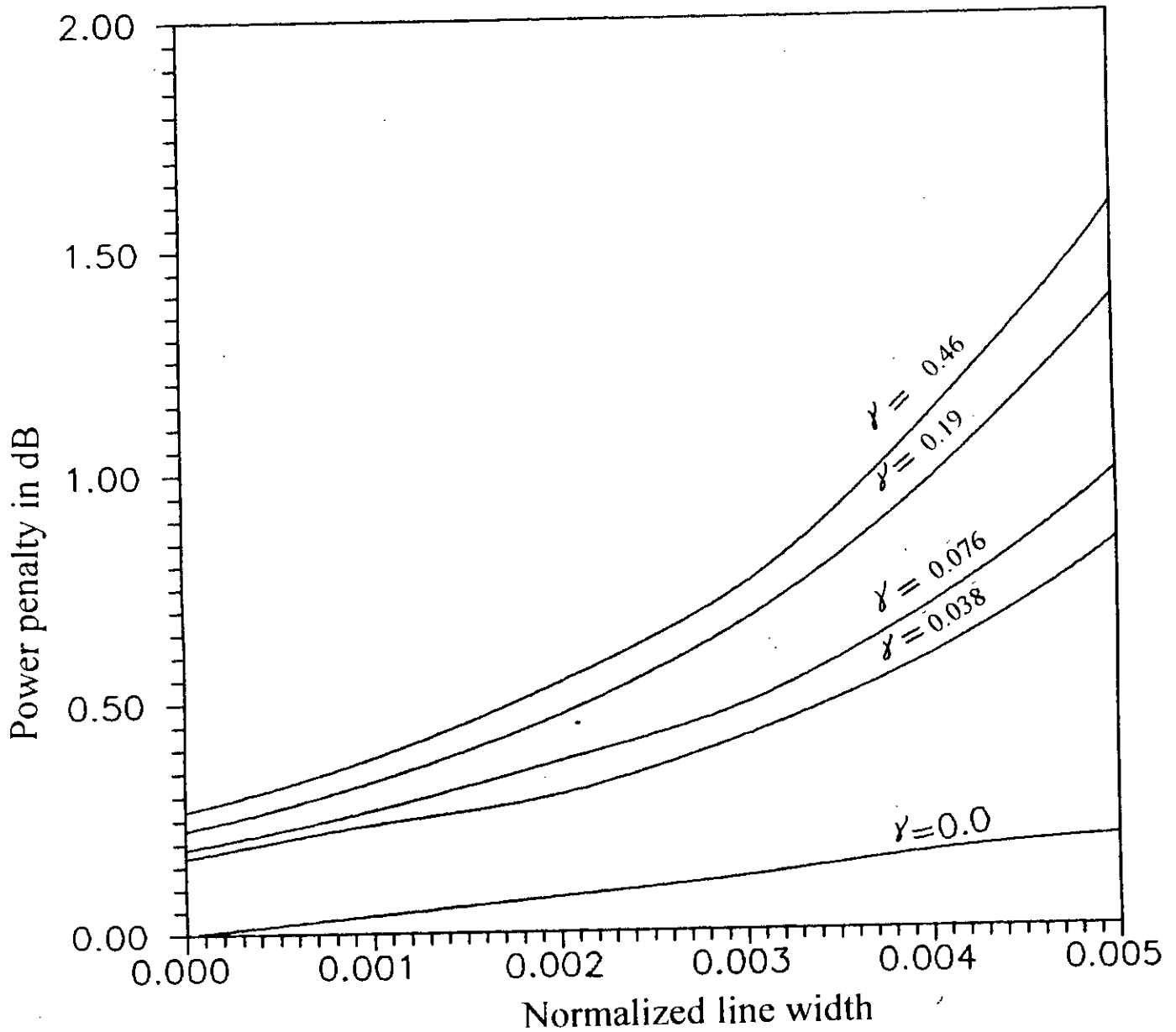


Fig. 3.22 Variation of power penalty (dB) due to combined effect of laser phase noise and fibre chromatic dispersion at $BER=10^{-9}$ with normalized linewidth $\Delta\nu T$ for modulation index $m=0.8$ and several values of dispersion factor γ .

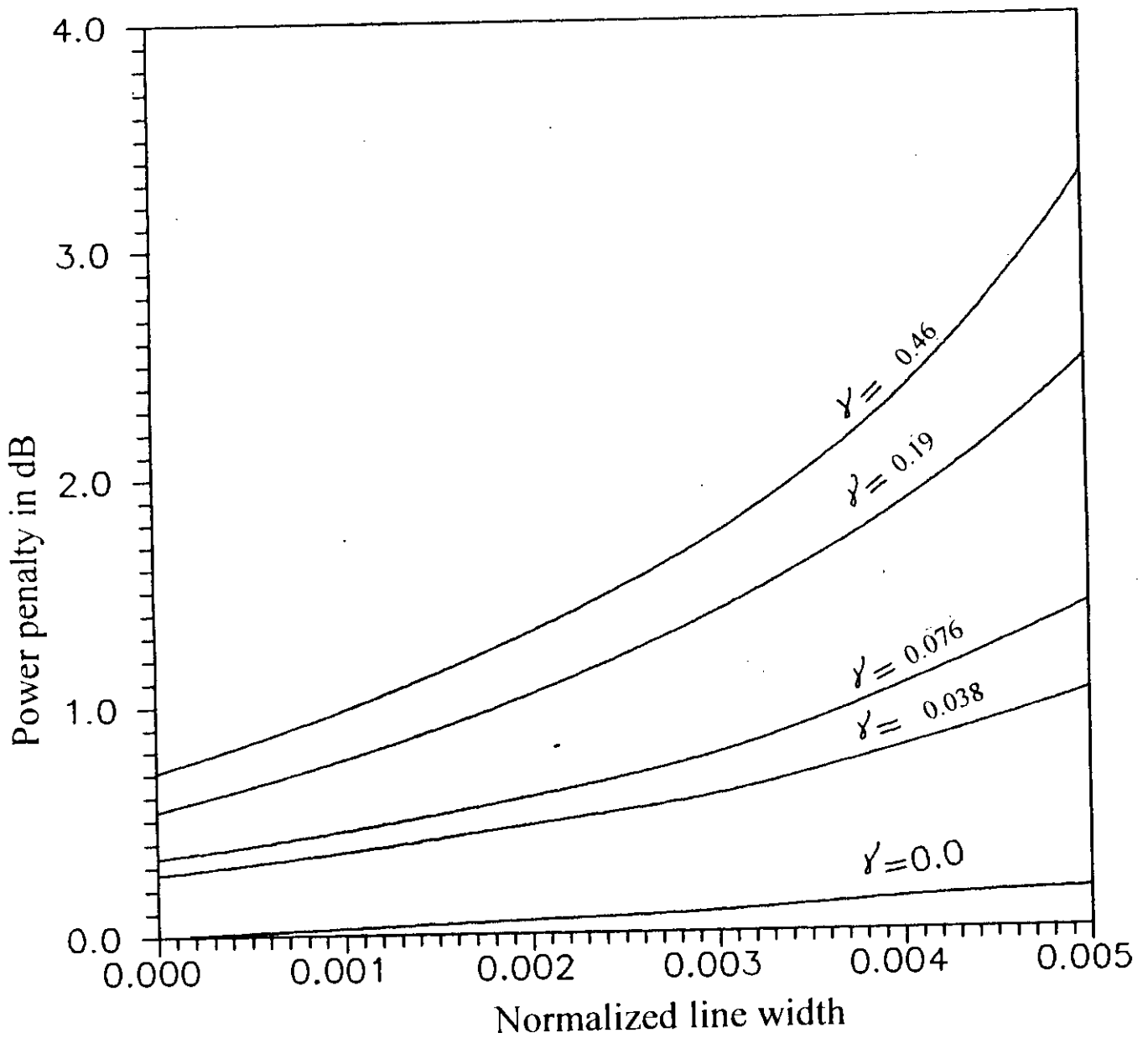


Fig. 3.23 Variation of power penalty (dB) due to combined effect of laser phase noise and fibre chromatic dispersion at BER= 10^{-9} with normalized linewidth $\Delta\nu T$ for modulation index $m=1.0$ and several values of dispersion factor γ .

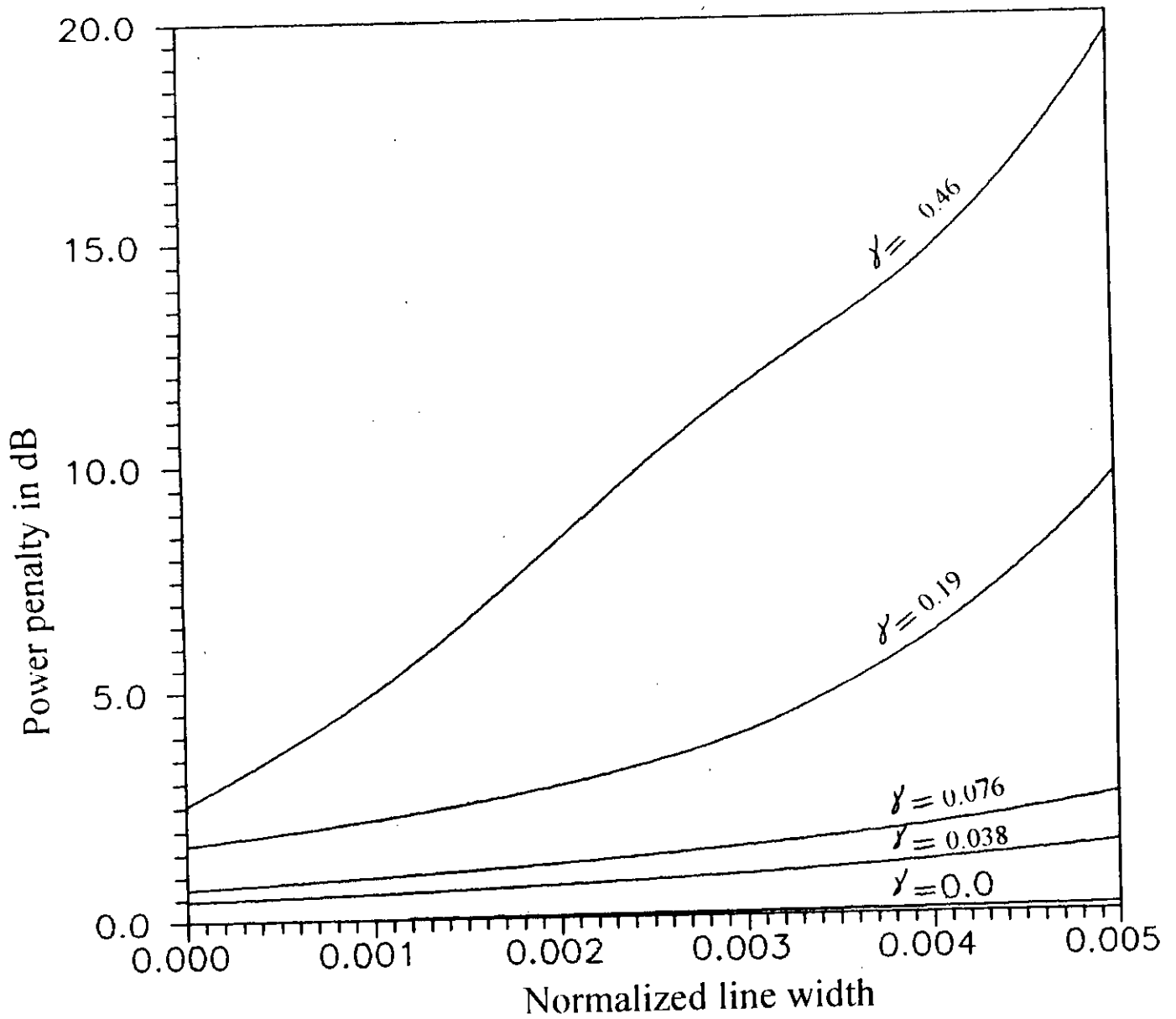


Fig. 3.24 Variation of power penalty (dB) due to combined effect of laser phase noise and fibre chromatic dispersion at $BER=10^{-9}$ with normalized linewidth $\Delta\nu T$ for modulation index $m=1.2$ and several values of dispersion factor γ .

The allowable laser linewidth for 1 dB penalty is further reduced at increased modulation index as is evident from fig. 3.23 and fig. 3.24 corresponding to $m=1.0$ and 1.2 respectively. When $m=1.0$ and $\gamma=0.46$, the allowable laser linewidth is approximately less than $0.0012/T$. At higher modulation index say $m=1.2$ (fig. 3.24), the penalty is much more higher than 1 dB when $\Delta\nu T=0.0$ and $\gamma\geq 0.076$.

The variation of power penalty with dispersion factor γ is plotted in fig. 3.25, fig. 3.26 and fig. 3.27 for different values of normalized linewidth $\Delta\nu T$. It is observed that the penalty increases with increasing values of dispersion factor γ and normalized linewidth $\Delta\nu T$. However, as mentioned before, the penalty is found to be higher at higher values of modulation index. Further, we also notice that for a given $\Delta\nu T$, at $BER=10^{-9}$ there is an upper limit on the dispersion factor γ for power penalty ≤ 1 dB. The upper limit or maximum allowable dispersion factor is less in the presence of phase noise and is significantly less at higher linewidth values. Corresponding to maximum allowable dispersion factor, we get an upper limit on the maximum fibre length for a given value of dispersion coefficient D_c corresponding to $BER=10^{-9}$ and penalty ≤ 1 dB. Further, the maximum allowable γ is also significantly less at higher modulation index as seen from fig. 3.26 and fig. 3.27 corresponding to $m=1.0$ and 1.2 respectively. For example, the maximum value of γ corresponding to 1 dB penalty at $BER=10^{-9}$ is 0.40 for $\Delta\nu T=0.004$ and

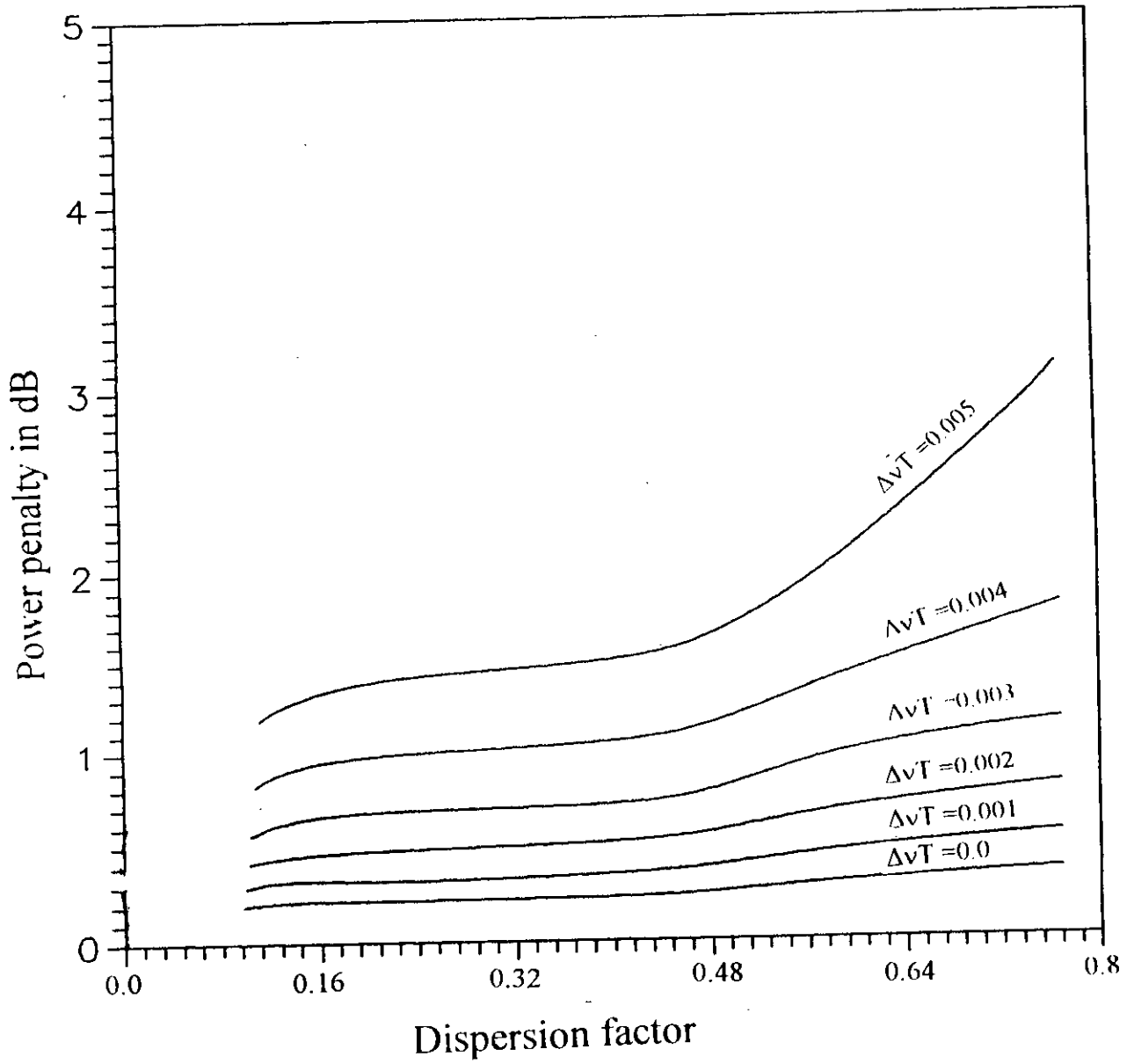


Fig. 3.25 Plots of power penalty (dB) at $BER=10^{-9}$ versus dispersion factor γ for modulation index $m=0.8$ with ΔvT as a parameter.

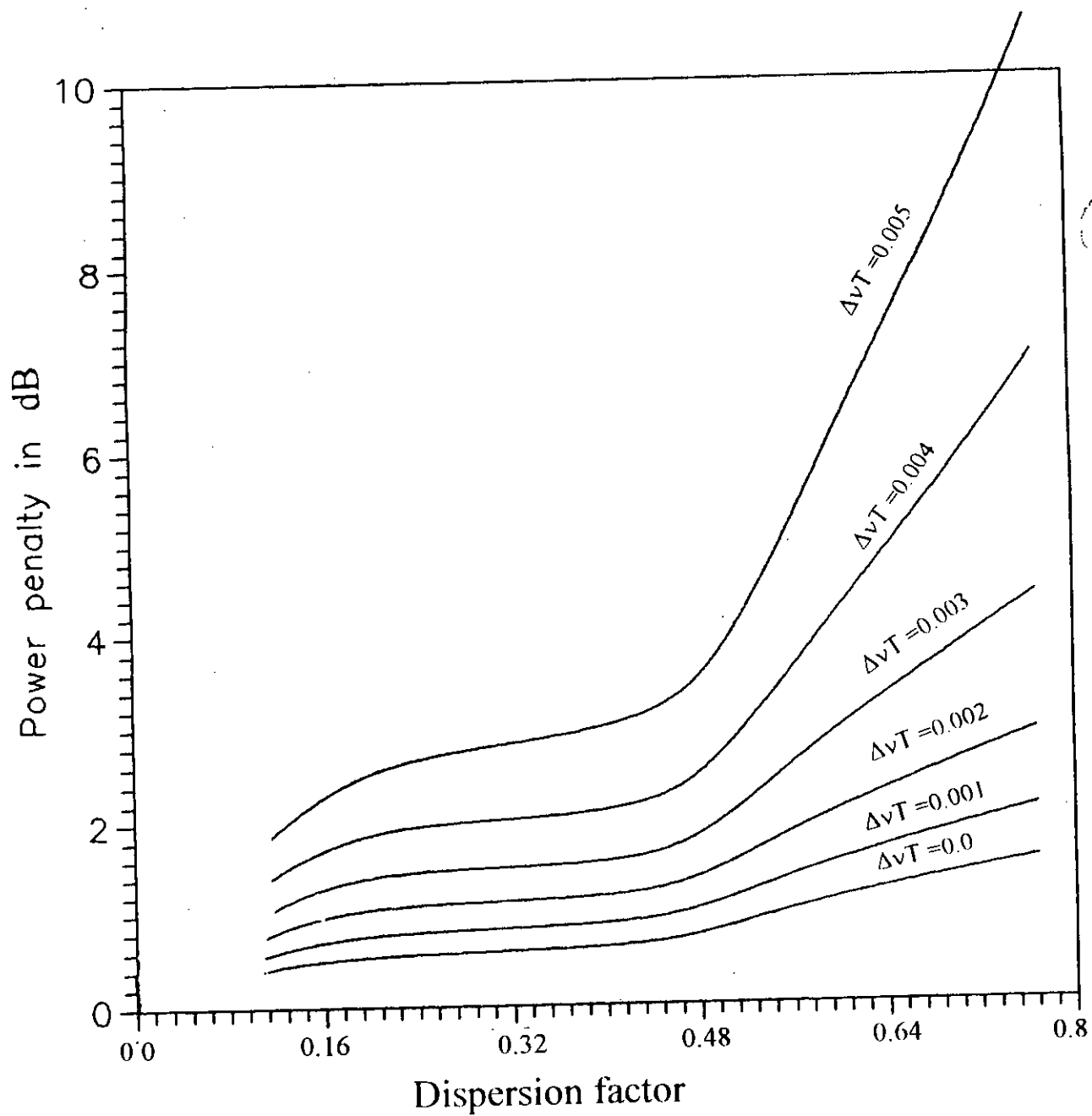


Fig. 3.26 Plots of power penalty (dB) at $BER=10^{-9}$ versus dispersion factor γ for modulation index $m=1.0$ with ΔvT as a parameter.

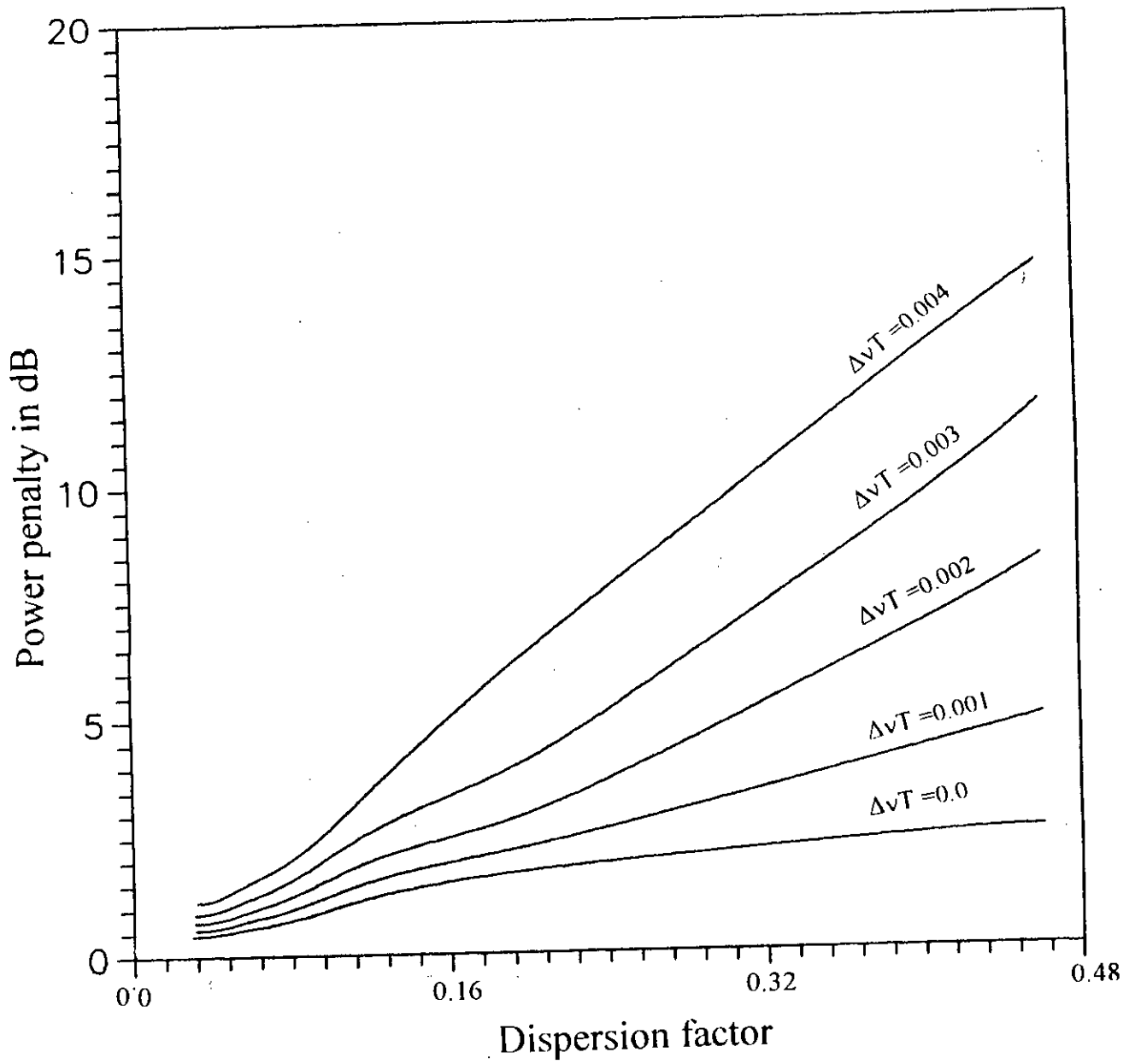


Fig. 3.27 Plots of power penalty (dB) at $BER=10^{-9}$ versus dispersion factor γ for modulation index $m=1.2$ with $\Delta\nu T$ as a parameter.

$m=0.8$. When $m=1.0$, for the same value of $\Delta\nu T$ the maximum allowable value of γ is found to be approximately 0.06 (fig. 3.26).

For 1 dB power penalty at $BER=10^{-9}$, the allowable fibre length (Km) is plotted in fig. 3.28 as a function of normalized linewidth $\Delta\nu T$ for chromatic dispersion coefficient $D_C=1.0$ and $m=0.8, 1.0, 1.2$. It is observed that the allowable fibre length is more than 12,000 Km when $\Delta\nu T=0.0$ and $m=0.8$. When m is increased to 1.0, the allowable fibre length reduces to around 2500 Km and is less than 500 Km for $m=1.2$. Further, the allowable fibre length exponentially decreases with increasing linewidth.

Similar plots are shown in fig. 3.29 and fig. 3.30 corresponding to $D_C=3.0$ and $D_C=15.0$ respectively. Comparison of these curves reveal that there is considerable reduction in the allowable fibre length at higher values of chromatic dispersion coefficient D_C . For $m=0.8$, the allowable fibre lengths are approximately 4000 Km and 800 Km for $D_C=3.0$ and $D_C=15.0$ respectively in the absence of laser noise. When the laser linewidth is 0.2 percent of bit rate, the corresponding values are significantly less, viz. 1100 Km and 220 Km respectively.

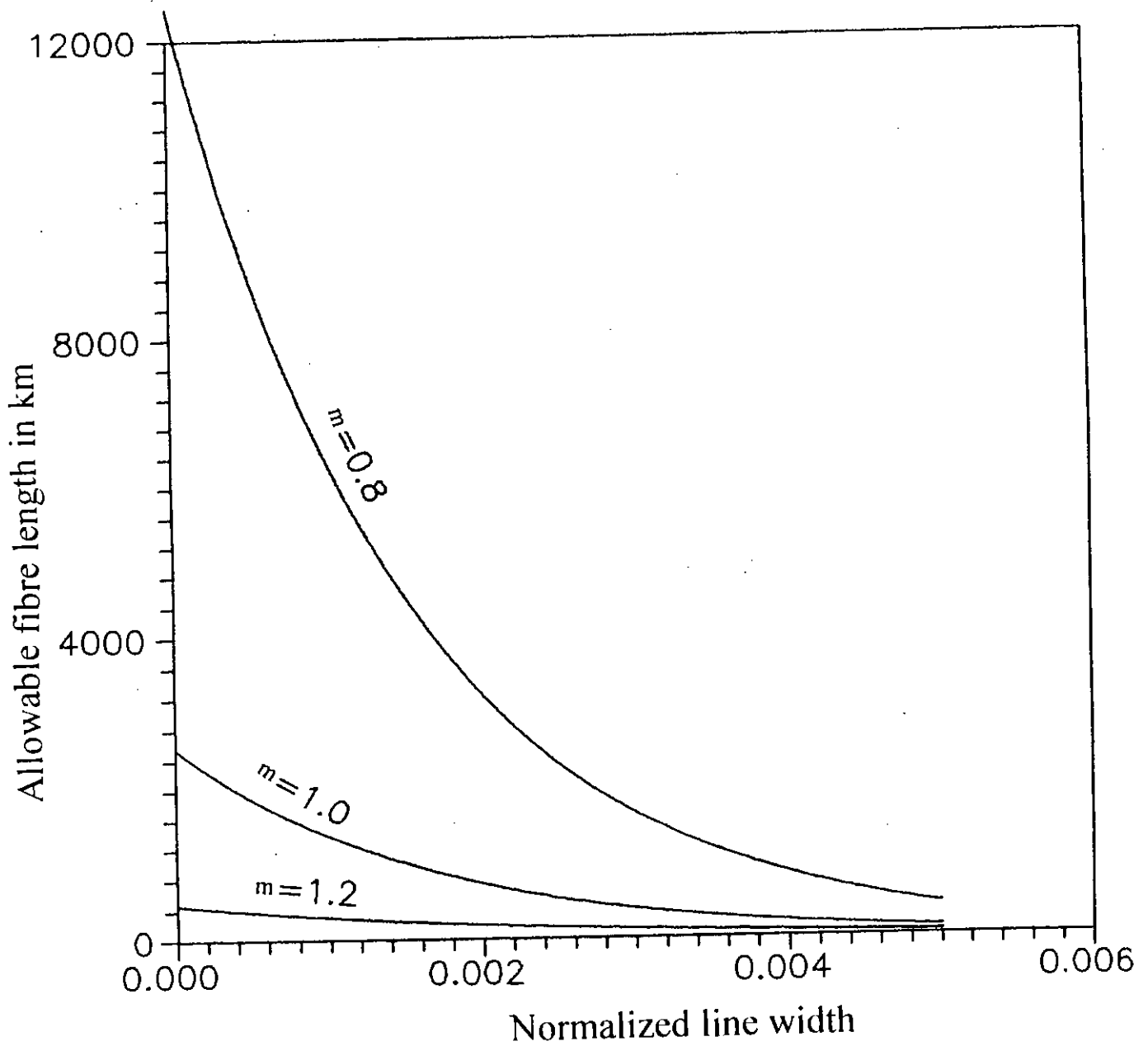


Fig. 3.28 Plots of allowable fibre length corresponding to 1 dB penalty at $BER=10^{-9}$ as a function of normalized linewidth $\Delta\nu T$ for modulation index $m=0.8, 1.0$ and 1.2 and dispersion coefficient $D_c=1.0$ ps/Km.nm.

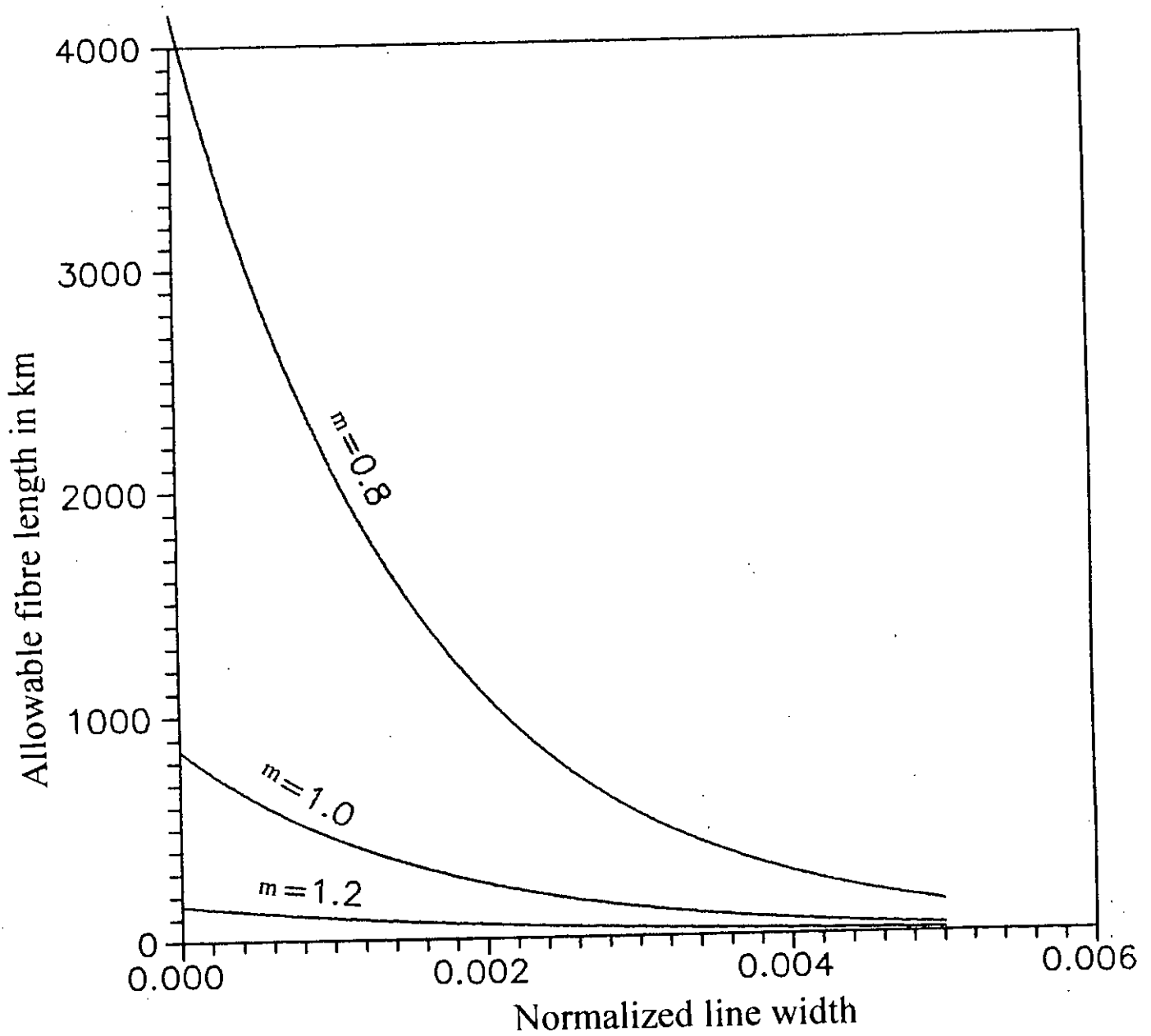


Fig. 3.29 Plots of allowable fibre length corresponding to 1 dB penalty at $BER=10^{-9}$ as a function of normalized linewidth ΔT for modulation index $m=0.8, 1.0$ and 1.2 and dispersion coefficient $D_c=3.0$ ps/Km.nm.

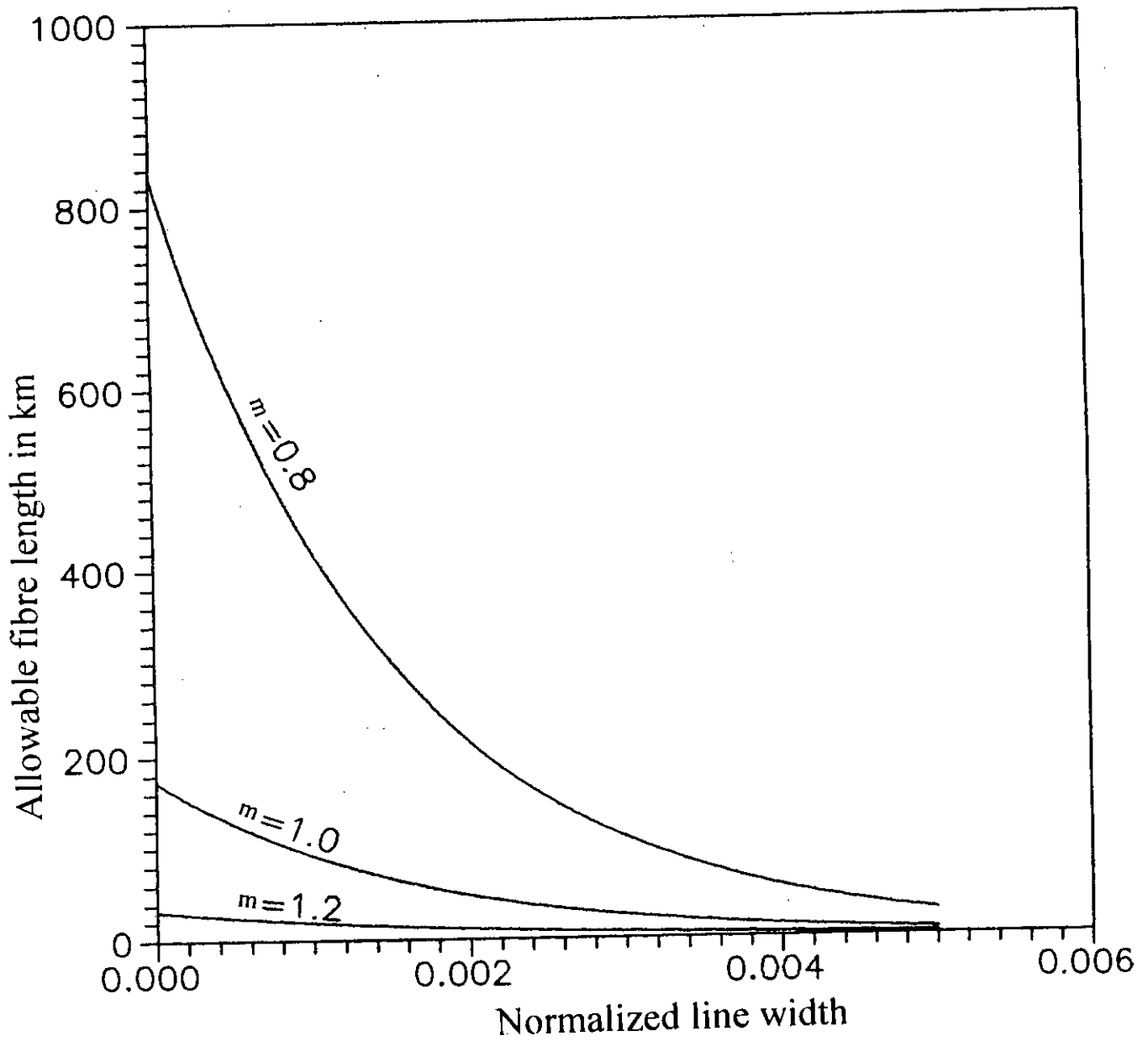


Fig. 3.30 Plots of allowable fibre length corresponding to 1 dB penalty at $BER=10^{-9}$ as a function of normalized linewidth $\Delta\nu T$ for modulation index $m=0.8, 1.0$ and 1.2 and dispersion coefficient $D_c=15.0$ ps/Km.nm.

CHAPTER - 4

CONCLUSIONS AND SUGGESTIONS FOR FUTURE WORKS

4.1 Conclusions:

A theoretical analysis is provided for optical FSK transmission system with direct detection receiver using Mach-Zender Interferometer (MZI) as an optical frequency discriminator. The analysis is carried out to evaluate the combined influence of fibre chromatic dispersion and laser phase noise on the system performance. The probability density function of the random phase fluctuation due to the effect of fibre chromatic dispersion is determined from its moments and the expression for bit error probability is developed.

Following the theoretical analysis the bit error rate performance results are evaluated at a bit rate of 10 Gb/s with single mode fibre at an wavelength of 1550 nm for different sets of values of chromatic dispersion coefficient, modulation index, laser linewidth etc.

The results show that in the absence of laser phase noise, the performance of direct detection optical FSK system is highly degraded due to the effect of fibre dispersion. For small values of dispersion coefficient D_C and dispersion factor γ , the

system suffers penalty in signal power at a specified BER of 10^{-9} compared to the case of no dispersion. In the presence of laser phase noise, the system performance is more degraded and the penalty is higher. For example, in the absence of laser phase noise ($\Delta\nu T=0.0$) the penalty suffered by the system at $\text{BER}=10^{-9}$ is approximately 0.13 dB for $D_C=1.0$, fibre span $L=150$ Km and modulation index $m=0.8$. In presence of phase noise, when $\Delta\nu T=0.005$, the above penalty is found to be 0.82 dB. It is further noticed that the penalty is higher for higher values of the modulation index m . For $L=150$ Km, $\Delta\nu T=0.005$, $D_C=12$ the penalty is 2.1 dB when $m=0.8$ whereas the penalty is approximately 4.0 dB when m is increased to 1.0. There is further increase in the penalty when the modulation index is further increased. Further, it is also observed that for zero and smaller values of linewidth, the penalty is below 1 dB. When the normalized linewidth $\Delta\nu T \geq 0.004$ and $D_C > 8$ ps/ Km.nm, the penalty is more than 1 dB and further increases with increase in $\Delta\nu T$ and/ or dispersion coefficient D_C and higher fibre length.

At increased value of normalized linewidth $\Delta\nu T$ and dispersion coefficient D_C there occurs bit error rate floor which can not be lowered by increasing the signal power. For example, the BER floor occurs around 10^{-12} corresponding to $\Delta\nu T=0.001$ and around 4×10^{-11} for $\Delta\nu T=0.003$. Also, the BER floor goes upward for the same value of $\Delta\nu T$ when γ is increased from 0.076 to 0.46.

For 1 dB power penalty at $BER=10^{-9}$, the maximum allowable laser linewidth is significantly less at higher values of dispersion factor γ . For example, corresponding to $m=0.8$ we observe that for penalty less than or equal to 1 dB, the allowable laser linewidth is sufficiently large ($>0.005/T$) when $\gamma=0.0$. When $\gamma=0.076$, the allowable laser linewidth is slightly higher than $0.005/T$. When γ is further increased to 0.46, the allowable laser linewidth is reduced to less than $0.004/T$. Thus chromatic dispersion imposes restriction on the laser specifications in terms of allowable laser linewidth for a specified system penalty at a given BER. The allowable laser linewidth for 1 dB penalty is further reduced at increased modulation index. When $m=1.0$ and $\gamma=0.46$, the allowable laser linewidth is approximately less than $0.0012/T$. At higher modulation index say $m=1.2$, the penalty is much more higher than 1 dB when $\Delta\nu T=0.0$ and $\gamma\geq 0.076$.

Further, we also notice that for a given $\Delta\nu T$, at $BER=10^{-9}$ there is an upper limit on the dispersion factor γ for power penalty ≤ 1 dB. The upper limit or maximum allowable dispersion factor is less in the presence of phase noise and is significantly less at higher linewidth values. Corresponding to maximum allowable dispersion factor, we get an upper limit on the maximum fibre length for a given value of dispersion coefficient D_C corresponding to $BER=10^{-9}$ and penalty ≤ 1 dB. Further, the maximum allowable γ is also significantly less at higher modulation index corresponding to $m=1.0$ and 1.2 respectively.

It is further observed that the allowable fibre length corresponding to 1 dB penalty at $BER=10^{-9}$ is more than 12,000 Km when $\Delta\nu T=0.0$ and $m=0.8$. When m is increased to 1.0, the allowable fibre length reduces to around 2500 Km and is less than 500 Km for $m=1.2$. The allowable fibre length exponentially decreases with increasing linewidth. Further, there is considerable reduction in the allowable fibre length at higher values of chromatic dispersion coefficient D_c . For $m=0.8$, the allowable fibre lengths are approximately 4000 Km and 800 Km for $D_c=3.0$ and $D_c=15.0$ respectively in the absence of laser noise. When the laser linewidth is 0.2 percent of bit rate, the corresponding values are significantly less, viz. 1100 Km and 220 Km respectively.

4.2 Suggestions for Future Works:

Further research related to this work can be carried out to investigate the influence of fibre chromatic dispersion on optical heterodyne FSK system with delay-demodulation as well as envelope detection receivers. The work can be extended to optical intensity modulation (IM) and differential phase shift keying (DPSK) transmission system with direct/ heterodyne detection receivers.

Further works can also be carried out to evaluate the impact of fibre dispersion on the performance of wavelength division multiplexed (WDM) optical FSK/ DPSK

transmission systems. The maximum number of wavelength channels, optimum channel separation, maximum fibre span limited by the effect of fibre chromatic dispersion at a bit rate of 10 Gb/s or higher are to be determined. Further investigations can also be initiated to analyze the performance of optical FSK/DPSK systems with fibre having nonuniform chromatic dispersion along the fibre length.

Further works of importance are to determine dispersion compensation techniques to reduce the power penalty due to fibre chromatic dispersion so as to increase the repeaterless transmission distance in single/ multi channel transmission systems with single-mode fibres.

REFERENCES:

- [1] F. M. Knox, W. Forsyiax and N. J. Doran, "10 Gbt/s Soliton Communication Systems over standard fiber at 1.55 μm and the use of dispersion compensation," *Journal of Lightwave Technology*, vol. 13, no.10, October 1995, pp. 1955-1962.
- [2] "Introduction to the optical fibre," Trainee's manual, Institute de formation, Alcatel CIT, March 1991, 14031.
- [3] J. R. Pierce, "Optical channel practical limits with photon counting," *IEEE Transaction on Communications*, vol. com-26, no. 12, December 1978, pp. 1819-1821.
- [4] B. L. Patel, E. M. Kimber, M. G. Taylor, A. N. Robinson, I. Hardcastle, A. Hadjifotiou, S. J. Wilson, R. Keys and J. E. Righton, "High performance 10 Gb/s optical transmission system using Erbium-doped fiber amplifier," *Electronic Letters*, vol. 27, no. 23, November 1991, pp. 2179-2180.
- [5] I. Garrett and G. Jacobsen, "Phase noise in weakly coherent systems," *IEE proceedings- J. opto electronics*, vol. 136, 1989, pp. 2179-2180.
- [6] G. Jacobsen, K. Emura, T. Ono and S. Yamazaki, "Requirements for LD FM characteristics in an optical CPFSK system," *Journal of Lightwave Technology*, vol. 9, 1991, pp. 1113-1123.

- [7] I. Garrett, "Introduction to the effect of phase noise on coherent optical system," Proceedings of Forth Tirrenia International workshop on digital communication, Tirrenia, Italy, September 19-23, 1989, pp. 103-116.
- [8] S. Kobayashi, Y. Yamamoto, M. Ito and T. Kimura, "Direct Frequency modulation in AlGaAs semiconductor lasers," IEEE Journal of Quantum Electron, vol. QE-18, no. 4, 1982, pp. 582-595.
- [9] K. Iwashita and T. Matsumoto, "Modulation and detection characteristics of optical continuous phase FSK transmission system," Journal of Lightwave Technology, vol. LT-5, April 1987, pp. 452-260.
- [10] R. S. Vodhanel, J. L. Gimlet, N. K. Cheung and S. Tsuji, "FSK heterodyne transmission experiments at 560 Mbit/s and 1 Gbit/s," Journal of Lightwave Technology, vol. LT-5, April 1987, pp. 461-468.
- [11] K. Nosu, H. Toba and K. Iwashita, "Optical FDM transmission technique," Journal of Lightwave Technology, vol. LT-5, no. 9, 1987, pp. 1301-1308.
- [12] D. J. Malyon and W. A. Stallard, "565 Mb/s FSK direct detection system operating with four cascaded photonic amplifiers," Electronics Letters, vol. 25, no. 8, 1989, pp. 495-496.

- [13] C. Rolland, R. S. Moore, F. Shepherd and G. Hillier, "10 Gb/s, 1.56 μm multi quantum well InP /InGaAsP Mach-Zender optical modulator," *Electronic Letters*, vol. 29, no. 5, March 1993, pp. 471-472.
- [14] A. R. Chraplyvy, "Limitations on Lightwave communications imposed by optical fiber nonlinearities," *Journal of Lightwave Technology*, vol. 8, no. 10, October 1990, pp. 1548-1557.
- [15] N. Shibata, K. Nosu, K. Iwashita and Y. Azuma, "Transmission Limitations due to fiber nonlinearities in optical FDM systems," *IEEE Journal on Selected Areas in Communications*, vol. 8, no. 6, August 1990, pp. 1068-1077.
- [16] D. Cotter, "Stimulated Brillouin scattering in mono mode optical fiber," *J. Opt. Communications*, vol. 4, 1983, pp. 10-19.
- [17] K. O. Hill, D. C. Johnson, B. S. Kawasaki and I. R. MacDonald, "CW three-wave mixing in single mode optical fibers," *J. Appl. Phy.*, vol. 49, 1978, pp. 5098-5106.
- [18] B. Glance, K. Pollock, C. A. Burrus, B. L. Kasper, G. Eisenstein and L. W. Stulz, "Density spaced WDM coherent optical star network," *Electronic Letters*, vol. 23, 1987, pp. 875-876.

- [19] H. Toba, K. Oda, K. Nosu, N. Takato and H. Miyazawa, "5 Ghz spaced eight channel optical FDM transmission experiment using guided wave tunable demultiplexer," *Electronic Letters*, vol. 24, 1988, pp. 78-80.
- [20] R. S. Vodhanel, A. F. Elrefaie, M. Z. Iqbal, R. E. Wagner, J. L. Gimlett and S. Tsuji, "Performance of directly modulated DFB lasers in 10 Gb/s ASK, FSK and DPSK Lightwave systems," *Journal of Lightwave Technology*, vol. 8, no. 9, September 1990, pp. 1379-1385.
- [21] A. F. Elrefaie and R. E. Wagner, "Chromatic dispersion limitations for FSK and DPSK systems with direct detection receivers," *IEEE Photonics Technology Letters*, vol. 8, no. 1, January 1991.
- [22] T. Okoshi, "Heterodyne and coherent optical fiber communications: Recent progress," *IEEE Transactions Microwave Theory Technology*, vol. MTT-30, August 1982, pp. 1138-1149.
- [23] M. Tamburrini, P. Spano and S. Piazzolla, "Influence of semiconductor laser phase noise on coherent optical communication systems," *Optics Letters*, vol. 8, no. 3, March 1983, pp. 174-176.
- [24] J. Salz, "Coherent Lightwave communications," *AT&T Tech. Journal*, vol. 64, no. 10, Dec. 1985, pp. 2153-2209.

- [25] I. Garrett and G. Jacobsen, "Theoretical analysis of heterodyne optical receivers for transmission systems using (semiconductor) lasers with non-negligible line width," *Journal of Lightwave Technology*, vol. LT-4, March 1986, pp. 323-334.
- [26] J. Franz, C. Rapp and G. Soder, "Influence of baseband filtering on laser phase noise in coherent optical transmission systems," *Journal of Optical Communications*, vol. 7, no. 1, March 1986, pp. 15-20.
- [27] K. Emura, S. Yamazaki, S. Fujita, M. Shikida, I. Mito and K. Minemura, "Over 300 km transmission experiment on an optical FSK heterodyne dual filter detection system," *Electronic Letters*, vol. 22, no. 21, October 9, 1986, pp. 1096-1097.
- [28] I. Garrett and G. Jacobsen, "The effect of laser line width on coherent optical receivers with non-synchronous demodulation," *Journal of Lightwave Technology*, vol. LT-5, April 1987, pp. 551-560.
- [29] Gerard J. Foschini, Larry J. Greenstein and Giovanni Vannucci, "Noncoherent detection of coherent Lightwave signals corrupted by phase noise," *IEEE Transactions on Communications*, vol. 36, no.3, March 1988, pp. 306-314.
- [30] H. Toba, K. Inoue and K. Nosu, "A conceptional design on optical frequency division multiplexing distribution system with optical tunable filters," *IEEE Journal on Selected Areas in Communication*, vol. SAC-4, no. 9, December 1986, pp. 1458-1467.

- [31] H. Toba, Z. Oda, K. Nakanishi, N. Shibata, K. Nosu, N. Takato and M. Fukuda, "A 100 channel optical FDM transmission /Distribution at 622 Mb/s over 50 km," *Journal of Lightwave Technology*, vol. 8, no. 9, September 1990. R. Gross and R. Olshansky, "Multi-channel coherent FSK experiments using subcarrier multiplexing techniques," *Journal of Lightwave Technology*, vol. 8, no. 3, March 1990, pp. 406-415.
- [33] R. G. McKay and J. G. Cartledge, "Performance of coherent optical CPFSK-DD with inter symbol interference, noise correlation and laser phase noise," *Journal*
- [32] *of Lightwave Technology*, vol. 11, no. 11, November 1993, pp. 1845-1853.
- [34] M. Shirasaki, H. Nishimoto, T. Okiyama and T. Touge, "Fibre transmission properties of optical pulses produced through direct phase modulation of DFB laser diode," *IEE Electronic Letters*, vol. 24, 1988, pp. 486-488.
- [35] J. Song and C. C. Fan, "A simplified dispersion limit formula for IM/DD systems and its comparison with experimental results," *Journal of Lightwave Technology*, vol. 13, no. 3, March 1995, pp. 456-550.

- [36] Md. Muzammel Haque Tarafder, "Effects of fibre chromatic dispersion on optical FSK and DPSK transmission systems," A project submitted to EEE dept. of BUET, Dhaka, December 1994.
- [37] Faizul Alam, "Study of optical direct detecton scheme using Mach-Zender discriminator," A project submitted to EEE dept. of BUET, Dhaka, March 1994.
- [38] E. Bedrosian and S. O. Rice, "Distortion and cross-talk of linearly filtered angle-modulated signals," Proc. IEEE, vol. 56, January 1968, pp. 2-13.
- [39] S. P. Majumder, R. Gangopadhyay, M. S. Alam and G. Prati, "Performance of line-coded heterodyne FSK system with non-uniform laser FM response," Journal of Lightwave Technology, vol. 13, no. 4, April 1995, pp. 628-638.

Appendix A EXPRESSIONS OF $W_\phi^c(f)$ AND $W_\phi^l(f)$

$$\Gamma(f) = e^{-j\alpha f^2}$$

$$\Gamma(\rho) = e^{-j\alpha \rho^2}$$

$$\Gamma(f + \rho) = e^{-j\alpha(f+\rho)^2} = e^{-j\alpha(f^2 + 2f\rho + \rho^2)}$$

$$\begin{aligned} \Gamma(f) \cdot \Gamma(\rho) \cdot \Gamma(f + \rho) &= e^{-j\alpha f^2} \cdot e^{-j\alpha \rho^2} \cdot e^{-j\alpha(f^2 + 2f\rho + \rho^2)} \\ &= e^{-j\alpha(f^2 + f\rho + \rho^2)} \end{aligned}$$

$$\begin{aligned} W_\phi^c(f) &= 2W_\phi(f) \int_{-\infty}^{\infty} d\rho W_\phi(\rho) \left\{ \text{Re} \Gamma(f) \Gamma(\rho) \Gamma(-f - \rho) - |\Gamma(\rho)|^2 |\Gamma(f)|^2 \right\} \\ &= 2W_\phi(f) \int_{-\infty}^{\infty} d\rho W_\phi(\rho) \left[\text{Re} \left(e^{-j2\alpha(f^2 + f\rho + \rho^2)} \right) - 1 \right] \\ &= 2W_\phi(f) \int_{-\infty}^{\infty} W_\phi(\rho) \left[\text{Cos} \{ 2\alpha(f^2 + f\rho + \rho^2) \} - 1 \right] d\rho \end{aligned}$$

$$W_\phi^l(f) = \frac{1}{6} \int_{-\infty}^{\infty} d\rho \int_{-\infty}^{\infty} d\sigma W_\phi(\rho) W_\phi(\sigma) W_\phi(f - \rho - \sigma) |X(f)|^2$$

where

$$\begin{aligned} X(f) &= 2\Gamma(f)\Gamma(\sigma)\Gamma(f - \rho - \sigma) - \Gamma(f - \rho - \sigma)\Gamma(\rho + \sigma) \\ &\quad - \Gamma(\rho)\Gamma(f - \rho) - \Gamma(\sigma)\Gamma(f - \sigma) + \Gamma(f) \end{aligned}$$

$$\Gamma(\rho) \cdot \Gamma(f - \rho) = e^{-j\alpha \rho^2} \cdot e^{-j\alpha(f-\rho)^2} = e^{-j\alpha[f^2 + 2\rho^2 - 2f\rho]}$$

$$\Gamma(\sigma) \cdot \Gamma(f - \sigma) = e^{-j\alpha \sigma^2} \cdot e^{-j\alpha(f-\sigma)^2} = e^{-j\alpha[f^2 + 2\sigma^2 - 2f\sigma]}$$

$$\Gamma(\rho) = e^{-j\alpha\rho^2}$$

$$\Gamma(f) = e^{-j\alpha f^2}$$

$$\Gamma(\sigma) = e^{-j\alpha\sigma^2}$$

$$\Gamma(\rho)\Gamma(\sigma)\Gamma(f - \rho - \sigma)$$

$$= e^{-j\alpha\rho^2} e^{-j\alpha\sigma^2} e^{-j\alpha(f^2 + \rho^2 + \sigma^2 - 2f\rho + 2\rho\sigma - 2f\sigma)}$$

$$= e^{-j\alpha[2\rho^2 + 2\sigma^2 + f^2 - 2f\rho + 2\rho\sigma - 2f\sigma]}$$

$$\Gamma(f - \rho - \sigma)\Gamma(\rho + \sigma)$$

$$= e^{-j\alpha(f^2 + \rho^2 + \sigma^2 - 2f\rho + 2\rho\sigma - 2f\sigma)} e^{-j\alpha(\rho^2 + 2\rho\sigma + \sigma^2)}$$

$$= e^{-j\alpha[f^2 + 2\rho^2 + 2\sigma^2 - 2f\rho + 4\rho\sigma - 2f\sigma]}$$

Therefore,

$$X(f) = 2\Gamma(f)\Gamma(\sigma)\Gamma(f - \rho - \sigma) - \Gamma(f - \rho - \sigma)\Gamma(\rho + \sigma)$$

$$- \Gamma(\rho)\Gamma(f - \rho) - \Gamma(\sigma)\Gamma(f - \sigma) + \Gamma(f)$$

$$= 2e^{-j\alpha[2\rho^2 + 2\sigma^2 + f^2 - 2f\rho + 2\rho\sigma - 2f\sigma]} - e^{-j\alpha[f^2 + 2\rho^2 + 2\sigma^2 - 2f\rho + 4\rho\sigma - 2f\sigma]}$$

$$- e^{-j\alpha[f^2 + 2\rho^2 - 2f\rho]} - e^{-j\alpha[f^2 + 2\sigma^2 - 2f\sigma]} + e^{-j\alpha f^2}$$

$$= 2e^{-j\alpha a} - e^{-j\alpha b} - e^{-j\alpha c} - e^{-j\alpha d} + e^{-j\alpha e}$$

where, $a = 2\rho^2 + 2\sigma^2 + f^2 - 2f\rho + 2\rho\sigma - 2f\sigma$

$$b = f^2 + 2\rho^2 + 2\sigma^2 - 2f\rho + 4\rho\sigma - 2f\sigma$$

$$c = f^2 + 2\rho^2 - 2f\rho$$

$$d = f^2 + 2\sigma^2 - 2f\sigma$$

$$e = f^2$$

Therefore,

$$\begin{aligned}
 |X(f)|^2 &= |2.e^{-j\alpha a} - e^{-j\alpha b} - e^{-j\alpha c} - e^{-j\alpha d} + e^{-j\alpha e}|^2 \\
 &= [2\cos(\alpha a) - \cos(\alpha b) - \cos(\alpha c) - \cos(\alpha d) + \cos(\alpha e)]^2 \\
 &\quad + [2\sin(\alpha a) + \sin(\alpha b) + \sin(\alpha c) + \sin(\alpha d) - \sin(\alpha e)]^2 \\
 &= |X_1(f)|^2 + |X_2(f)|^2
 \end{aligned}$$

$$\begin{aligned}
 |X_1(f)|^2 &= 4\cos^2\alpha a + \cos^2\alpha b + \cos^2\alpha c + \cos^2\alpha d + \cos^2\alpha e \\
 &\quad - 4\cos\alpha a \cdot \cos\alpha b - 4\cos\alpha a \cdot \cos\alpha c - 4\cos\alpha a \cdot \cos\alpha d + 4\cos\alpha a \cdot \cos\alpha e \\
 &\quad + 2\cos\alpha b \cdot \cos\alpha d - 2\cos\alpha b \cdot \cos\alpha e + 2\cos\alpha c \cdot \cos\alpha e \\
 &\quad + 2\cos\alpha c \cdot \cos\alpha d - 2\cos\alpha c \cdot \cos\alpha e - 2\cos\alpha d \cdot \cos\alpha e
 \end{aligned}$$

$$\begin{aligned}
 |X_2(f)|^2 &= 4\sin^2\alpha a + \sin^2\alpha b + \sin^2\alpha c + \sin^2\alpha d + \sin^2\alpha e \\
 &\quad + 4\sin\alpha a \cdot \sin\alpha b + 4\sin\alpha a \cdot \sin\alpha c + 4\sin\alpha a \cdot \sin\alpha d + 4\sin\alpha a \cdot \sin\alpha e \\
 &\quad + 2\sin\alpha b \cdot \sin\alpha d + 2\sin\alpha b \cdot \sin\alpha e + 2\sin\alpha c \cdot \sin\alpha e \\
 &\quad + 2\sin\alpha c \cdot \sin\alpha d + 2\sin\alpha d \cdot \sin\alpha e
 \end{aligned}$$

Therefore,

$$\begin{aligned}
 |X(f)|^2 &= |X_1(f)|^2 + |X_2(f)|^2 \\
 &= 4(\sin^2\alpha a + \cos^2\alpha a) + (\sin^2\alpha b + \cos^2\alpha b) + (\sin^2\alpha c + \cos^2\alpha c) \\
 &\quad + (\sin^2\alpha d + \cos^2\alpha d) + (\sin^2\alpha e + \cos^2\alpha e) \\
 &\quad - 4\{\cos\alpha a \cdot \cos\alpha b - \sin\alpha a \cdot \sin\alpha b\} - 4\{\cos\alpha a \cdot \cos\alpha c - \sin\alpha a \cdot \sin\alpha c\} \\
 &\quad - 4\{\cos\alpha a \cdot \cos\alpha d - \sin\alpha a \cdot \sin\alpha d\} + 4\{\cos\alpha a \cdot \cos\alpha e + \sin\alpha a \cdot \sin\alpha e\}
 \end{aligned}$$

$$\begin{aligned}
&+2\{\text{Cos}\alpha b.\text{Cos}\alpha d + \text{Sin}\alpha b.\text{Sin}\alpha d\} - 2\{\text{Cos}\alpha b.\text{Cos}\alpha c - \text{Sin}\alpha b.\text{Sin}\alpha c\} \\
&+2\{\text{Cos}\alpha b.\text{Cos}\alpha c + \text{Sin}\alpha b.\text{Sin}\alpha c\} + 2\{\text{Cos}\alpha c.\text{Cos}\alpha d - \text{Sin}\alpha c.\text{Sin}\alpha d\} \\
&-2\{\text{Cos}\alpha c.\text{Cos}\alpha e - \text{Sin}\alpha c.\text{Sin}\alpha e\} - 2\{\text{Cos}\alpha d.\text{Cos}\alpha e - \text{Sin}\alpha d.\text{Sin}\alpha e\} \\
&= 8 - 4\text{Cos}\alpha(a + b) - 4\text{Cos}\alpha(a + c) - 4\text{Cos}\alpha(a + d) + 4\text{Cos}\alpha(a - e) \\
&-2\text{Cos}\alpha(b - d) - 2\text{Cos}\alpha(b + e) + 2\text{Cos}\alpha(b - c) \\
&+2\text{Cos}\alpha(c - d) - 2\text{Cos}\alpha(c + e) - 2\text{Cos}\alpha(d + c)
\end{aligned}$$

Appendix B PROGRAM LISTING

```

1.     PROGRAM TO FIND CROSS POWER COMPONENT

PROGRAM WFC
DOUBLE PRECISION Y(8193)
COMMON BR,FMX,Y,N
OPEN(10,FILE='C:\WATFOR\DOC\WFCIN.DAT',STATUS='OLD')
OPEN(20,FILE='C:\WATFOR\DOC\WFCOUT.DAT',STATUS='OLD')
C     VALUES OF A,B,C,D ARE NORMALIZED BY BR(BIT RATE)
BR=10.0E9
READ(10,*)A,B,NF,D
WRITE(20,90)A,B,NF,D
FMX=B
IF(D.GT.B) FMX=D
N=2**13
CALL PSDFSK()
DELF=(B-A)/NF
F=A
DO 10 I=1,NF
NFF=INT(F*N/FMX)+1
FUNF=Y(NFF)
CALL INTGRL(F,0.0,D,VALINT)
W=2.0*FUNF*VALINT*2.0
WRITE(20,91)F,W
F=F+DELF
PRINT*,I
10    CONTINUE
90    FORMAT(1X,'A=',F6.2,2X,'B=',F6.2,2X,'N=',I3,
+       2X,'D=',F6.2//1X,'FREQUENCY',3X,'WF_C')
91    FORMAT(1X,F6.2,2X,E10.3)
STOP
END

C     SUBROUTINE INTGRL(F,A,B,SY)
DELY=1.0E-3
IMAXY=13
S11Y=0.0
SY=0.0
BA=B - A
IF(BA) 20,19,20
19    IERY1=1
PRINT*, 'IERY1=',IERY1
STOP
20    IF(DELY)22,22,23
22    IERY1=2
PRINT*, 'IERY1=',IERY1
STOP
23    IF(IMAXY-1)24,24,25
24    IERY1=3
PRINT*, 'IERY1=',IERY1
STOP
25    HX=BA/2.0+A
NHALFY=1
CALL FUN1(F,HX,FUNHX)

```

```

SUMKY=FUNHX*BA*2.0/3.0
CALL FUN1(F.A.FUNA)
CALL FUN1(F.B.FUNB)
SY=SUMKY+(FUNA+FUNB)*BA/6.0
DO 28 IY=2,IMAXY
S11Y=SY
SY=(SY-(SUMKY/2.0))/2.0
NHALFY=NHALFY*2.0
ANHLFY=NHALFY
FRSTY=A+(BA/ANHLFY)/2.0
CALL FUN1(F.FRSTY,FUNFTY)
SUMKY=FUNFTY
YK=FRSTY
KLASTY=NHALFY-1
FENCY=BA/ANHLFY
DO 26 KY=1,KLASTY
YK=YK+FENCY
CALL FUN1(F.YK.FUNYK)
SUMKY=SUMKY+FUNYK
26 CONTINUE
SUMKY=SUMKY*2.0*BA/(3.0*ANHLFY)
SY=SY+SUMKY
WRITE(*,*)'SY=',SY,' S11Y=',S11Y
27 IF(ABS(SY-S11Y)-ABS(DELTA*SY))29,28,28
28 CONTINUE
IERY1=4
GO TO 30
29 IERY1=0
30 CONTINUE
NOY=2*NHALFY
RETURN
END

```

C

```

SUBROUTINE FUN1(F,R,YVAL)
DOUBLE PRECISION Y(8193),W
COMMON BR,FMX,Y,N
NR=INT(R*N/FMX)+1
W=Y(NR)
ALFA=1.89E-20
TEMP=2.0*ALFA*(F*F+F*R+R*R)*BR*BR
YVAL=W*(COS(TEMP)-1)
RETURN
END

```

C

```

SUBROUTINE PSDFSK()
DOUBLE PRECISION Y(8193)
COMMON BR,FMX,Y,N
FD=0.5*BR
FC=0.0
F=FMX*BR/N
T=1.0/BR
AM=2*FD/BR
DO 10 I=1,N+1
BETA=T*((I-1)*F-FC)
THETA=BETA+AM/2.0
CALL SUB12(THETA,A1)
THETA=BETA-AM/2.0
CALL SUB12(THETA,A2)

```

```

CALL SUB3(BETA,AM,A1,A2,A3)
Y(I)=(A1*A1+A2*A2+A3)/8.0
10 CONTINUE
RETURN
END

C
SUBROUTINE SUB12(THETA,A)
IF(THETA.EQ.0.0)THEN
A=1.0
ELSE
A=SIN(THETA)/THETA
ENDIF
RETURN
END

C
SUBROUTINE SUB3(BETA,AM,A1,A2,A3)
PI=22.0/7.0
A3=0.0
DO 20 I=1,2
DO 10 K=1,2
IF(I.EQ.K)THEN
IF(I.EQ.1)THEN
ALPHA=-PI*AM
ELSE
ALPHA=PI*AM
ENDIF
ELSE
ALPHA=0.0
ENDIF
ZI=COS(PI*AM)
ANUM=COS(2.0*PI*BETA-ALPHA)-ZI*COS(ALPHA)
DNUM=1.0+(ZI*ZI)-2.0*ZI*COS(2.0*PI*BETA)
IF(DNUM.EQ.0.0)THEN
PRINT*,'DNUM=0'
PRINT*,'ZI=',ZI,'M=',AM,'BETA=',BETA
DNUM=1E-9
ENDIF
B=ANUM/DNUM
IF(I.EQ.1)THEN
P1=A1
ELSE
P1=A2
ENDIF
IF(K.EQ.1)THEN
P2=A1
ELSE
P2=A2
ENDIF
A3=A3+B*P1*P2
10 CONTINUE
20 CONTINUE
RETURN
END

```

2. PROGRAM TO FIND INTERMODULATION POWER COMPONENT

```

PROGRAM WFIM
COMMON /B/BR,FMX
OPEN(10,FILE='DOC\WFIP1.DAT',STATUS='OLD')
OPEN(20,FILE='DOC\WFOP1.DAT',STATUS='OLD')
C ALL VALUES ARE NORMALIZED BY BIT RATE
C PRINT*,'ENTER VALUES OF A,B,N,C,D,C1,D1'
READ(10,*)A,B,N,RMX,SMX
WRITE(20,90)A,B,N,RMX,SMX
90 FORMAT(' A=',F4.1,2X,'B=',F4.1,2X,'N=',I2/1X,'RMX=',
+ F4.1/1X,'SMX=',F4.1)
FMX=RMX+SMX
IF(B.GT.FMX) FMX=B
BR=1E9
T=1/BR
CALL PSDFSK()
DELF=(B-A)/N
F=A
DO 10 I=1,N
CALL INTGL1(F,0.0,RMX,0.0,SMX,VALINT)
WF=T*T*VALINT*4.0/6.0
WRITE(20,91)F,WF
91 FORMAT(1X,'F=',F5.2,3X,'W(F)='E8.3)
F=F+DELF
PRINT*,I
10 CONTINUE
STOP
END
C
SUBROUTINE INTGL1(F,A,B,C1,D1,SY)
DELY=1.0E-2
IMAXY=10
BA=B - A
IF(BA) 20,19,20
19 IERY1=1
PRINT*,'IERY1=',IERY1
STOP
20 IF(DELY)22,22,23
22 IERY1=2
PRINT*,'IERY1=',IERY1
STOP
23 IF(IMAXY-1)24,24,25
24 IERY1=3
PRINT*,'IERY1=',IERY1
STOP
25 HX=BA/2.0+A
NHALFY=1
CALL INTGL2(F,C1,D1,HX,FUNHX)
SUMKY=FUNHX*BA*2.0/3.0
CALL INTGL2(F,C1,D1,A,FUNA)
CALL INTGL2(F,C1,D1,B,FUNB)
SY=SUMKY+(FUNA+FUNB)*BA/6.0
DO 28 IY=2,IMAXY
S1IY=SY
SY=(SY-(SUMKY/2.0))/2.0
NHALFY=NHALFY*2.0
ANHLFY=NHALFY

```

```

FRSTY=A+(BA/ANHLFY)/2.0
CALL INTGL2(F,C1,D1,FRSTY,FUNFTY)
SUMKY=FUNFTY
YK=FRSTY
KLASTY=NHALFY-1
FENCY=BA/ANHLFY
DO 26 KY=1,KLASTY
YK=YK+FENCY
CALL INTGL2(F,C1,D1,YK,FUNYK)
SUMKY=SUMKY+FUNYK
26 CONTINUE
SUMKY=SUMKY*2.0*BA/(3.0*ANHLFY)
SY=SY+SUMKY
27 IF(ABS(SY-S11Y)-ABS(DELY*SY))29,28,28
28 CONTINUE
IERY1=4
GO TO 30
29 IERY1=0
30 CONTINUE
NOY=2*NHALFY
WRITE(*,*)'ITERATIONS IN INTEGRAL1='.NOY
RETURN
END.

```

C

```

SUBROUTINE INTGL2(F,A,B,ROW,SY)
DELY=1.0E-2
IMAXY=10
BA=B - A
IF(BA) 20,19,20
19 IERY1=1
PRINT*, 'IERY1='.IERY1
STOP
20 IF(DELY)22,22,23
22 IERY1=2
PRINT*, 'IERY1='.IERY1
STOP
23 IF(IMAXY-1)24,24,25
24 IERY1=3
PRINT*, 'IERY1='.IERY1
STOP
25 HX=BA/2.0+A
NHALFY=1
CALL FUN2(F,ROW,HX,FUNHX)
SUMKY=FUNHX*BA*2.0/3.0
CALL FUN2(F,ROW,A,FUNA)
CALL FUN2(F,ROW,B,FUNB)
SY=SUMKY+(FUNA+FUNB)*BA/6.0
DO 28 IY=2,IMAXY
S11Y=SY
SY=(SY-(SUMKY/2.0))/2.0
NHALFY=NHALFY*2.0
ANHLFY=NHALFY
FRSTY=A+(BA/ANHLFY)/2.0
CALL FUN2(F,ROW,FRSTY,FUNFTY)
SUMKY=FUNFTY
YK=FRSTY
KLASTY=NHALFY-1
FENCY=BA/ANHLFY

```



```

DO 26 KY=1,KLASTY
YK=YK+FICY
CALL FUN2(F,ROW,YK,FUNYK)
SUMKY=SUMKY+FUNYK
26 CONTINUE
SUMKY=SUMKY*2.0*BA/(3.0*ANHLFY)
SY=SY+SUMKY
27 IF(ABS(SY-S11Y)-ABS(DELY*SY))29.28.28
28 CONTINUE
IERY1=4
GO TO 30
29 IERY1=0
30 CONTINUE
NOY=2*NHALFY
WRITE(*,*) ITERATIONS IN INTEGRAL2=',NOY
RETURN
END

```

```

C
SUBROUTINE FUN2(F,ROW,SIG,FUN)
DOUBLE PRECISION F1,F2,F3,F4,Y(8193)
COMMON /B/BR,FMX, /Y
N=2**13
NR=INT(ROW*N/FMX)+1
F1=Y(NR)
NS=INT(SIG*N/FMX)+1
F2=Y(NS)
C=F-ROW-SIG
IF(C.LT.0)C=-C
NC=INT(C*N/FMX)+1
F3=Y(NC)
FF=F*BR
R=ROW*BR
S=SIG*BR
CALL FUNX(FF,R,S,F4)
FUN=F1*F2*F3*F4*F4
RETURN
END

```

```

C
SUBROUTINE FUNX(F,R,S,FUN)
DOUBLE PRECISION FUN
DOUBLE PRECISION A,B,C,D,E,AL
A=2*R*R+2*S*S+F*F-2*F*R+2*R*S-2*F*S
B=F*F+2*R*R+2*S*S-2*F*R+4*R*S-2*F*S
C=F*F+2*R*R-2*F*R
D=F*F+2*S*S-2*F*S
E=F*F
AL=1.89E-20
FUN=8-4*COS(AL*(A+B))-4*COS(AL*(A+C))-4*COS(AL*(A+D))
1 +4*COS(AL*(A-E))+2*COS(AL*(B-D))-2*COS(AL*(B+E))
1 +2*COS(AL*(B-C))+2*COS(AL*(C-D))-2*COS(AL*(C+E))
1 -2*COS(AL*(D+E))
RETURN
END

```

```

C
SUBROUTINE PSDFSK()
DOUBLE PRECISION Y(8193)
COMMON /B/BR,FMX, /Y

```

```

FD=0.5*BR
FC=0.0
M=13
N=2**M
F=FMX*BR/N
T=1.0/BR
AM=2*FD/BR
DO 10 I=1,N+1
  BETA=T*((I-1)*F-FC)
  THETA=BETA+AM/2.0
  CALL SUB12(THETA,A1)
  THETA=BETA-AM/2.0
  CALL SUB12(THETA,A2)
  CALL SUB3(BETA,AM,A1,A2,A3)
  Y(I)=(A1*A1+A2*A2+A3)/8.0
10 CONTINUE
RETURN
END

C
SUBROUTINE SUB12(THETA,A)
IF(THETA.EQ.0.0)THEN
  A=1.0
ELSE
  A=SIN(THETA)/THETA
ENDIF
RETURN
END

C
SUBROUTINE SUB3(BETA,AM,A1,A2,A3)
PI=22.0/7.0
A3=0.0
DO 20 I=1,2
DO 10 K=1,2
IF(I.EQ.K)THEN
  IF(I.EQ.1)THEN
    ALPHA=-PI*AM
  ELSE
    ALPHA=PI*AM
  ENDIF
ELSE
  ALPHA=0.0
ENDIF
ZI=COS(PI*AM)
ANUM=COS(2.0*PI*BETA-ALPHA)-ZI*COS(ALPHA)
DNUM=1.0+(ZI*ZI)-2.0*ZI*COS(2.0*PI*BETA)
IF(DNUM.EQ.0.0)THEN
  PRINT*,'DNUM=0'
  PRINT*,'ZI=',ZI,'M=',AM,'BETA=',BETA
  DNUM=1E-9
ENDIF
B=ANUM/DNUM
IF(I.EQ.1)THEN
  P1=A1
ELSE
  P1=A2
ENDIF
IF(K.EQ.1)THEN
  P2=A1

```

```
ELSE
    P2=A2
ENDIF
A3=A3+B*P1*P2
10 CONTINUE
20 CONTINUE
RETURN
END
```

3. PROGRAM TO FIND IMPULSE RESPONSE OF FIBRE

```

PROGRAM IMPULS
DOUBLE PRECISION X(4096),X1(4096),Y(4096),Y1(4096)
DOUBLE PRECISION F,FSA,TS,T,Z(4096)
OPEN(20,FILE='BER\IR2.DAT')
PI=22.0/7.0
C=3E8
BR=10E9
NSB=8
M=10
N=2**M
F=12*BR/N
FSA=F*N
TS=1.0/FSA
DO 1 I=1,NSB
X(I)=1.0
Y(I)=0.0
1 CONTINUE
CALL TRANSF(X,Y,NSB,TS,M,T)
NH=N/2
WRITE(*,*) 'ENTER FIBRE LENGTH L IN KM'
READ(*,*) L
WRITE(*,*) 'ENTER CROMATIC DISPERSION IN PS/KM.NM'
READ(*,*) D
WRITE(*,*) 'ENTER LAMDA IN NM'
READ(*,*) LAMDA
ALFA=PI*D*1E-12*LAMDA*LAMDA*1E-9*L/C
GAMA=(BR**2.0)*ALFA/PI**2
PRINT *, 'L=',L,'DC=',D,'LAMDA=',LAMDA,'ALFA=',ALFA,
+ 'GAMA=',GAMA
WRITE(20,*)L,D,LAMDA,GAMA
DO 2 I=1,NH+1
FF=F*(1-I)
TEMP=ALFA*FF**2
X1(I)=COS(TEMP)
Y1(I)=-SIN(TEMP)
2 CONTINUE
INC=1
DO 3 I=NH+2,N
J=I-2*INC
X1(I)=X1(J)
Y1(I)=Y1(J)
INC=INC+1
3 CONTINUE
DO 4 I=1,N
AA=X(I)*X1(I)-Y(I)*Y1(I)
BB=X(I)*Y1(I)+X1(I)*Y(I)
X(I)=AA
Y(I)=-BB
4 CONTINUE
CALL DFT(X,Y,N,M)
DO 5 I=1,N/2+1
X(I)=X(I)/N
Y(I)=Y(I)/N
Z(I)=SQRT(X(I)**2+Y(I)**2)
WRITE(20,*) SNGL(Z(I))
WRITE(*,*)SNGL(X(I)), SNGL(Z(I))

```

```

5  CONTINUE
   STOP
   END

C
SUBROUTINE TRANSF(X,Y,NSB,TS,M,T)
DOUBLE PRECISION X(4096),Y(4096),TS,T
N=2**M
NH=N/2
FSA=1.0/TS
F=FSA/N
DO 1 I=NSB+1,NH+1
X(I)=0.0
Y(I)=0.0
1  CONTINUE
   INC=1
   DO 2 I=NH+2,N
J=I-2*INC
X(I)=X(J)
Y(I)=Y(J)
INC=INC+1
2  CONTINUE
   CALL DFT(X,Y,N,M)
   RETURN
   END

C
SUBROUTINE DFT(X,Y,N,M)
COMPLEX AX(4096),U,W,T
DOUBLE PRECISION PL,X(4096),Y(4096)
DO 1 I=1,N
AX(I)=CMPLX(X(I),Y(I))
1  CONTINUE
   NV2=N/2
   NM1=N-1
   J=1
   DO 5 I=1,NM1
IF(I.GE.J) GO TO 2
T=AX(J)
AX(J)=AX(I)
AX(I)=T
2  K=NV2
3  IF(K.GE.J) GO TO 4
J=J-K
K=K/2
GO TO 3
4  J=J+K
5  CONTINUE
   PI=22.0/7.0
   DO 20 L=1,M
LE=2**L
LE1=LE/2
U=CMPLX(1.0,0.0)
W=CMPLX(COS(PI/LE1),SIN(PI/LE1))
DO 20 J=1,LE1
DO 10 I=J,N,LE
IP=I+LE1
T=AX(IP)*U
AX(IP)=AX(I)-T

```

```
AX(I)=AX(I)+T
10 CONTINUE
U=U*W
20 CONTINUE
DO 25 I=1,N
X(I)=REAL(AX(I))
Y(I)=AIMAG(AX(I))
25 CONTINUE
RETURN
END
```

```

4.  PROGRAM TO FIND EVEN ORDER MOMENTS
C   PROGRAM FOR COMPUTATION OF EVEN ORDER MOMENTS
C   OF LASER FREQUENCY NOISE
DIMENSION X(8192),SUMY(10,1026),A(8192)
DIMENSION Y(20,32)
OPEN(70,FILE='\\WATFOR\BER\IR2.DAT')
OPEN(40,FILE='\\WATFOR\BER\MOMENT.DAT')
NSB=8
N=512
READ(70,*)LL,D,LAMDA,ALFA
WRITE(*,*)'GIVE MOD. INDEX'
READ(*,*)AMOD
WRITE(40,*) AMOD
WRITE(*,*)'AMOD=',AMOD
AMAX=1.0
DO 2 I=1,N+1
  READ(70,*)A(I)
  IF(A(I) .GT. AMAX) AMAX=A(I)
2  CONTINUE
  WRITE(*,*)'AMAX=',AMAX
  DO 1 I=1,N+1
    A(I)=A(I)*AMOD/4.0
    WRITE(*,*)I,A(I)
1  CONTINUE
  S=0.0
  DO 6 I=1,NSB
    S=S+A(I)
6  CONTINUE
  DELF=S/NSB
  WRITE(*,*)'AVG. DEV. M0=',DELF
  WRITE(40,*)DELF
  NB=N/NSB
  DO 10 L=NSB,1,-1
    DO 11 K=1,10
      K2=K*2
      DO 12 I=1,NB-1
        SUMY(K,I)=0.0
      DO 13 J=0,K
        AK=2.0*K
        AJ=2.0*J
        CALL COMBN(AK,AJ,CKJ)
        IF(I .EQ. 1) THEN
          IF(J .EQ. 0) THEN
            SY=1.0
          ELSE
            SY=0.0
          ENDIF
        ELSE
          IF(J .EQ. 0) THEN
            SY=1.0
          ELSE
            SY=SUMY(J,I-1)
          ENDIF
        ENDIF
      ENDIF
    ENDIF
    II=I*NSB+L
    NKJ=2*(K-J)
    AI=ABS(A(II))

```

```

SUMY(K,I)=SUMY(K,I)+CKJ*SY*(AI**NKJ)
SMY=SUMY(K,I)
13 CONTINUE
12 CONTINUE
Y(K2,L)=SMY
WRITE(*,*)'M('K2,',',L,')=',Y(K2,L)
IF(L .EQ. 1) THEN
    WRITE(40,*)Y(K2,L)
ENDIF
11 CONTINUE
10 CONTINUE
WRITE(40,*)LL,D,LAMDA,ALFA
STOP
END

```

```

SUBROUTINE COMBN(AN,AR,ANCR)
IF(AR .EQ. 0.0) THEN
    ANCR=1.0
ELSE
    CALL FACTN(AN,FAN)
    CALL FACTN(AR,FAR)
    ANMR=AN-AR
    CALL FACTN(ANMR,FANMR)
    ANCR=FAN/(FAR*FANMR)
ENDIF
RETURN
END

```

C

```

SUBROUTINE FACTN(C,FAC)
IF(C .EQ. 0.0) THEN
    FAC=1.0
ELSE
    M=ANINT(C)
    FAC=1.0
    DO 100 I=1,M
        FAC=FAC*FLOAT(I)
        CONTINUE
100
ENDIF
RETURN
END

```



```

5. PROGRAM TO FIND BER FOR DIFFERENT PS dBm DUE TO FIBRE CHROMATIC DISPERSION
C PROGRAM TO FIND BER FOR DIFFERENT VALUE OF PS-DBM DUE TO FIBRE
CHROMATIC
C DISPERSION
IMPLICIT DOUBLE PRECISION (A-H,J-M,O-Z)
DIMENSION DBM(20),BERM(20,10)
REAL NU,NUT(10)
COMMON M(10),/X/XMEAN
OPEN(12,FILE='\\WATFOR\BER\DELNU.DAT')
OPEN(11,FILE='\\WATFOR\BER\MOMENT.DAT')
OPEN(10,FILE='\\WATFOR\BER\BERMQM.DAT')
* VARIABLE DEFINITION: RD=RESPONSIVITY=1.0, FE= NOISE * FIGURE= 3DB
* MOD. INDEX,H=(2*DELF/RB),
* LINEWIDTH=NU(NORMALIZED)=DT=(DELNEW*T)
* TAO=(T/2*H), VARIANCE=VAR=2*PI*(NU/T)*TAO=2*PI*DT1
RB=10.0*(10.0**9.0)
BW=(2.0*RB)
T=(1.0/RB)
PI=22.0/7.0
* ??? CHOOSE THE VALUE OF MOD.INDEX, H
READ(11,*) H
READ(11,*)XMEAN
READ(11,*) (M(I),I=1,10)
WRITE(*,*) 'IF DC ZERO THEN ENTER 0 ELSE ENTER 9'
READ(*,*) DC
WRITE(*,*) 'H=' ,H
TAO=T/(2.0*H)
* CHOOSE THETA0BAR=XMEAN, FOR A PARTICULAR H
WRITE(*,*)'XMEAN=',XMEAN
READ(12,*) NNU,(NUT(I),I=1,NNU)
IF(DC.NE.0) GOTO 10

* FOR FIBRE CROMATIC DISPERSION DC=0.0
DO 7 I=1,NNU
NU=NUT(I)
DT=NU
DT1=(NU/T)*TAO
C SET THE VALUE OF PS_DBM
PS_DBM=-25.0
WRITE(*,*)'DT1=' ,DT1
WRITE(*,*)'DT=' ,DT
DO 5 IJ=1,20
PSIG= .001*(10.0)**(PS_DBM/10.0)
CALL SNRT(PSIG,SNR,BW,DT1)
JITA=SQRT(SNR/2.0)
X=0.0
C FOR X=0.0, PDF=PDFN=1.0 AS, PDFN=PDF[1+...*HE(X)], AND HE.N(0) IS ALWAYS ZERO FOR
ANY C VALUE OF N
CALL ERFC(X,ERFCZ,JITA)
BER=0.5*ERFCZ
WRITE(*,*)PS_DBM,BER,I
DBM(IJ)=PS_DBM
BERM(IJ,I)=BER
IF(BER.LE.1E-12) GOTO 7
PS_DBM=PS_DBM+1.0
5 CONTINUE
7 CONTINUE

```

GO TO 20

```
* FOR NON-ZERO FIBRE CHROMATIC DISPERSION
10 DO 17 I=1, NNU
    NU=NUT(I)
    DT=NU
    DT1=(NU/T)*TAO
    WRITE(*,*)'DT=' .DT
    PS_DBM=-25.0
    DO 15 IJ=1,20
        PSIG=.001*(10.0)**(PS_DBM/10.0)
        CALL SNRT(PSIG,SNR,BW,DT1)
        JITA=SQRT(SNR/2.0)
        C=(XMEAN-5.0)
        D=(XMEAN+5.0)
        CALL SMPSNY(C,D,DT1,JITA,SY)
        BER=(0.5*SY)
        DBM(IJ)=PS_DBM
        BERM(IJ,I)=BER
        WRITE(*,*)'PS_DBM=',PS_DBM,'BER=',BER,I
        IF(BER.LE.1E-12) GOTO 17
        PS_DBM=PS_DBM+1.0
15 CONTINUE
17 CONTINUE
20 DO 25 IJ=1,20
    WRITE(10,90) DBM(IJ),(BERM(IJ,N),N=1,NNU)
25 CONTINUE
90 FORMAT(1X,F6.2,1X,10(E8.2,1X))
100 STOP
    END
```

```
    SUBROUTINE SMPSNY(C,D,DT1,JITA,SY)
    IMPLICIT DOUBLE PRECISION (A-H,I-M,O-Z)
    COMMON /X/XMEAN
C    SET THE ACCURACY LIMIT YOU DESIRE FROM THE INTEGRATION
    DELY=0.01
C    SET THE MAXIMUM ITERATION YOU DESIRE,IMAX
    IMAX=10
    S11Y=0.00
    SY=0.0
    DC=D-C
    IF(DC)20,19,20
19    WRITE(*,*) 'ERROR IN BOUNDARY VALUE'
    RETURN
20    IF(DELY)22,22,23
22    WRITE(*,*)'ERROR: CHOOSE +VE VALUE FOR DELY'
    RETURN
23    IF(IMAX-1)24,24,25
24    WRITE(*,*)'ERROR: CHOOSE +VE VALUE FOR MAXIMUM ITERATION'
    RETURN
25    HY=DC/2.0+C
    NHALFY=1
    X=HY
    XX=X-XMEAN
    CALL PDF(XX,PDF1,DT1)
    CALL ERFC(X,ERFCZ,JITA)
    FUNHY=PDF1*ERFCZ
```

```

SUMKY=FUNHY*DC*2.0/3.0
X=C
XX=X-XMEAN
CALL PDF(XX.PDF1.DT1)
CALL ERFC(X.ERFCZ.JITA)
FUNC=PDF1*ERFCZ
X=D
XX=X-XMEAN
CALL PDF(XX.PDF1.DT1)
CALL ERFC(X.ERFCZ.JITA)
C GET THE VALUE OF F(X)=PDF1*ERFCZ
FUND=PDF1*ERFCZ
C BER OBTAINED FROM THE FIRST ITERATION IN SIMPSON.BER=SY
SY=SUMKY+(FUNC+FUND)*DC/6.0
DO 28 IY=2.IMAX
S11Y=SY
C FOR 2ND ITERATION KEEP THE CONTRIBUTION OF F(X) AT C.D & HY IN SY
SY=(SY-(SUMKY/2.0))/2.0
NHALFY=NHALFY*2.0
ANHLFY=NHALFY
FRSTY=C+(DC/ANHLFY)/2.0
X=FRSTY
XX=X-XMEAN
CALL PDF(XX.PDF1.DT1)
CALL ERFC(X.ERFCZ.JITA)
C GET THE VALUE OF F(X)=PDF1*ERFCZ
FUNFTY=PDF1*ERFCZ
SUMKY=FUNFTY
YK=FRSTY
KLASTY=NHALFY-I
FENCY=DC/ANHLFY
DO 26 KY=1.KLASTY
YK=YK+FENCY
X=YK
XX=X-XMEAN
CALL PDF(XX.PDF1.DT1)
CALL ERFC(X.ERFCZ.JITA)
C GET THE VALUE OF F(X)=PDF1*ERFCZ
FUNYK=PDF1*ERFCZ
SUMKY=SUMKY+FUNYK
26 CONTINUE
SUMKY=(SUMKY*2.0*DC)/(3.0*ANHLFY)
SY=SY+SUMKY
27 IF(ABS(SY-S11Y)-ABS(DELY*SY)) 29.28.28
28 CONTINUE
29 AINTE=SY
RETURN
END

```

```

C SUBROUTINE TO OBTAIN PROBABILITY DENSITY FUNCTION

SUBROUTINE PDF(X.PDFX.DT1)
IMPLICIT DOUBLE PRECISION (A-Z)
COMMON M(10)
C CONSTANT IDENTIFICATION
PI=22.0/7.0

```

```

XAVG=0.0
VAR=(2.0*PI*DT1)+M(1)
EXPO=((X-XAVG)**2)/(2.0*VAR)
IF(EXPO.GE.708.9.AND.EXPO.LT.709.8)THEN
ANUMER=0.0
ELSE
ANUMER=EXP(-1.0*EXPO)
ENDIF
DENO=SQRT(2.0*PI*VAR)
PDFX=ANUMER/DENO
RETURN
END
*****

```

```

C PROGRAM TO FIND ERFC(Z)

SUBROUTINE ERFC(X,ERFCZ,JITA)
IMPLICIT DOUBLE PRECISION (A-H,I-M,O-Z)
C CONSTANT IDENTIFICATION
Z=JITA*COS(X)
C DOUBLE PRECISION Z,Y,P,PP,Q1,Q2,A1,A2,A3,A4,A5,PI,ZZ
PI=22.0/7.0
ZZ=ABS(Z)
SIGN=Z/ZZ
A1=0.2548295920
A2=-0.284496736
A3=1.4214137410
A4=-1.453152027
A5=1.0614054290
C ERROR=1.5E-7
P=0.3275911
PP=1.0/(1.0+P*ZZ)
Q1=EXP(-(ZZ**2.))
Q2=A1*PP+A2*(PP**2.)+A3*(PP**3.)+A4*(PP**4.)+A5*(PP**5.)
Y=(1.0-Q1*Q2)*SIGN
Y=1.0-Y
ERFCZ=Y
RETURN
END

```

C*****

```

C PROGRAM TO FIND SIGNAL TO NOISE RATIO
SUBROUTINE SNRT(PSIG, SNR, BW, DT1)
IMPLICIT DOUBLE PRECISION(A-Z)
COMMON M(10)
C CONSTANT IDENTIFICATION
E=1.6E-19
PI=(22.0/7.0)
RD=1.0
CUR=(RD*PSIG)
XAVG=1.0
C VARIANCE= PROD= 2*PI*DT1, RES=LOAD RESISTANCE, FE=NOISE C FIGURE
K=1.38E-23
TEMP=300.0
RES=50.0
FE_DBM=3.0
FE=(10.0)**(FE_DBM/10.0)
VAR=2.0*PI*DT1

```

NSHOT=2.0*E*BW*CUR*(1.0+XAVG)
NEXCSS=0.5*(CUR**2.0)*VAR
NTHRM=(4.0*K*TEMP*FE*BW)/RES
NTOT=NSHOT+NEXCSS+NTHRM
AMP=2.0*RD*PSIG
C SNR=(AMP**2)/(TOTAL NOISE. NTOT)
SNR=(AMP**2.0)/NTOT
RETURN
END

